Doctoral Dissertation

The role of membrane proteins in abiotic stresses in *Arabidopsis thaliana*

Division: Thermo-Biosystem Relations

Specialty: Cryobiosystems

United Graduate School of Agricultural Sciences

Iwate University

Ashraf Mohammad Arif

2018. 12

Contents	

Summary

The growth and development of plants are constantly challenged due to the change in the environment or stressful conditions. These unfavorable environmental conditions include biotic stresses, such as invasion of virus, parasites, and insects, and abiotic stresses, such as drought, heat, cold, salinity, nutrient deficiency, and excess of toxic compounds like arsenate, cadmium, cesium in the soil. Among these, temperature stress has become the major concern as heat and cold stress lead to other abiotic stresses. For instance, heat and cold stresses cause drought and osmotic stress, respectively. Between high and low temperature stresses, the decrease in temperature and the increased length of winter have become the major limiting factor to provide the favorable growth temperature for most of the crop plants (Chapter 1).

Altered response of plants' growth and development due to abiotic stress is the summation of cellular response. From the cellular perspective, plasma membrane acts as boundary and helps to maintain the cell – cell communication. Additionally, plasma membrane residing proteins function as transporter, receptor, and receptor kinases. The perception of stress is mediated through plasma membrane proteins and manipulation of membrane proteins restrict the uptake of toxic metal and perturbs the stress signal transduction inside the cell. Hence, the membrane proteins play pivotal role in abiotic stress regulation (Chapter 1).

In recent years, temperature stresses, more specifically low temperature stress, has become the cause of huge economic loss in most part of the world. Despite the huge financial loss due to low temperature stress, our understanding about cold stress response in plant is still elusive. Till date, our knowledge about cold stress regulation is mostly based on stress hormone Abscisic acid (ABA) and the major cold stress inducible transcription factor CBFs (C-Repeat Binding Factors). But, the plant growth and regulation is mediated through multiple hormones and cold stress mediated transcriptional regulation follows both CBF-dependent and –independent pathway. Recent discoveries pointed out the role of auxin in low temperature stress regulation. The study of auxin depicted a cold stress-mediated inhibition of intracellular trafficking model (Chapter 2).

In this research, I have used known protein trafficking mutants and identified GNOM, Guanine nucleotide Exchange Factors for ADP Ribosylation Factor (ARF-GEF), as one of the master regulator of cold stress response. GNOM is localized in the both cytosol and PM. Weak

mutant of GNOM, *gnom*$^{B/E}$, is hypersensitive to cold and GNOM-engineered BFA resistant line (GNOM^{M696L}) is resistant to cold from root phenotype and whole plant level. I have found that the point mutation in the BFA res. line results in overexpression of GNOM both at transcriptional and translational levels. GNOM participates in the recycling endosomal pathway and facilitates trafficking of proteins, including auxin efflux carrier PIN2, between PM and cytosol. Using PIN2-GFP, it had been demonstrated that recycling endosomal trafficking is disappeared during cold stress and in contrast, persistent trafficking is observed in BFA resistant line background. Altogether, it suggests that the overexpression of GNOM retains protein trafficking between plasma membrane and cytosol even after cold stress treatment (Chapter 2).

Another major abiotic stress is metal stress, because toxic metals exploit plants' transport system and easily incorporate in our food chain. In these recent years, cesium drew our attention most due to the nuclear power plant accident in Fukushiam, Japan during the Tsunami of 2011. Due to its chemical similarity with potassium, plants easily uptake cesium using potassium transporters. Consistently, so far identified cesium transporters are mostly known potassium transporters. As a result, most of the low cesium uptake strategy employed the alteration of potassium transporters to reduce cesium uptake. Unfortunately, this approach is irrational as it changes the intracellular concentration of important nutrient potassium. Gene expression analysis of cesium intoxicated plants compared with potassium starved plants highlighted that a group of potassium independent transporters, including ABC (ATP-binding cassette) transporters, are differentially expressed. Among these group of transporters, ABC transporters have less substrate specificity and are involved in detoxification of metal in both animal and plant cells. Hence, I focused on the screening of ABC transporters to find alternative cesium transporter (Chapter 3).

Based on the screening of ABC transporters, I have identified two ABC transporters, ABCG33 and ABCG37, as cesium influx carriers, which function redundantly. The gain-of-function mutant of ABCG37, *abcg37-1*, is hypersensitive to cesium. However, single knockout mutants of ABCG37 (*abcg37-2*, *abcg37-3*, and *abcg37-4*) have wild-type like phenotype. The unexpected wild-type like response of single mutants prompted us to hypothesize that loss of ABCG37 may be compensated by another ABC protein. Based on phylogenetic analysis, ABCG33 turned out to be the closest homolog of ABCG37, residing in the same clade and have ~80% identity at protein level. Double knockout mutant (*abcg37-2 abcg33-1*) shows the resistant

phenotype and reduce uptake of cesium. Combining the knowledge of these transporters with existing low cesium containing crop plants will help to develop varieties capable of growing in cesium contaminated soil (Chapter 3).

Interestingly, study of these abiotic stresses (cold and cesium stress) helped to identify three membrane proteins as major regulators. Among them, GNOM was identified as response regulator of cold stress and two ABCG transporters, ABCG37 and ABCG33, were characterized as plasma membrane-localized potassium-independent cesium influx carriers (Chapter 2, 3, 4).

Chapter 1

General Introduction

Abiotic stress for plant

As sessile organism plants are unable to escape from the adverse conditions and experience both biotic and abiotic stresses. Between these two, abiotic stress has become the most prominent cause for the agricultural loss. The reason is the damage caused by biotic stress can be solved by manipulating single target genes or receptors. In opposite, one abiotic stress leads to other or plants are subjected to multiple abiotic stresses at the same time (Mittler, 2006). For instance, synergistic effect of drought and heat is more destructive compared to individual stress (Mittler, 2006; Prasad et al., 2011). Low temperature causes mechanical constrains, alters signaling molecule and reduces osmotic pressure in the cellular level (Xiong et al., 2002). During the submergence, plants experience the combination of flooding, salinity stress and hypoxia at the same time (Tamang and Fukao, 2015).

Among abiotic stresses, temperature stress has become the major issues due to global warming. According to the latest data of National Centers for Environmental Information, USA (NOAA), the global land surface temperature for March 2018 was 1.49°C (2.86°F) above average and it was seventh highest since global records began in 1880. At the same time, cooler-than-average conditions engulfed much of Europe and western Russia during March 2018. For example, the Leon (France) observed an average maximum temperature of 8.6°C (47.5°F), the lowest of March since its record began in 1938 (Based on recent data of National Oceanic and Atmospheric Administration, USA). This statistics suggest the anomaly of both low and high temperature in various parts of the world in recent years.

NOAA temperature statistics correlate with the agricultural economic data published by developed countries in the past years. Heat, drought, low temperature, and flooding caused damages with more than 1 billion USD between 1980 and 2004 (Mittler, 2006; Suzuki et al., 2014). In 2009, low temperature resulted in approximately 158 billion yen of crop damage in Japan (Rahman, 2013). Additionally, early and late frost causes the damage of vegetable and fruits which is approximately 5 – 6 billion yen per year (Rahman, 2013).

Plant growth and low temperature

Low temperature affects the metabolic pathways and physiological development of plants. Cold stress is divided into non-freezing or chilling stress (above 0°C and below 15°C) and freezing stress (below 0°C) (Shi and Yang, 2014). However, in natural condition, temperature decreases gradually over time. Most of the temperate plants are capable of tolerating freezing stress after the exposure at non-freezing or chilling condition for a certain amount of time. This is known as cold acclimation (CA) (Thomashow, 1999). If plants are directly placed to freezing temperature without prior treatment or exposure at non-freezing temperature, they are referred as non-acclimated (NA) plants. During chilling stress and freezing stress conditions, plants go through diverse physiological and molecular changes. Chilling stress severely disrupts biochemical processes required for photosynthesis (Oliveira and Peñuelas, 2005), reactive oxygen species (ROS) scavenging (Rizhsky et al., 2004) and hormonal homeostasis (Shibasaki et al., 2009; Bielach et al., 2017). These disruptions lead to cell death and subsequently crop damage (Hong et al., 2017). On the other hand, freezing stress induces ice crystal formation in the extracellular regions. Due to ice formation, cells perceive dehydration and osmotic stress, which eventually cause membrane and tissue injury (Uemura et al., 1995). In contrast, cold acclimated plants initiate the physiological and biochemical modifications. Additionally, cold acclimated condition alters the expression patterns of cold responsive genes, proteins and metabolites (Miura and Furumoto, 2013). As a result, cold acclimated plants can survive during freezing temperature by accumulating osmolytes and anti-freezing proteins. Plants go through transcriptional and translational modification during the non-freezing temperature, which helps to modify membrane composition to withstand the freezing stress (Yamada et al., 2002).

Low temperature and plasma membrane

The phenotypic changes observed in the plant and organ level is actually the cumulative effect of individual cells and cell – cell communication (Eckardt, 2014). Understanding the cellular mechanism provides the insight about the overall growth dynamics. In the cellular level, plasma membrane acts as the primary sensor for temperature change. Analysis of various genomes suggested that 10% plasma membrane-localized proteins functions as transporters (Rai et al., 2012) and rest others are mostly involved in signal transduction.

Apart from providing transport facility, plasma membrane proteins help to perceive and respond to environmental stimuli (Yadeta et al., 2013). As a result, a direct and the earliest effect of an alteration of temperature on cells is the change in their membrane fluidity (Levitt, 1972). It has been demonstrated that low temperature reduces membrane fluidity and high temperature increases membrane fluidity (Mejía et al., 1995; Alonso et al., 1997). The change in membrane fluidity and permeability alters the interactions between plasma membrane and cell wall (Kazemi-Shahandashti and Maali-Amiri, 2018). Additionally, elevated level of the cytosolic Ca^{2+} concentrations is observed in every kinds of abiotic stresses (Wilkins et al., 2016). Interestingly, the increase in Ca^{2+} is moderated by membrane rigidification-activated mechano-sensitive or ligand-activated Ca^{2+} channels (Kazemi-Shahandashti and Maali-Amiri, 2018).

Cold stress modulates cellular response by altering both transcriptome (Hannah et al., 2005; Lee et al., 2005a) and protein expression profiles (Amme et al., 2006; Li et al., 2014) of *Arabidopsis thaliana*. It has been shown that the cold stress alters the expression of approximately 4%-20% genes in Arabidopsis (Hannah et al., 2005; Lee et al., 2005a). Similarly a range of proteins have also been shown to be affected by cold stress (Amme et al., 2006; Li et al., 2014). Cold stress is perceived by plasma membrane-localized proteins and subsequently transduce the signal inside the cell. Recent studies highlighted the role of membrane proteins in cold stress perception and regulation. For instance, it has been found that the phosphorylation of 14-3-3 proteins is conducted by the plasma membrane localized cold-responsive protein kinase 1 (CRPK1). The phosphorylated 14-3-3 proteins translocate from cytosol to nucleus and interact with CBFs proteins in order to attenuate the CBF signaling (Liu et al., 2017). In rice, plasma membrane-localized *COLD1* regulates G-protein signaling to activate the Ca^{2+} channel to confer chilling tolerance (Ma et al., 2015). In other study, it has been shown that cold stress inhibits the protein trafficking of plasma membrane-localized auxin efflux carrier PIN2 and consequently alters the auxin response to inhibit the root growth (Shibasaki et al., 2009). Altogether, plasma membrane-localized protein-mediated cold stress response and regulation is emerging from the current studies.

Membrane proteins are also involved in other abiotic stresses such as metal stress

Plants interact with soil through roots to take up nutrients and water and transport them to other parts of the plants to support photosynthesis, plant growth and development (Zelazny and Vert, 2014). Unfortunately, soil contains the combination of necessary and toxic metals. Hyper accumulation of necessary metals or minimal uptake of toxic metals is detrimental for plant growth (Grennan, 2009). Interestingly, it has been found that most of the dispensable toxic metals use transporters of chemically similar essential components. For example, As (V) uses phosphate transporters (Zhao et al., 2009), As (III) utilizes aquaporin-like water transporter (Ma et al., 2008; Kamiya et al., 2009), Cd is taken up by iron transporter IRT1 (Nakanishi et al., 2006) and cesium is take up by multiple known potassium transporters (Kobayashi et al., 2010; Nieves-Cordones et al., 2017; Rai et al., 2017).

Apart from using known transporters of indispensable nutrients, toxic metals exploit non-specific transporters, such as ABC transporters. One of the reasons is that among 200 families of transporters, ABC is the largest family (Rai et al., 2012). Additionally, ABC transporters are ubiquitous in both plant and animal kingdom and function in cellular detoxification processes. Supporting this idea, ABC transporters have been reported for As, Cd, Hg, Pd transport (Lee et al., 2005b; Kim et al., 2006; Kim et al., 2007; Song et al., 2010; Park et al., 2012).

One of the major contaminants of soil which has become the pressing issue in last few decades is cesium. Although the soil contains a very low amount of cesium, the nuclear power plant incidences, such as Chernobyl disaster at Soviet Union in 1986 and Fukushima (Japan) incidence during Tsunami in 2011, have released an alarming amount of radio cesium in the environment (Cooghtrey et al., 1983; Isaure et al., 2006). Two major radio cesium isotopes (^{134}Cs and ^{137}Cs) have longer half-lives, ranging from 2 years to 30 years, and these are capable to be incorporated into animal system due to their higher chemical similarity with potassium (White and Broadley, 2000; Kinoshita et al., 2011). As a result, understanding of cesium transport mechanism resulted in the identification of known potassium transporter till now (Kobayashi et al., 2010; Nieves‐Cordones et al., 2017; Rai et al., 2017). But, it is also intriguing that potassium transporters are not only source for cesium transport in plants (Zhu and Smolders, 2000), which suggest the existence of potassium-independent cesium transport system. At the same time, the microarray data of cesium intoxicated plants showed the up-regulation of a group of ABC

transporters compared with potassium starved plants (Hampton et al., 2004). Altogether, it suggests that ABC transporters may act as potassium-independent cesium transporters.

Research objectives

Although the plasma membrane proteins play crucial role in abiotic stress regulation, their precise functions in both cold stress and cesium stress are still unknown. In this thesis work, I have focused on deciphering the role of membrane proteins and the objective is divided into two parts.

(1) The role of plasma membrane proteins in regulating cold stress response (Chapter 2).
(2) Identification of plasma membrane-localized potassium-independent cesium transporters (Chapter 3).

Chapter 2

Cold stress response in Arabidopsis thaliana is mediated by GNOM ARF-GEF

2.1. Introduction

Intracellular protein trafficking plays vital roles in regulating growth and development of model organisms ranging from unicellular (*Saccharomyces cerevisiae*) to multicellular (*Drosophila melanogaster*, *Caenorhabditis elegans*) eukaryotes and plants (Smith, 1999; Kandachar and Roegiers, 2012; Feyder et al., 2015; Pal et al., 2017). Mutants defective in internalization of proteins, vacuolar protein sorting and vacuolar morphogenesis showed multiple developmental abnormalities in *Saccharomyces cerevisiae* (Wiederkehr et al., 2001). In *Schizosaccharomyces pombe* , deletion of particular SNARE protein results in the absence of normal vacuoles (Hosomi et al., 2011). Perturbation of intracellular protein trafficking affects eye and wing development of *Drosophila melanogaster* (Stewart, 2002). Defective endocytic trafficking mutants alter cytoskeletal localization, oocyte growth and polar localization of proteins in *Caenorhabditis elegans* (Pal et al., 2017).

Similarly, alteration of intracellular trafficking disturbs myriad indispensable developmental processes in the model plant *Arabidopsis thaliana,* including growth and development in biotic and abiotic stresses. As for biotic stresses, ENDOSOMAL RETICULUM ARRESTED PEN3 (EAP3) BTB/POZ-domain dependent membrane trafficking is involved in conferring resistance to root-penetrating fungus (Mao et al., 2017). Weak mutant of GNOM, $gnom^{B/E}$, shows a delay in papilla formation and reduced penetration resistance to barley powdery mildew fungus (Nielsen et al., 2012). *RabA4c* overexpression causes complete resistance to the virulent powdery mildew *Golovinomyces cichoracearum* due to enhanced callose deposition at the early time point of infection (Ellinger et al., 2014). VPS9a is required for both pre-and post-invasive immunity against a non-adaptive powdery mildew fungus (*Blumeria graminis* f. sp *hordei*) in *Arabidopsis thaliana* (Nielsen et al., 2017). For abiotic stresses, RabA4c plays vital role in glycine betaine-mediated root growth recovery after chilling stress (Einset et al., 2007). GNOM-mediated trafficking is an absolute requirement in hydrotropic response (Miyazawa et al., 2009). RabF1 or plant specific Rab5 GTPase ARA6 is involved in salt stress (Ebine et al., 2011; Yin et al., 2017). In case of temperature stress, SORTING NEXIN 1 (SNX1) dependent endosomal trafficking regulates intracellular auxin

homeostasis during high temperature stress (Hanzawa et al., 2013). In contrast, cold stress primarily inhibits shootward auxin transport by blocking the intracellular trafficking of the auxin efflux carriers (Shibasaki et al., 2009; Shibasaki and Rahman, 2013).

Evidence of endosomal trafficking regulating temperature stress in plant is reminiscent of studies from other model system, most prominently from yeast. P-type ATPase Drs2p is a membrane localized protein, which interacts directly and functionally with ARF GEF Gea2p in *Saccharomyces cerevisiae*. Single mutant *drs2Δ* cells are viable, but show a cold-sensitive phenotype. Moreover, double mutant *drs2Δgea2Δ* strain shows severe cold-sensitive growth defect. Gea2^{V698G} mutant fails to interact with Drs2p and consequently becomes temperature and BFA sensitive (Chantalat et al., 2004). These genetic analyses pin-pointed the importance of GTPase and BFA (Brefeldin A)-sensitive trafficking pathways in regulating cold response in yeast. In ARF- GEF, the central catalytic domain SEC7 domain plays pivotal role in GTPase activity, BFA-sensitive response and thermo-sensitivity. Yeast cells of *sec7-4*, containing mutation within SEC7 domain, show reduced ARF-GEF activity and temperature sensitivity. In contrast, *sec7-1*, containing mutation outside of SEC7 domain, does not show temperature sensitive response (Jones et al., 1999). Interestingly, plant counterpart of SEC7 domain containing GNOM is able to rescue temperature sensitive yeast mutant *gea1-19 gea2Δ* (Steinmann et al., 1999). These findings suggest that SEC7-mediated trafficking plays an important role for temperature sensitivity. However, in plant, the role of GNOM ARF-GEF in regulating temperature response remains obscure.

Previously it was demonstrated that plants responses to both high and low temperatures are directly linked to intracellular trafficking of auxin efflux carriers and auxin homeostasis (Gray et al., 1998; Koini et al., 2009; Shibasaki et al., 2009; Sakata et al., 2010; Franklin et al., 2011; Sun et al., 2012; Hanzawa et al., 2013; Wang et al., 2016). This along with studies of protein trafficking and temperature response in yeast prompted us to hypothesize that intracellular protein trafficking components may play important roles in regulating plant cold temperature response too. By screening a large number of protein trafficking mutants, I identified GNOM, a SEC7 containing ARF-GEF, as an important regulator of cold response in plant. Partial loss of function transheterozygote GNOM mutant *gnom* $^{B4049/emb30-1}$ (*gnom*$^{B/E}$), in which two mutations in SEC7 domain partially complement the nonfunctional domains of each

other (Geldner et al., 2004), shows hypersensitive response to both short and long term cold (4°C) stresses. On the other hand, the engineered BFA resistant transgenic GNOM line, which has a point mutation at 696 position (Methionine to Leucine mutation M→L) (Geldner et al., 2003) of SEC7 domain shows strong resistance to both short and long term cold stresses. Cold stress selectively and transiently inhibits GNOM expression. Overexpression and altered cellular localization of GNOM were found to be directly linked to confer cold resistance in Arabidopsis. Taken together, these results identify GNOM as a unique regulator of cold stress response and pave the pathway to engineer cold resistant plant.

2.2 Materials and Methods

2.2.1. Plant materials

All lines are in the Columbia background of *Arabidopsis thaliana*, except EGFP-LTI6b (C24 background) (Kurup et al., 2005). *ara6-1*, *ara7*, *rha1-1* (Ebine et al., 2011), *vps9a-2* (Goh et al., 2007), *erex1-2*, *erex2-1*, *erex3-2* (Sakurai et al., 2016), *syp41*, *syp42*, *syp43* (Uemura et al., 2012), *vam3-1*/*syp22-1*(Ebine et al., 2008), *vamp727* (Ebine et al., 2008), *pen1-1*/*syp121-1* (Collins et al., 2003), *puf2*, *ara6ara7*, *ara6rha1*, *ara7syp22*, *ara6pen1*, *ara6vamp727*, *erex1-2erex3-2*, *erex2-1erex3-2*, *puf2vam3*, *ara6pen1vamp727* were provided by Takashi Ueda (National Institute of Basic Biology, Aichi, Japan). *snx1-1* and *snx1-2* were described earlier (Jaillais et al., 2006), *gnom*$^{B/E}$(Geldner et al., 2004), *miz2* (Miyazawa et al., 2009), *gnl1-1* (Teh and Moore, 2007) were provided by Nobuharu Fujii (Tohoku University, Japan). *gnl1-2* ST-mRFP and *gnl1-3* (Teh and Moore, 2007) were obtained from Satoshi Naramoto (Tohoku University, Japan). BFA resistant line (Geldner et al., 2003) was provided by Wu Shuang (Fujian Agriculture and Forestry University, China). *fwr* (Okumura et al., 2013) was a gift from Hidehiro Fukaki (Kobe University, Japan).

pAtCCS52A1::AtCCS52A1::GFP (Vanstraelen et al., 2009), *pAtPCNA1:: AtPCNA1-sGFP* (Yokoyama et al., 2016), GNOM-GFP (Naramoto et al., 2014), PIN2-GFP (Xu and Scheres, 2005), and EGFP-LTI6b (Kurup et al., 2005) were provided by Peter Mergaert (French National Center for Scientific Research, France), Sachihiro Matsunaga (Tokyo University of Science, Japan), Satoshi Naramoto (Tohoku University, Japan), Ben Scheres (University of Utrecht, The Netherlands), and Gloria Muday (Wake Forest University, Winston-Salem, NC), respectively. G2-M phase specific cell cycle marker pCYCB1; 1::GUS was described earlier (Colón‐Carmona et al., 1999).

BFA res. GNOM-GFP, pCYCB1; 1::GUS , IAA2-GUS, DII Venus, and PIN2-GFP transgenic lines were generated by crossing, and F3 homozygous lines were used for microscopy observations. At least three independent crossed-lines were tested.

2.2.2. Growth conditions

Surface-sterilized seeds were placed on modified Hoagland medium (Baskin and Wilson, 1997) containing 1% (w/v) sucrose and 1% (w/v) agar (Difco Bacto agar; BD Laboratories).

Two days after stratification at 4°C in the dark, plates were transferred to a growth chamber (NK System; LH-70CCFL-CT) at 23°C under continuous white light at an irradiance of ~80 µmolm^{-2}s^{-1}. The seedlings were grown vertically for 5d.

For the root growth study, 5-d-old seedlings were transferred to new Hoagland plates and kept at 23°C (NK System; LH-70CCFL-CT) and 4°C growth chamber (NK System; LH-1-120.S) for 24h treatment under continuous white light at an irradiance of ~80 µmolm^{-2}s^{-1}.

For root growth recovery study, 5-d-old seedlings were transferred to 23°C (NK System; LH-70CCFL-CT) and 4°C growth chamber (NK System; LH-1-120.S) for 12 h treatment under continuous white light at an irradiance of ~80 µmolm^{-2}s^{-1}. For recovery, 12 h treated seedlings were transferred to 23°C growth chamber (NK System; LH-70CCFL-CT) and root length was measured at 6 h, 12 h and 24 h time point.

All phenotypic images were taken by Canon Power Shot A640 (Canon, Japan) without flash and using micro focus function. Root lengths were measured using ImageJ (https://imagej.nih.gov/ij/) software.

For soil grown plants, 10-d-old seedlings from Hoagland plates were transferred to soil and grown at 4°C growth chamber (NK System; LH-1-120.S) for 7 weeks under continuous white light at an irradiance of ~80 µmolm^{-2}s^{-1}.

2.2.3. Chemicals

BFA was purchased from Sigma-Aldrich Chemical Co. FM 4-64 was purchased from Invitrogen. Cell clearing solution (Visikol®) was purchased from Visikol (https://visikol.com/). All other chemicals were purchased from Wako Pure Chemical Industries, Japan.

2.2.4. GUS staining

GUS staining was performed based on previously described method (Okamoto et al., 2008). In brief, 5-d-old seedlings were transferred to a new agar plate and grown vertically at 4°C or 23°C under continuous white light. After 24 h, seedlings were transferred to GUS staining buffer (100 mM sodium phosphate, pH 7.0, 10 mM EDTA, 0.5 mM potassium ferricyanide, 0.5 mM potassium ferrocyanide, and 0.1% Triton X-100) containing 1 mM X-gluc and incubated at 37°C in the dark for 1 h. For cell clearing, Visikol was used as per manufacturer's instruction

(https://visikol.com/). The roots were imaged with a light microscope (Nikon Diaphot) equipped with a digital camera control unit (Digital Sight [DS-L2]; Nikon).

2.2.5. Live-cell imaging

To image GFP, the transferred seedlings were incubated at 23°C or 4°C under continuous light for various time lengths as mentioned. For BFA treatment, 5-d old control or cold-stressed seedlings were incubated in liquid Hoagland medium containing 20 μM BFA for 30 min. For FM4-64 staining, 2 μM concentration was used in liquid Hoagland medium and incubated for 5 minutes. After mounting on a large cover glass, the roots were imaged using a Nikon laser scanning microscope (Eclipse Ti equipped with Nikon C2 Si laser scanning unit) with a X20 objective. For the sub-cellular localization study (Figure 20) and PIN2 endocytosis observation (Figure 21), X40 water immersion objective was used. Same confocal settings were used for each group of experiments. To minimize the effect of room temperature during imaging, the imaging of cold-treated seedlings was completed within 30 min. Fluorescence intensities were measured by drawing a region of interest (ROI) in the images obtained from live-cell imaging using Image J software. For sub-cellular localization study, ROI is drawn around the endosome and plasma membrane region.

2.2.6. Gene Expression Analysis

5-d-old vertically grown *Arabidopsis thaliana* seedlings were transferred to agar plate and incubated at 23°C or 4°C for 12 h. After cold stress treatment, the plants were kept at 23°C for 6h for recovery). RNA was extracted from the root tissue using RNA Extraction Kit (APRO Science, Japan) with on-column DNA digestion to remove residual genomic DNA using RNase-free DNase according to manufacturer's protocol. Extracted RNA was tested for quality and quantity. Each RNA concentration was normalized with RNase free water. 500 ng RNA was used to synthesize cDNA using Rever Tra Ace qPCR RT master mix (Toyobo, Japan). Quantitative PCR reactions were performed using the Takara TP-850 thermal cycler (Takara Bio, Japan) and SsoAdvanced™ Universal SYBR® Green Supermix (BIO-RAD, USA).The reaction was performed as per manufacturer's instruction. For quantification of GNOM expression, we used the 2-ΔΔCT (cycle threshold) method with a normalization to the ef1α expression (Hanzawa et al., 2013). Data were obtained from three biological replicates.

2.2.7. Western blotting

Total protein extracts were obtained from the 7-d-old whole seedlings. The whole seedlings were homogenized in SDS-PAGE sample buffer. Total 50 µg protein was resolved by SDS-PAGE, transferred to Immobilon-P PVDF membrane, and probed with antibodies against anti-Living Colors-GFP (1:1000) (Clontech) and anti-actin (1:2500) (C4; Chemicon). Proteins were detected with a luminoimage analyzer (AE-6972C; ATTO) using Amersham ECL prime western blotting detection reagent kit (GE Healthcare), as described previously (Rahman et al., 2010). Band intensity was quantified using ImageJ (https://imagej.nih.gov/ij/) software.

2.2.8. Electrolyte leakage assay

Freezing injury of leaves was assayed by electrolyte leakage based on a modified version of previously published method (Uemura et al., 1995). In brief, 14-d-old 4 leaves were placed in a test tube (10 X 100 mm) with 100 µL Milli-Q water, and the samples were then cooled to -2°C. After 15 min, ice formation was facilitated by introducing a small piece of ice into the test tubes. After an additional 2 h incubation at -2°C, the samples were cooled in decrements of 1°C at 15-min intervals and took out at specific temperatures such as -4°C, -5°C, -6°C, and -8°C. Samples were kept in ice for addition 30 min, and then thawed overnight at 4°C. Next day, samples were incubated with 4 mL of distilled water and shaken at room temperature for 2 h at 160 rpm in dark. 135 µL solution was taken from each sample and electrolyte leakage was measured with a compact conductivity meter (LAQUAtwin b-771, HORIBA Scientific). Next, samples were treated at 95°C for 20 min, shaken at room temperature for 2 h at 160 rpm in dark and subjected to electrolyte leakage measurement. Non-freezing and liquid nitrogen indicate without freezing stress and liquid nitrogen-treated samples, respectively. Electrolyte leakage was calculated for respective leaf area and expressed in percentage scale.

2.2.9. Statistical analysis

Results are expressed as the means ± SE from appropriate number of experiments as described in the figure legends. A two-tailed Students t test was used to analyze statistical significance.

2.3. Results

2.3.1. Effect of cold stress on *Arabidopsis* root growth

Exposure of plant at 4°C results in severe stresses, which is unique in nature. Previous work showed that 12 h 4°C treatment severely affected the root's ability to grow during recovery at 23°C (Shibasaki et al., 2009). To understand the root developmental mechanism under severe cold stress, we incubated Arabidopsis seedlings at 4°C for 24 h. This treatment results in only 10% root growth compared with the growth at 23°C (Figure 1A and 1B). Since the root growth consists of both cell elongation and cell division, we next investigated whether 4°C affects both the processes by measuring cell length, and analyzing the expression of cell cycle markers. Measurement of mature cortical cell length (to avoid the variability in cell length) (Rahman et al., 2007) in 4°C treated roots revealed a surprising fact that cold stress does not inhibit the cell elongation process. The average cell length of mature root cortical cells was found to be similar in 4°C and 23°C treated plants (Figure 2A and 3). This surprising finding was confirmed by observing and measuring cell lengths in GFP marker lines LTI6b and PIN2-GFP (Figure 3B-3D). The drastic reduction of root growth at 4°C and the inability of the cold stress to inhibit the cell elongation process indicate that the cold stress solely affects the cell division process. Consistently, analysis of G2-M phase specific cell cycle marker, pCYCB1; 1::GUS (Colón-Carmona et al., 1999), revealed extremely reduced GUS-staining in 4°C treated seedlings compared with control plants grown at 23°C, confirming lower mitotic divisional events at severe low temperature stress (Figure 2B). Inhibition of G2-M phase marker indicates the possibility of the interruption of an earlier stage of cell cycle progression. To further clarify which stages of cell cycle are affected by 4°C treatment, we used a recently developed cell cycle marker PROLIFERATING CELL NUCLEAR ANTIGEN (PCNA) (*pAtPCNA1:: AtPCNA1-sGFP* (Yokoyama et al., 2016). Distinct GFP signals of this marker facilitate the recognition of different phases of cell cycle. Typically, the whole GFP signal represents the cells that are in G1/G2 phase, dotted signal represents the cells in early S and speckled signal represents the cells in late S phase (Figure 4) (Yokoyama et al., 2016). Comparative analyses of the cellular GFP signals in the meristem of cold treated and control roots revealed more cells in G1/G2 phase and less number of cells in S phase in 4°C treated seedlings (Figure 5, inset). These results, for the first time, provide a clear picture on how the cold stress regulates the cell cycle progression.

The reduction in mitotic cell division produces less number of new cells which affects the meristem size. Consistent with the idea, using elongation zone specific/endoreduplication onset marker, *pAtCCS52A1::AtCCS52A1::GFP* (Vanstraelen et al., 2009), I also found that cold stress treated roots show approximately 30% reduction in meristem size (Figure 6A and 6B). Taken together, these results clarify the mechanisms how the cold stress affects cell division, meristem size and the total root growth.

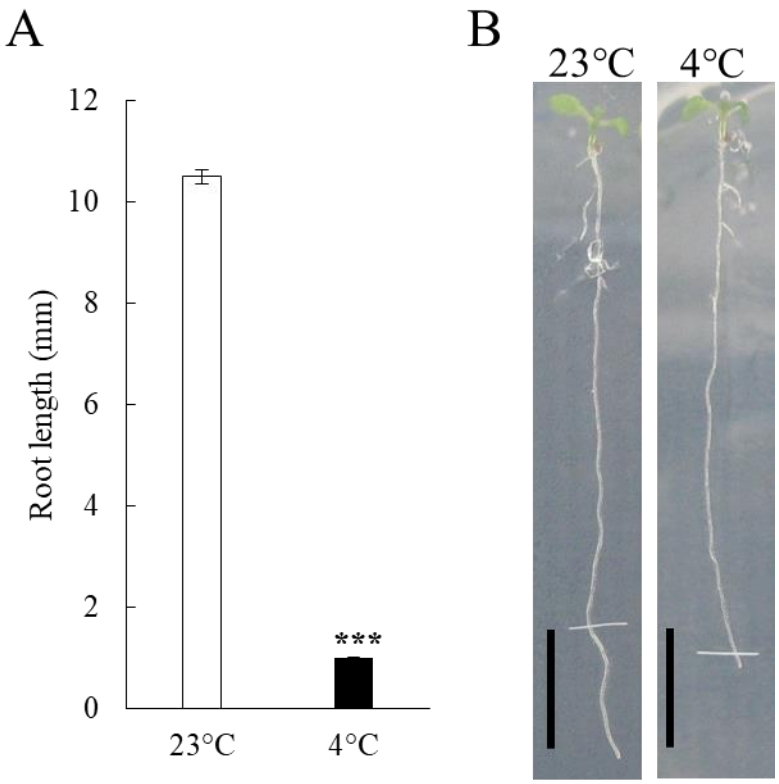

Figure 1. Cold stress inhibits primary root elongation of *Arabidopsis thaliana*

Five-day-old light grown wild-type (Col-0) seedlings were transferred to new agar plates and incubated at 23°C and 4°C for 24h.

(A) Cold-induced inhibition of primary root growth elongation in wild-type (Col-0) after 24h.

(B) Root phenotype of wild-type (Col-0) after grown at 23°C and 4°C for 24h. Scale bar =10mm.

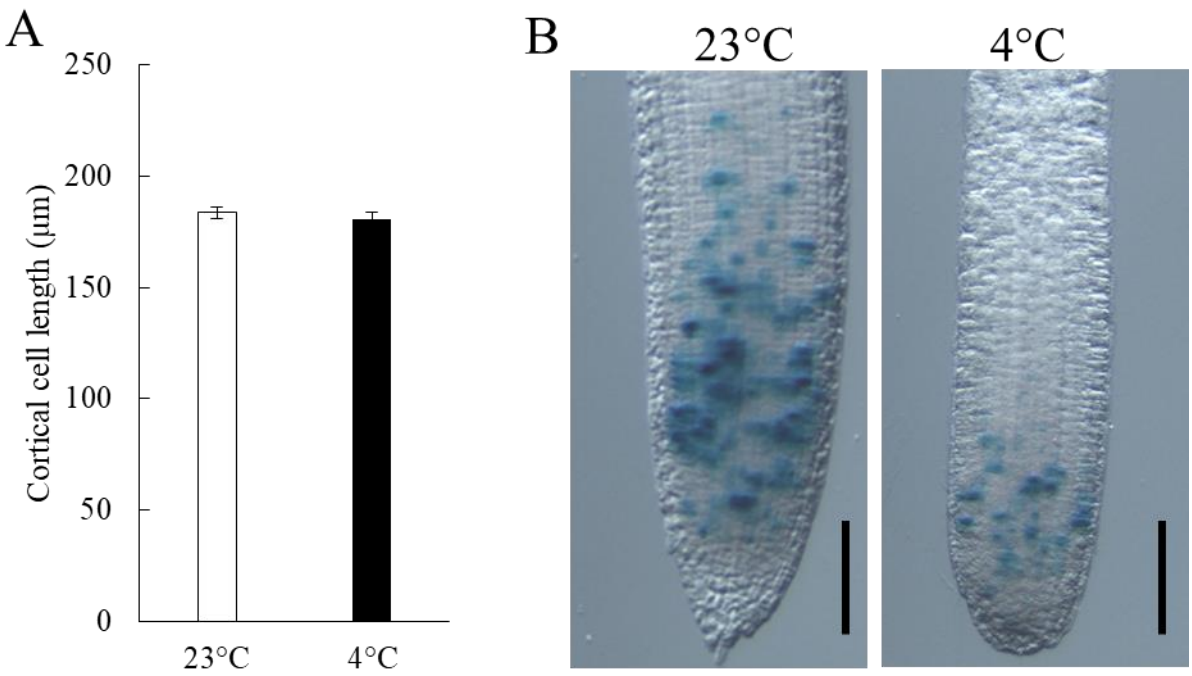

Figure 2. Cold stress inhibits cell division rather than cell elongation in *Arabidopsis thaliana* root

(A) Cortical cell length of wild-type (Col-0) after grown for 24h at 23°C and 4°C.

(B) Effect of cold (4°C) on expression of CycB1;1-Gus in the primary root tip. Images are representative of three independent experiments with 5 seedlings observed per experiment. Scale bar = 100 μm.

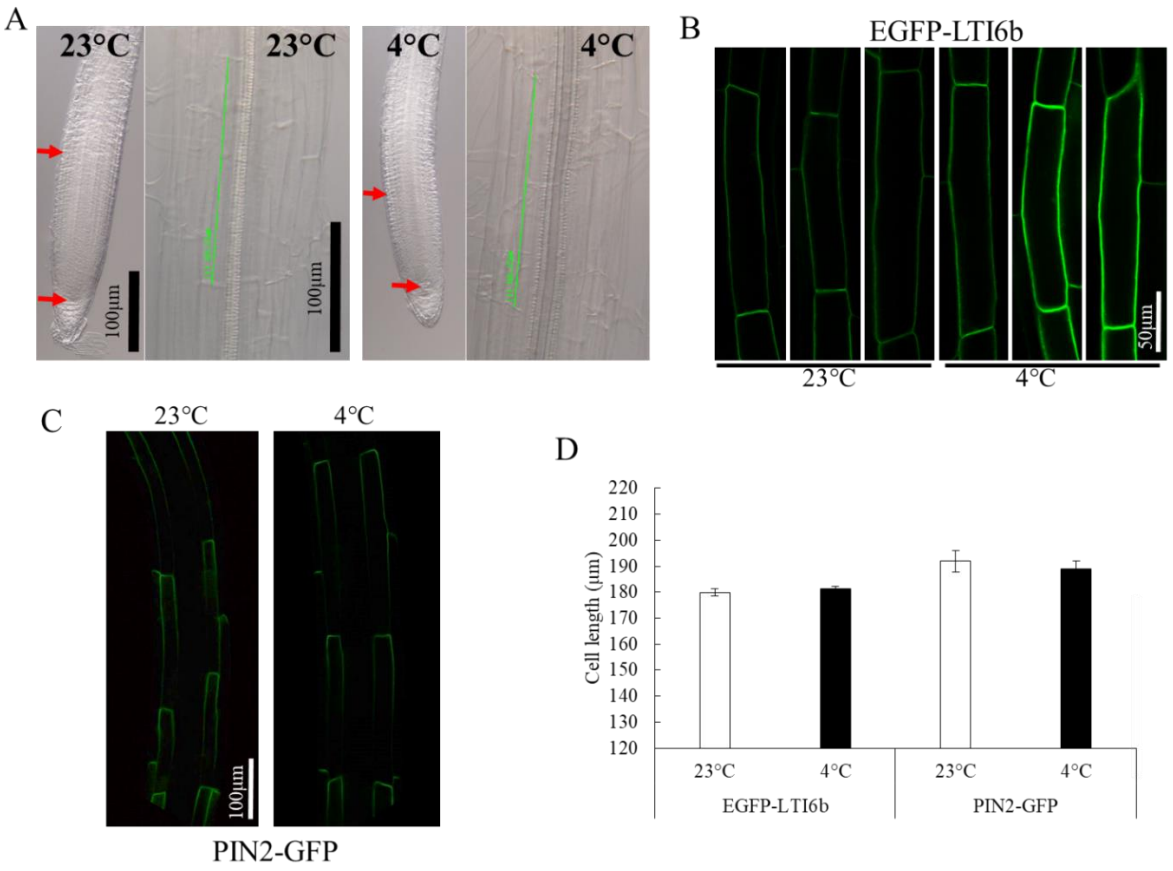

Figure 3. Cold stress the cell meristem size instead of cell length

Five-day-old light grown wild-type (Col-0) seedlings were transferred to new agar plates and incubated at 23°C and 4°C for 24h.

(A) represents seedlings grown at 23°C and 4°C. Red arrows indicate the region from QC to the first onset of endoreduplication. Cortical cell length from maturation zone at 23°C and 4°C was demonstrated through green line. The images are representative of three independent experiments with 5 seedlings observed per experiment. Scale bars are embedded in the images.

(B) Five-day-old light grown EGFP-LTI6b seedlings were transferred to new agar plates and incubated at 23°C and 4°C for 24h. The images are representative of three independent experiments with 5 seedling observed per experiment. Scale bars are embedded in the images.

(C) Five-day-old light grown PIN2-GFP seedlings were transferred to new agar plates and incubated at 23°C and 4°C for 24h. The images are representative of three independent experiments with 5 seedling observed per experiment. Scale bars are embedded in the images.

(D) Quantification of cell length from figure (B) and (C). Vertical bars in the graph indicate ±SE.

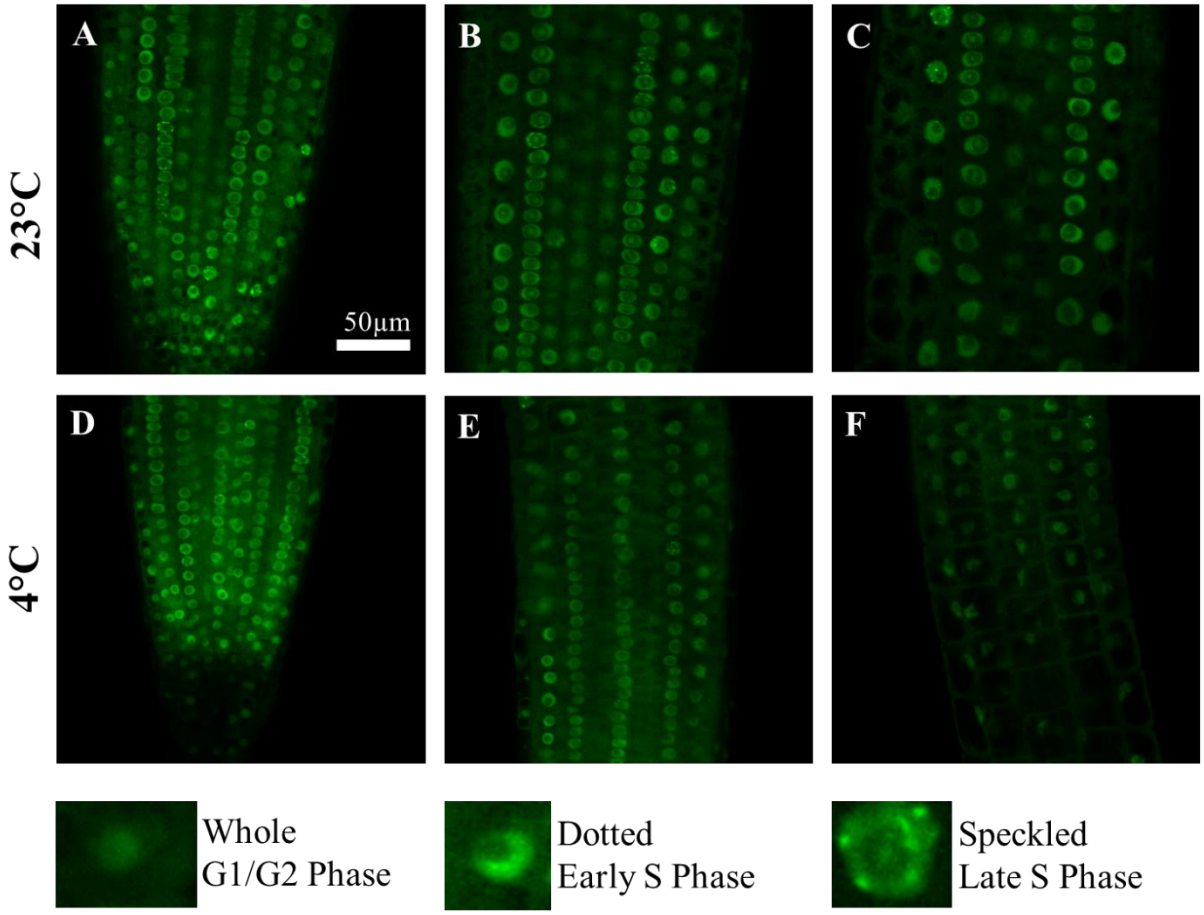

Figure 4. Cold stress targets gap phase (G1/G2) in the cell cycle

Five-day-old light grown *pAtPCNA1::AtPCNA1-sGFP* seedlings were transferred to new agar plates and incubated at 23°C and 4°C for 24h.

(A), (B), (C) represent seedlings at 23°C and (D), (E), (F) represents seedlings at 4°C. These data represents more than 100 individual cells of single root from meristematic, transition, and elongation zones. The images are representative of three independent experiments with 5 seedlings observed per experiment. Scale bars = 50µm.

Bottom row represents characteristic patterns for specific cell cycle phase. Whole, dotted, and speckled indicate G1/G2, early S and late S phase, respectively.

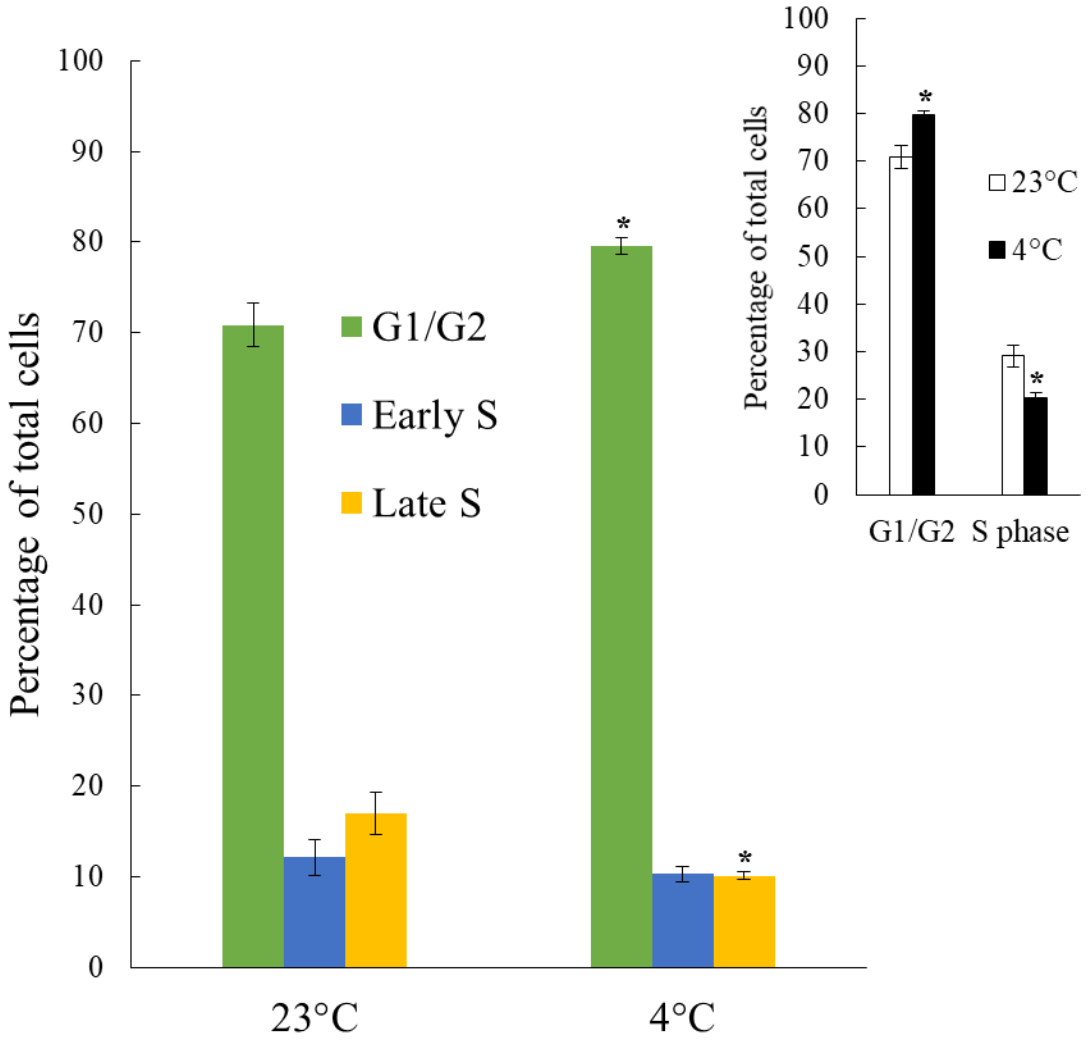

Figure 5. Cold stress affects differential stages of cell cycle

5-day-old grown *pAtPCNA1::AtPCNA1-sGFP* cell cycle marker was subjected to cold stress at 4°C for 24 h and cell cycle progression was compared with the plants grown at 23°C. Data are average of more than 100 individual cells from meristematic, transition, elongation zone obtained from three independent experiments with at least 5 seedlings observed per experiment. Inset: Percentage of cells in G1/G2 and S (early + late) phase at 23°C and 4°C.

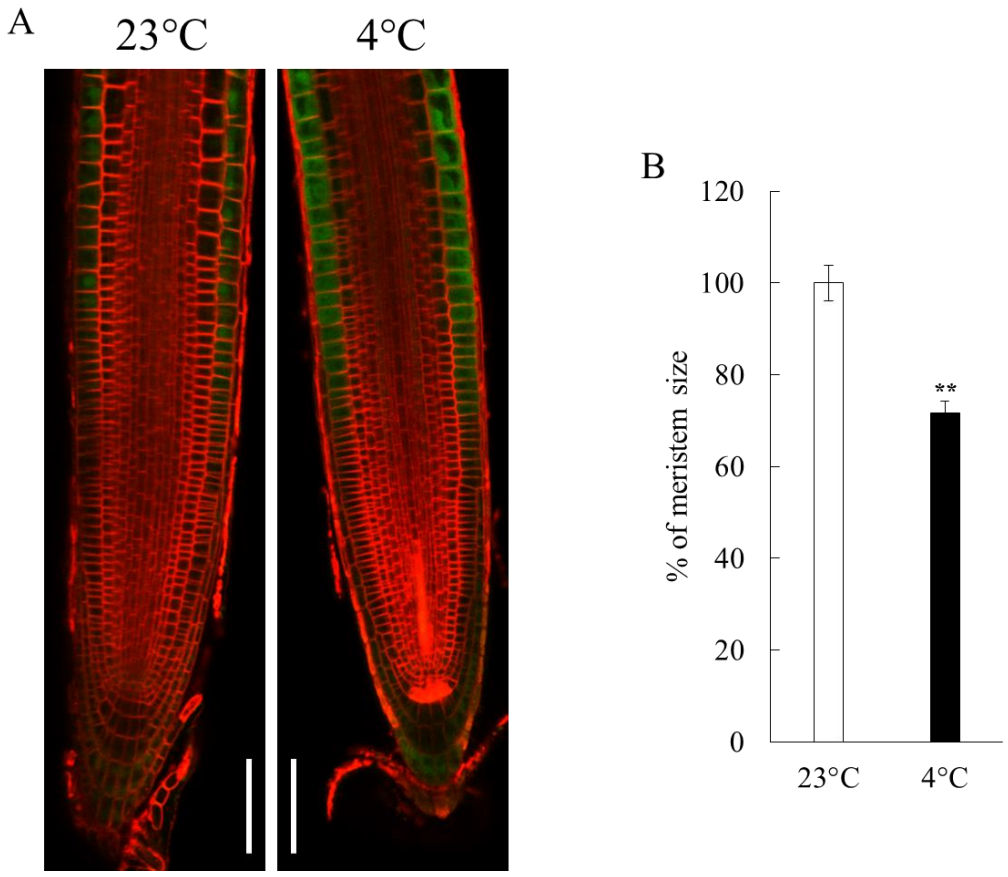

Figure 6. Cold stress affects meristem size negatively

(A) Transition zone marker *pAtCCS52A1::AtCCS52A1::GFP* was subjected to cold stress at 4°C for 24h and stained with FM4-64. Images are representative of three independent biological experiments with 5 seedlings observed per experiment. Scale bar = 50µm.

(B) Effect of cold stress on meristem length. Quantitative data obtained from experiment A.

Asterisks represent the statistical significance between the means for each treatment. ***P < 0.001. Vertical bars in the graph represent mean ±SE.

2.3.2. Screening of endocytic trafficking mutants identified ARF-GEF protein, GNOM as a potential regulator of cold stress

Earlier it was demonstrated that one of the major mechanisms of cold stress-induced inhibition of root growth is linked to the altered endosomal trafficking of a subset of intracellular proteins that include auxin efflux carrier PIN2 and PIN3 (Shibasaki et al., 2009; Rahman, 2013; Shibasaki and Rahman, 2013). However, it remains obscure which endocytic pathway; early, recycling or late endosomal is primarily targeted by cold stress. To elucidate the target, 22 available single mutants, and 9 double and triple mutants (for reducing the possibility of redundant function of homologous proteins) from three trafficking pathways were screened for cold stress response in root (Figure 8). To this end, we used the root growth recovery response assay after cold stress as described earlier (Shibasaki et al., 2009). Arabidopsis seedlings placed at 23°C after 12h 4°C treatment show a characteristic root growth recovery response. Typically, 50% root growth is recovered at 6 h followed by 65% and 75% recovery at 12 h and 24 h respectively (Figure 7). Screening of mutants in different endocytic pathways (Figure 8A) for root growth recovery revealed few candidates, such as *gnom* $^{B/E}$, *vam3*, *snx1-1*, *snx1-2* with altered recovery response at 6 h time point (Figure 8 and 9). However, in longer recovery assay, except *gnom* $^{B/E}$, all other mutants showed wild-type like recovery response (Figure 8). Hence, we focused on GNOM for further experiments.

GNOM encodes Guanine nucleotide Exchange Factors for ADP Ribosylation Factor (ARF-GEF) (Steinmann et al., 1999), and is required both for correct patterning of apical-basal pattern formation of early embryo and root formation (Mayer et al., 1993). GNOM protein consists of 6 domains: DCB (Dimerization and Cyclophilin Binding domain), HUS (Homology Upstream of SEC7 domain), SEC7 (Secretory7- Catalytic domain of GEF), and HDS1-3 (Homology Downstream of SEC7 domains 1-3) (Moriwaki et al., 2014). Dimerization of GNOM is regulated by DCB-DCB interaction, a heterotypic interaction between the DCB domain and the remainder of the protein, while the GEF catalytic activity on the membrane is regulated by the conserved SEC7 domain (Steinmann et al., 1999; Anders et al., 2008). Mutation in SEC7 domain results in strong phenotype characterized by disordered vascular system, defective establishment of the embryonic axis, loss of root meristem and fused cotyledons (Mayer et al.,

1993), while the mutations in other domains result in relatively mild phenotypes. For instance, *fwr*, which has a mutation in HDS domain, shows a slightly reduced root growth and fewer lateral root phenotypes (Okumura et al., 2013). Similarly, *miz2* which has a mutation between HDS1 and HDS2 domains shows no apparent growth phenotype except altered hydrotropic response (Miyazawa et al., 2009). Since $gnom^{B/E}$ mutations reside in SEC7 domain, and shows slower root growth recovery response, I screened other available alleles of *gnom*, containing mutations in other domains, to confirm whether the altered cold stress response is linked to the domain specific function. In addition, I also investigated the roles of GNOM like (GNL) proteins, which have high homology to GNOM (Richter et al., 2007). The root growth recovery screening results revealed that only $gnom^{B/E}$ shows slower recovery response after cold stress (Figure 9). Taken together, these results suggest that GNOM, possibly the SEC7 domain of GNOM plays an important role in regulating plant cold stress response. To validate the functional role of GNOM in cold stress regulation, complemented GNOM (*pGNOM::GNOM-GFP*) was subjected to cold stress recovery. The wild-type like response of *pGNOM::GNOM-GFP* (for convenience, mentioned as GNOM-GFP in the later part) confirms that GNOM specifically regulates cold stress response (Figure 10 and 11).

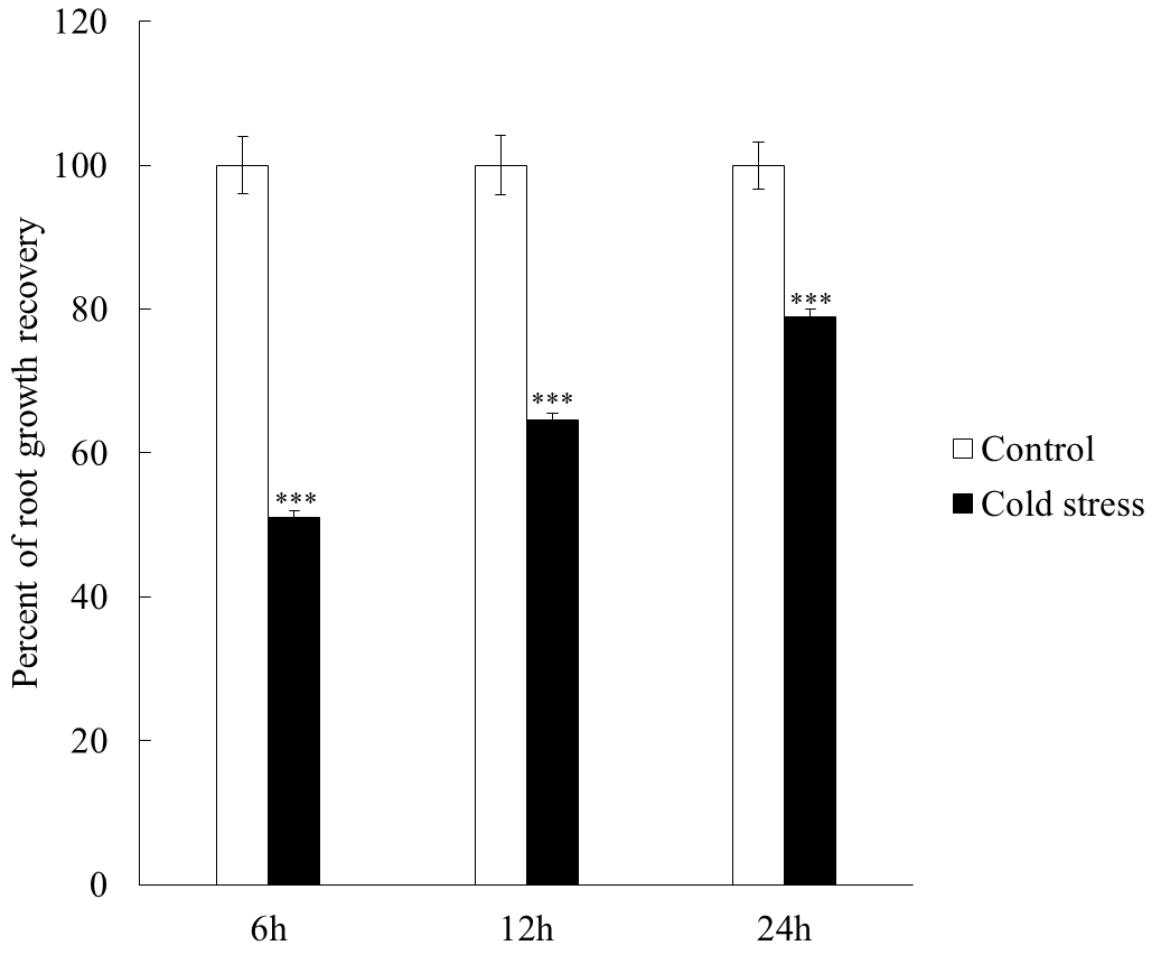

Figure 7. Root growth recovery of wild-type (Col-0)

Five-day-old light grown wild-type (Col-0) seedlings were transferred to new agar plates and incubated at 23°C and 4°C for 12h. After the treatment, root growth was measured for 6h, 12h and 24h at 23°C.

Asterisks represent the statistical significance between the means for each treatment. ***P < 0.001. Vertical bars in the graph indicate ±SE.

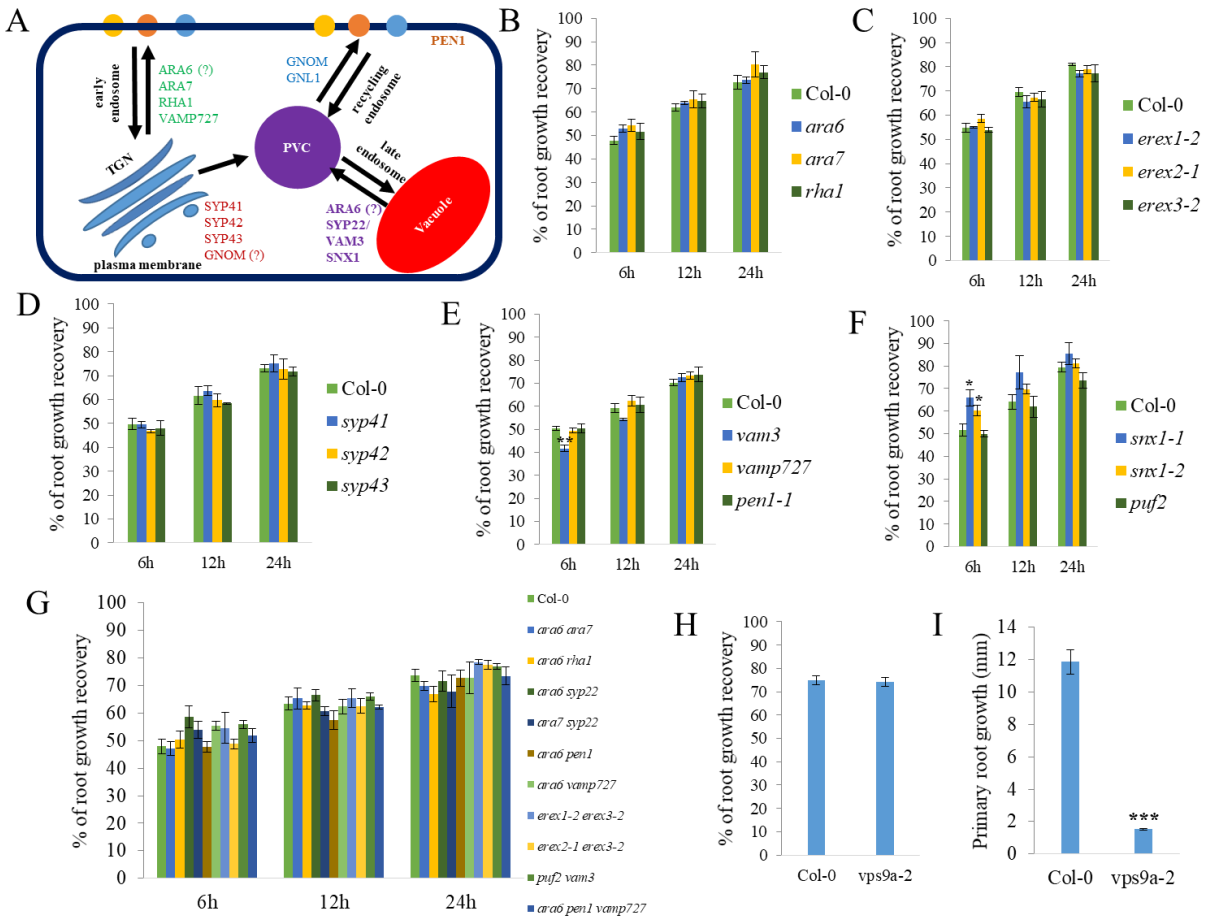

Figure 8. Root growth recovery of mutants of endosomal trafficking pathways in cold stress screening

(A) Overview of endosomal trafficking pathway and localization of characteristic proteins.

Five-day-old light grown wild-type (Col-0) and mutant seedlings were transferred to new agar plates and incubated at 23°C and 4°C for 12h. After the treatment, root growth was measured for 6h, 12h and 24h at 23°C.

Percentage of root growth recovery of Col-0 with *ara6-1*, *ara7*, *rha1-1* (B); *erex1-2*, *erex2-1*, *erex3-2* (C); *syp41*, *syp42*, *syp43* (D); *vam3*, *vamp727*, *pen1-1* (E); *snx1-1*, *snx1-2*, *puf2* (F); *ara6 ara7*, *ara6 rha1*, *ara6 syp22*, *ara7 syp22*, *ara6 pen1*, *ara6 vamp727*, *erex1-2 erex3-2*, *erex2-1 erex3-2*, *puf2 vam3*, *ara6 pen1 vamp727* (G) in 6h, 12h and 24h at 23°C. Percent of root growth recovery (H) and primary root growth (I) of Col-0 and *vps9a-2* in 24h.

*P < 0.05, **P < 0.01 and ***P < 0.001. Vertical bars in the graph indicate ±SE.

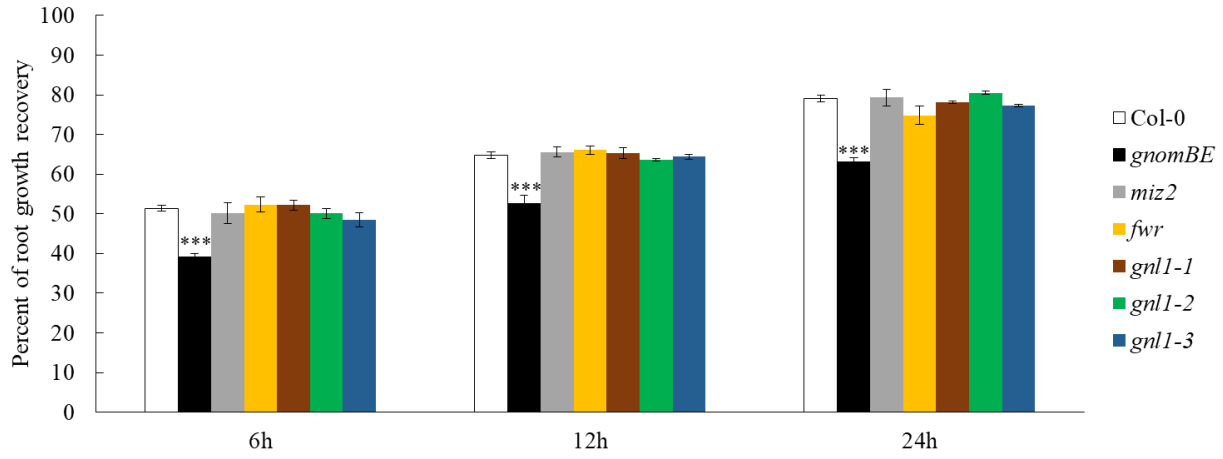

Figure 9. Root elongation response of various GNOM lines to cold stress

Five-day-old light grown wild-type (Col-0) and mutant seedlings were transferred to new agar plates and incubated at 23°C and 4°C for 12h. After the treatment, root growth was measured for 6h, 12h and 24h at 23°C.

Primary root elongation recovery at 23°C for 6h, 12h and 24h after incubation at 23°C and 4°C for 12h in wild-type, *gnom* mutants (*gnom*$^{B/E}$, *miz2*, *fwr*) and *gnl1* mutants (*gnl1-1*, *gnl1-2*, *gnl1-3*).

Asterisks represent the statistical significance between the means for each treatment. ***P < 0.001. Vertical bars in the graph indicate ±SE.

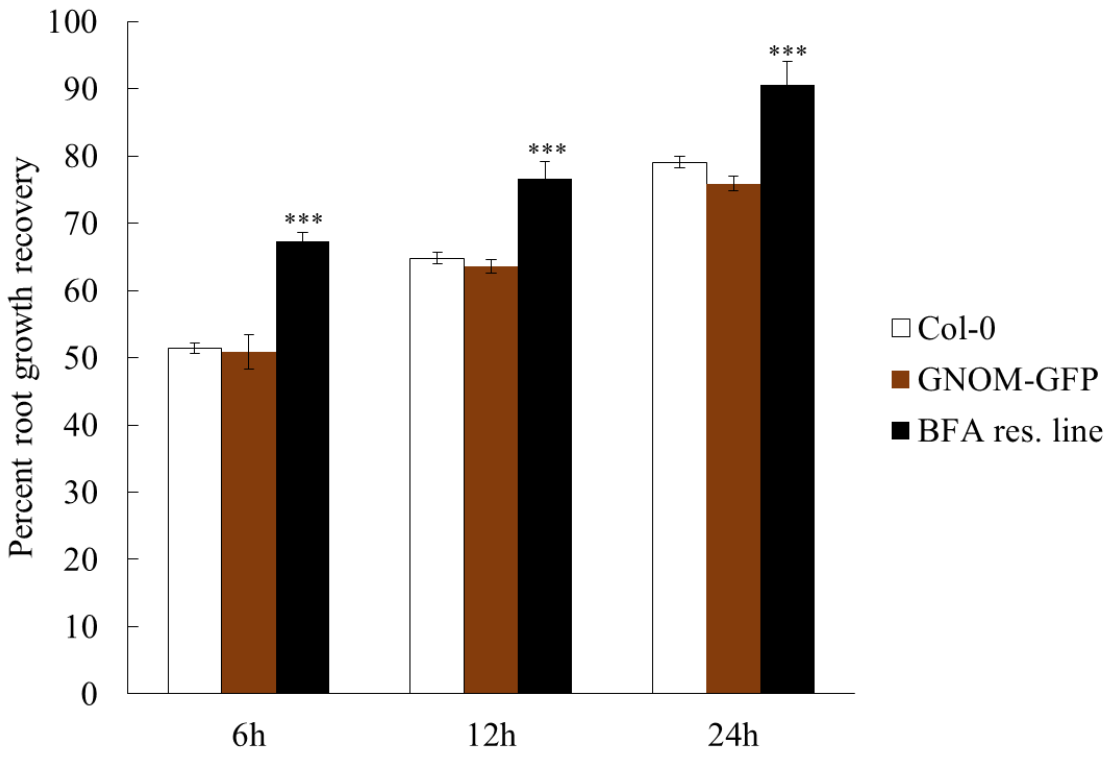

Figure 10. GNOM is required for cold stress response

Five-day-old light grown seedlings were transferred to new agar plates and incubated at 23°C and 4°C for 12h. After the treatment, root growth was measured for 6h, 12h and 24h at 23°C.

Primary root elongation recovery at 23°C for 6h, 12h and 24h after incubation at 23°C and 4°C for 12h in wild-type, GNOM-GFP and BFA res. line

Asterisks represent the statistical significance between the means for each treatment. ***P < 0.001. Vertical bars in the graph indicate ±SE.

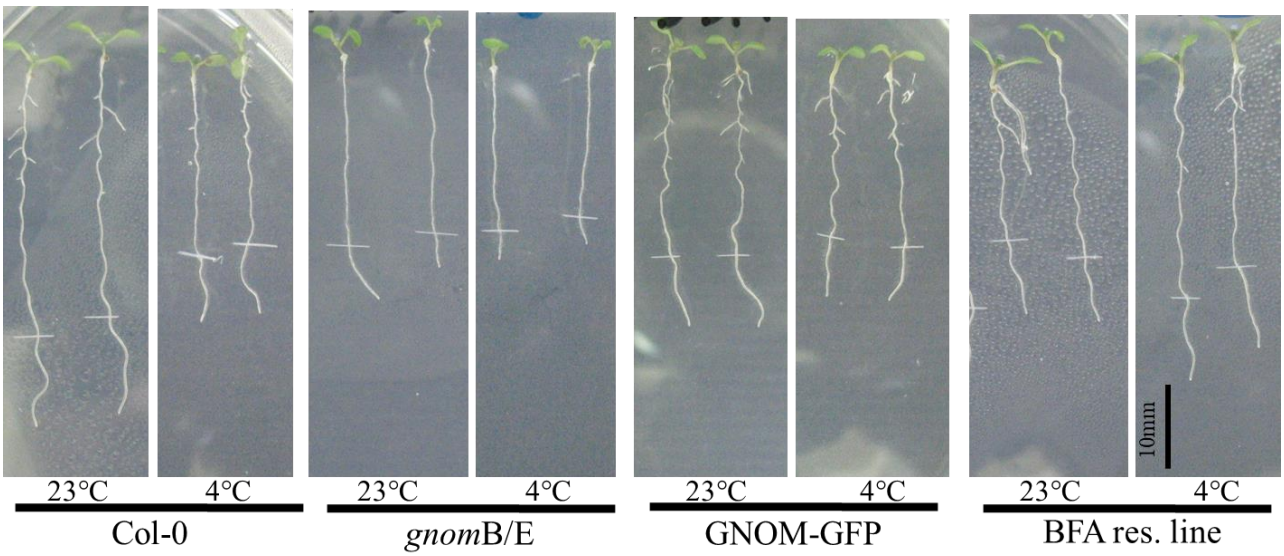

Figure 11. Root growth recovery of Col-0, *gnom*$^{B/E}$, GNOM-GFP and BFA res. line

Root phenotype of Col-0, *gnom*$^{B/E}$, GNOM-GFP and BFA res. line in 24h recovery period at 23°C after incubation at 23°C and 4°C for 12h. Tick marks indicate the starting point of the recovery at 23°C. Scale bar = 10mm.

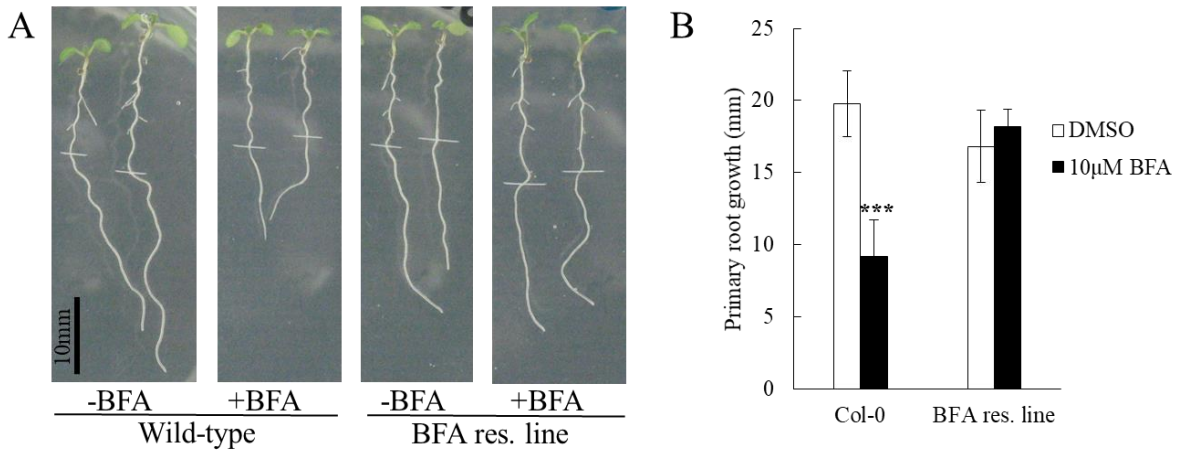

Figure 12. Root growth phenotype of BFA res. line

(A) Phenotype of Col-0 and BFA res. line in presence of DMSO (-BFA) and 10μM BFA (+BFA). Four-day-old light grown Col-0 and BFA res. line seedlings were transferred to DMSO (-BFA) and 10μM BFA (+BFA) plates and incubated for three days.

(B) Primary root growth of Col-0 and BFA res. line in presence of DMSO (-BFA) and 10μM BFA (+BFA). Vertical bars in the graph indicate ±SD. Scale bar = 10mm.

2.3.3. Cold stress targets GNOM at translational level

Cold stress alters both transcriptome and protein expression profiles of *Arabidopsis thaliana*. It has been shown that the cold stress alters the expression of approximately 4%-20% genes in Arabidopsis (Hannah et al., 2005; Lee et al., 2005a). Similarly a range of proteins have also been shown to be affected by cold stress (Amme et al., 2006; Li et al., 2014). To understand whether cold stress affects GNOM expression at transcriptional or translational levels, we investigated the *GNOM* expression by quantitative PCR and monitored GNOM expression using a transgenic line where GNOM is translationally fused to GFP (GNOM-GFP). The GNOM transcript profiling during control (23°C), cold (4°C) and recovery (6 h at 23°C after 12 h treatment at 4°C) conditions revealed no significant differences in *GNOM* expression, suggesting that cold stress does not regulate GNOM at transcriptional level (Figure 13).

At 23°C, intracellular localization of GNOM, using GNOM-GFP, revealed a typical cytosolic and membrane localization as described earlier (Figure 4) (Geldner et al., 2003; Naramoto et al., 2014). The dotted cytosolic GFP fluorescent signal represents the characteristic of trafficking protein, while the membrane localization represents the GTPase activity of GNOM, which occurs at membrane. Cold treatment for 12 h at 4°C drastically inhibited the GNOM expression as observed by the reduced GFP signal. The characteristic dotted cytosolic signal of GNOM also completely disappeared (Figure 15 and Figure 16). These results suggest that GNOM is possibly a direct target of cold stress at translational level. To confirm the specificity of the effect of cold stress on GNOM, we used root specific plasma membrane proteins fused with GFP such as PIN2-GFP and LTI6b-GFP (Kurup et al., 2005; Xu and Scheres, 2005). Same cold treatment did not induce any changes in localization or expression of PIN2 or LTI6b (Figure 17), confirming that cold-induced inhibition of GNOM expression and localization is not a general effect of stress rather a specific event.

Since the root growth started to recover during the recovery process (Figure 7), I hypothesized that this recovery may also be linked to the recovery of the GNOM expression and localization. To test this hypothesis, I monitored the GNOM expression and localization using recovery experiment. Consistent with this idea, after 6 h recovery, both expression and localization of GNOM returned to almost control (signals observed at 23°C) level (Figure 15A-

15C). To further clarify the effect of cold stress on GNOM expression, I performed a time course assay analyzing the GFP signal intensity during cold and recovery treatments. During cold treatment, GFP signal intensity started to decline after 5 h, and the signal completely disappeared at 8 h (Figure 15D). Interestingly, within 2 h of recovery GNOM signal reverted back to almost control level (Figure 15D). These results provide compelling evidence that cold stress transiently regulates GNOM expression, and a wild-type level of GNOM expression recovery is an absolute requirement for root growth.

2.3.4. GNOM-engineered BFA resistant line shows resistance to cold stress

GNOM functions as Guanine nucleotide Exchange Factor which takes place at plasma membrane. However, the majority of GNOM localizes in the cytosol (Figure 5) (Anders et al., 2008). Hence, a continuous cytosol-membrane-cytosol trafficking is required for GNOMs functionality (Geldner et al., 2003). In addition, GNOM has been shown to play a pivotal role in regulating the trafficking of the proteins that reside in recycling endosomal pathway (Geldner et al., 2003). GNOM trafficking is also subjected to the regulation of the non-specific endosomal trafficking inhibitor Brefeldin A (BFA) (Steinmann et al., 1999; Geldner et al., 2003). BFA treatment inhibits the trafficking of GNOM and results in formation of characteristic BFA bodies (Geldner et al., 2003) (Figure 19). To understand whether GNOM-mediated BFA sensitive protein trafficking is linked to plants cold stress response, I used the engineered BFA resistant GNOM transgenic line (mentioned as BFA res. line in the later part). A single point mutation at 696 amino acid position (alteration from M→L) in the conserved SEC7 domain confers BFA resistance (Geldner et al., 2003). Consistent with previous report, we also found that BFA res. line shows strong resistance to BFA-induced root growth inhibition and intracellular accumulation of BFA bodies (Figure 12 and 19). Interestingly, this BFA res. line shows significantly higher root growth recovery rate at all time points of recovery after 12 h 4°C treatment (Figure 10). The mutations in the same SEC7 domain result in two completely opposite responses for root growth under cold stress; while *gnom*$^{B/E}$ shows slower root growth recovery after cold stress, the BFA res. line shows faster root growth recovery under same condition (Figure 9, 10 and 11). These findings further confirm the involvement of GNOM in cold stress response regulation, and also highlight the importance of SEC7 domain as a central regulator of this response.

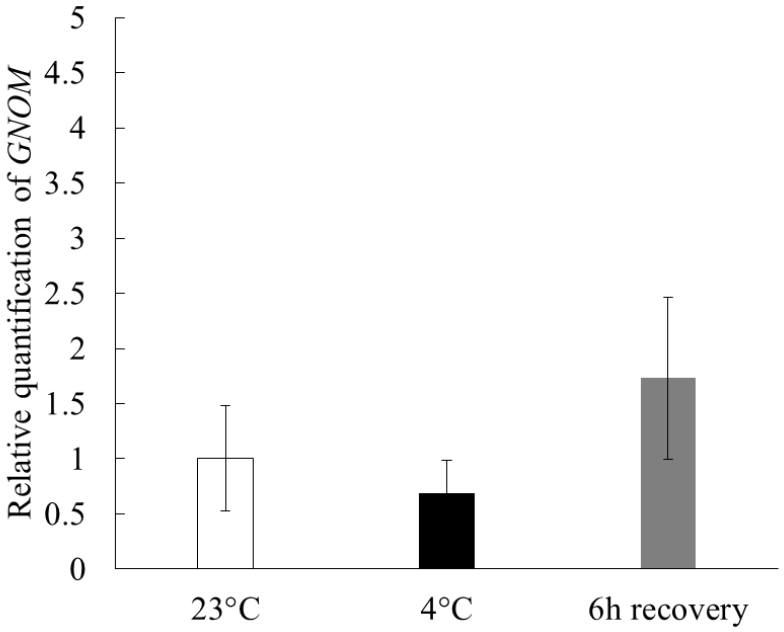

Figure 13. Transcriptional regulation of *GNOM*

Relative quantification of *GNOM* at 23°C, 4°C and 6h recovery at 23°C after 12h treatment at 4°C. Five-day-old light grown seedlings were transferred to fresh plates and treated for 12h at 23°C and 4°C. After the respective treatments, root samples were collected for RNA isolation, cDNA preparation and qRT-PCR analysis. All the data were normalized against EF1α. The data were obtained from three biological replicates.

Vertical bars in the graph represent mean ±SE.

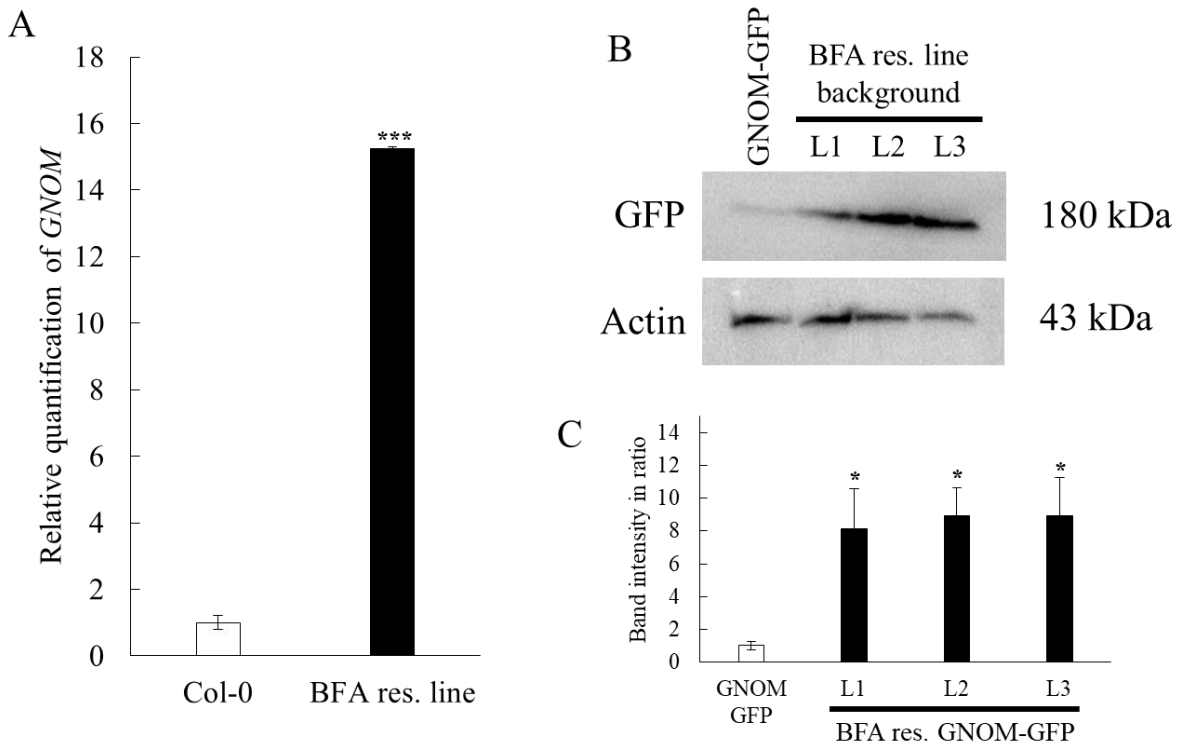

Figure 14. BFA resistant transgenic line overexpresses GNOM both at transcriptional and translational levels

(A) Relative quantification of *GNOM* in wild-type and BFA res. line. Seven-day-old light grown seedlings were used for the experiment. Root samples were collected for RNA isolation, cDNA preparation and qRT-PCR analysis. All the data were normalized against EF1α. The data were obtained from three biological replicates. (B) Comparison of GNOM protein expression in Col-0 and BFA res. line. Seven-day-old whole seedlings were collected for total protein isolation, resolved by gradient (5-20%) SDS-PAGE, and probed with monoclonal antibody against GFP and actin for GNOM-GFP and three independent lines (L1, L2, L3) of BFA res. GNOM-GFP. Total 50µg protein was loaded in each lane. The blot is representative of three independent experiments. GNOM fused with GFP (~180KDa) and actin (43KDa) bands are indicated. (C) Relative quantification of Western blot analysis from experiment B. GNOM-GFP expression was considered as 1 and three independent lines (L1, L2, L3) of BFA res. GNOM-GFP were compared with GNOM-GFP.

Asterisks represent the statistical significance between the means for each treatment. *$P < 0.05$ and ***$P < 0.001$. Vertical bars in the graph represent mean ±SE.

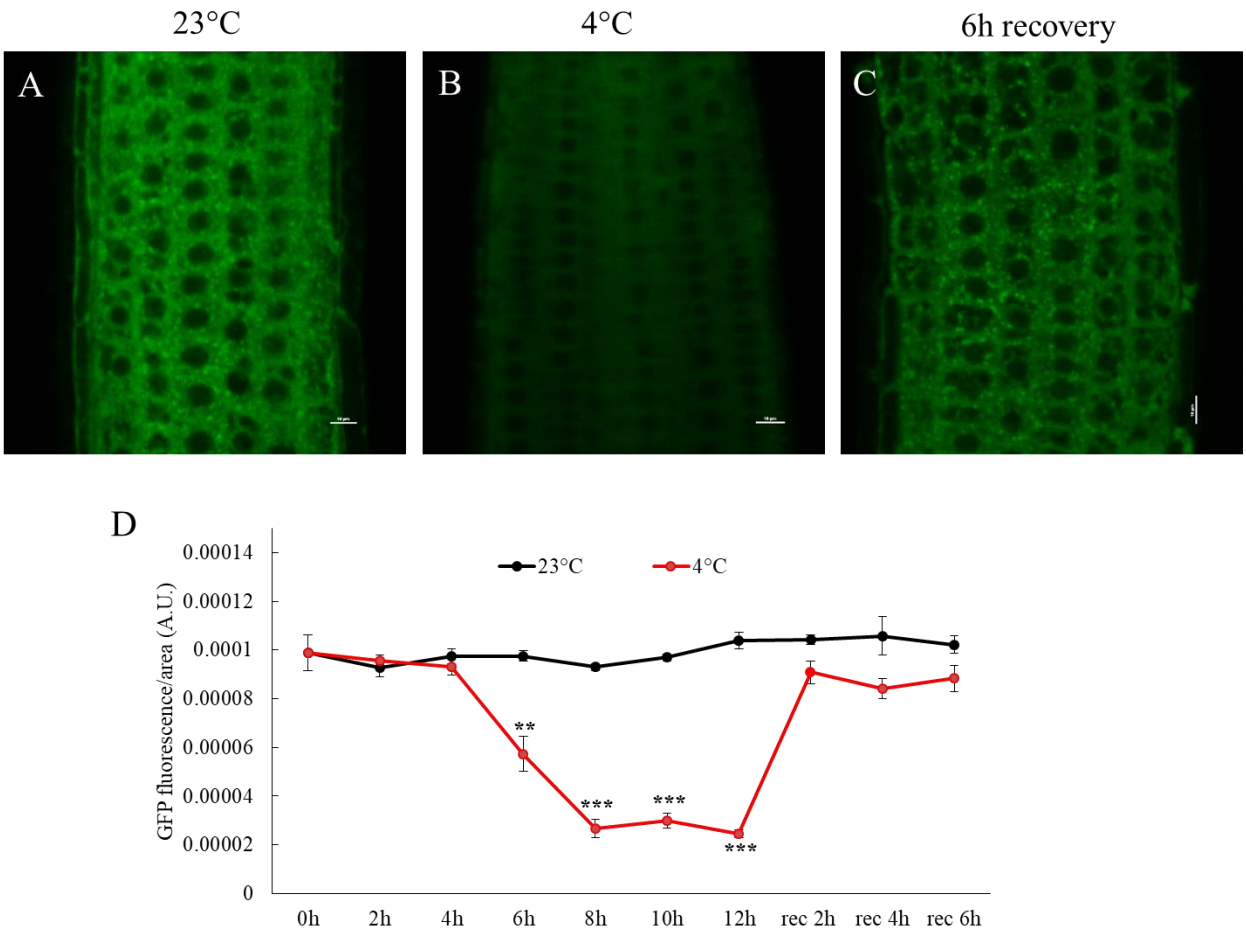

Figure 15. Cold stress transiently inhibits the GNOM expression

Five-day-old light grown GNOM-GFP seedlings were transferred to new agar plates and incubated at 23°C and 4°C for 12h. For the recovery, seedlings grown at 4°C for 12h were kept at 23°C for 6h.

(A), (B), (C) represent the signal of GNOM-GFP at 23°C, 4°C and 6h recovery, respectively. Scale bar = 10µm. The images are representative of three independent experiments with 5 seedlings observed per experiment. (D) Quantification of GFP fluorescence intensity based on time course experiment. The images were captured using same confocal setting.

Asterisks represent the statistical significance between the means for each treatment. **P < 0.01 and ***P < 0.001. Vertical bars in the graph represent mean ±SE.

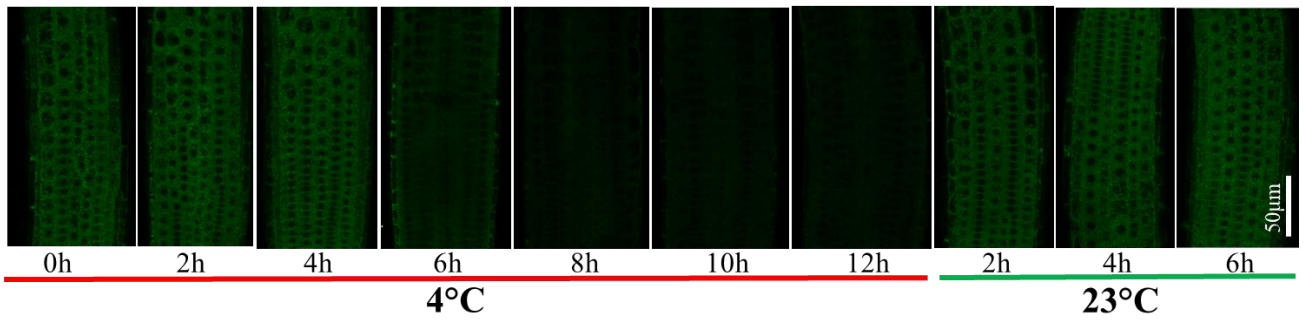

Figure 16. Cold stress exerts transient effect on GNOM-GFP

Five-day-old light grown GNOM-GFP seedlings were transferred to new agar plates and incubated at 4°C from 0h to 12h and recovery period at 23°C up to 6h.

Time course cellular imaging of GNOM-GFP in every 2 hours interval during cold stress and recovery period. Scale bars = 50µm. The images are representative of three independent experiments with 5 seedlings observed per experiment.

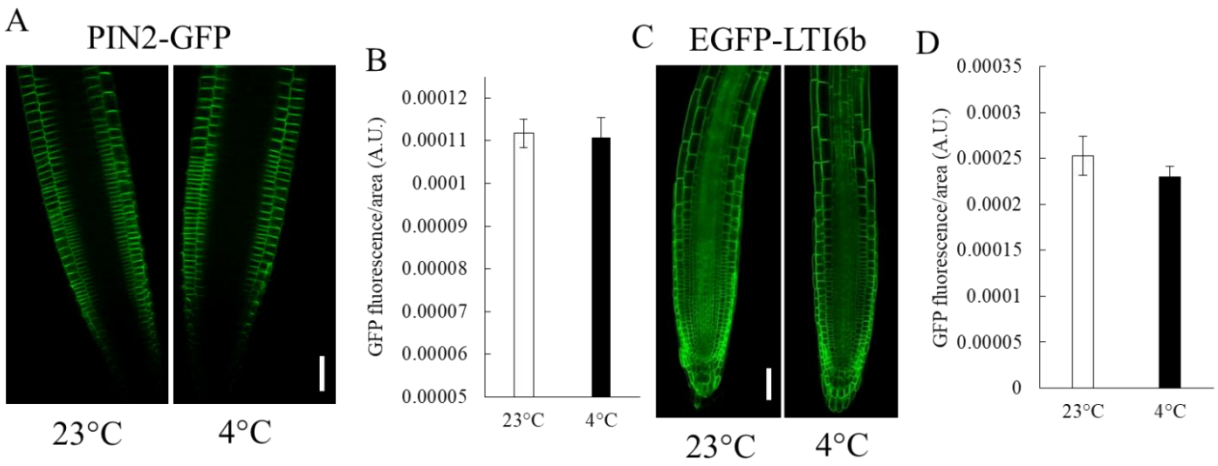

Figure 17. Cold stress does not inhibit PIN2-GFP and EGFP-LTI6b signal

Five-day-old light grown PIN2-GFP and EGFP-LTI6b seedlings were transferred to new agar plates and incubated at 23°C and 4°C for 12h.

(A) and (C) represent the signal of PIN2-GFP and EGFP-LTI6b at 23°C and 4°C. Scale bars = 50µm. The images are representative of three independent experiments with 5 seedlings observed per experiment.

(B) and (D) represent the quantification from (A) and (C), respectively.

Vertical bars in the graph indicate ±SE.

2.3.5. Overexpression and altered cellular localization of GNOM confer cold stress tolerance

To understand the underlying molecular and cellular mechanisms of GNOM in cold stress response regulation, I took the advantage of the BFA res. line which shows a cold resistant behavior (Figure 10 and 11). Since cold stress directly affects the GNOM expression and localization, we hypothesized that the abundance of GNOM in BFA res. line may contribute for its resistance to cold. To confirm the hypothesis, GNOM expression was investigated both at translational and transcriptional levels. Surprisingly and consistent with our hypothesis, transcript analysis of *GNOM* in BFA res. line revealed a ~ 15 fold increase in *GNOM* expression compared with wild-type (Figure 14A). The increase in the transcript level was also reflected at the translational level. Comparative GNOM expression analysis in GNOM-GFP and BFA res.-GNOM-GFP lines by western blotting using GFP antibody revealed ~ 8 fold increase in the GNOM abundance (Figure 14B and 14C) in BFA res. line, confirming that BFA res. line indeed is an overexpression line. This is a unique finding, as for the first time it has been demonstrated that the single point mutation in BFA res. line results in overexpression of GNOM.

One of the major features of cold stress effect on GNOM is the down regulation of GNOM expression and altered cellular localization (Figure 4). Further, the recovery of root growth of cold-stressed seedlings required the appropriate GNOM expression and localization (Figure 15). To understand the cellular basis of the resistance of BFA res. line, I monitored expression and localization of GNOM using BFA res.-GNOM-GFP lines. Unlike GNOM-GFP, the BFA res.-GNOM-GFP lines retain both the expression and sub-cellular localization of GNOM after cold treatment (Figure 18). Additionally, in these crossed lines, GNOM shows preferential plasma membrane localization instead of cytosolic localization found in wild-type (Figure 20). Three independent cross lines were investigated for cellular localization, BFA resistance for root growth, and capabilities of making BFA bodies after BFA treatment (Figure 18 and 19). All three lines show similar responses to all the experiments that I performed, suggesting that overexpression of GNOM and subsequent altered cellular localization induced by point mutation make the BFA res. line root growth resistant to cold stress.

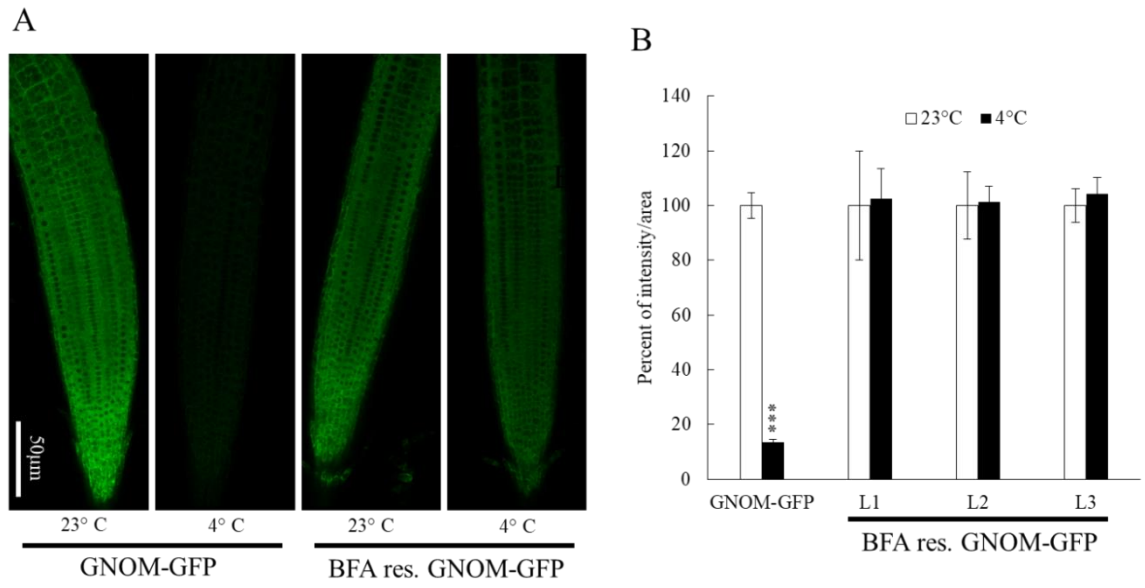

Figure 18. Cold stress does not inhibit GNOM expression in GNOM-engineered BFA res. line

Five-day-old light grown GNOM-GFP and BFA res. GNOM-GFP seedlings were transferred to new agar plates and incubated at 23°C and 4°C for 12h.

(A) Cellular imaging of GNOM-GFP and BFA res. GNOM-GFP at 23°C and 4°C after 12h. Scale bar = 50µm. (B) GFP quantification of GNOM-GFP and three independent lines (L1, L2, L3) of BFA res. GNOM-GFP at 23°C and 4°C after 12h. The images and quantitative data are representative of three independent experiments with 5 seedlings observed per experiment.

Asterisks represent the statistical significance between the means for each treatment. ***P < 0.001. Vertical bars in the graph represent mean ±SE.

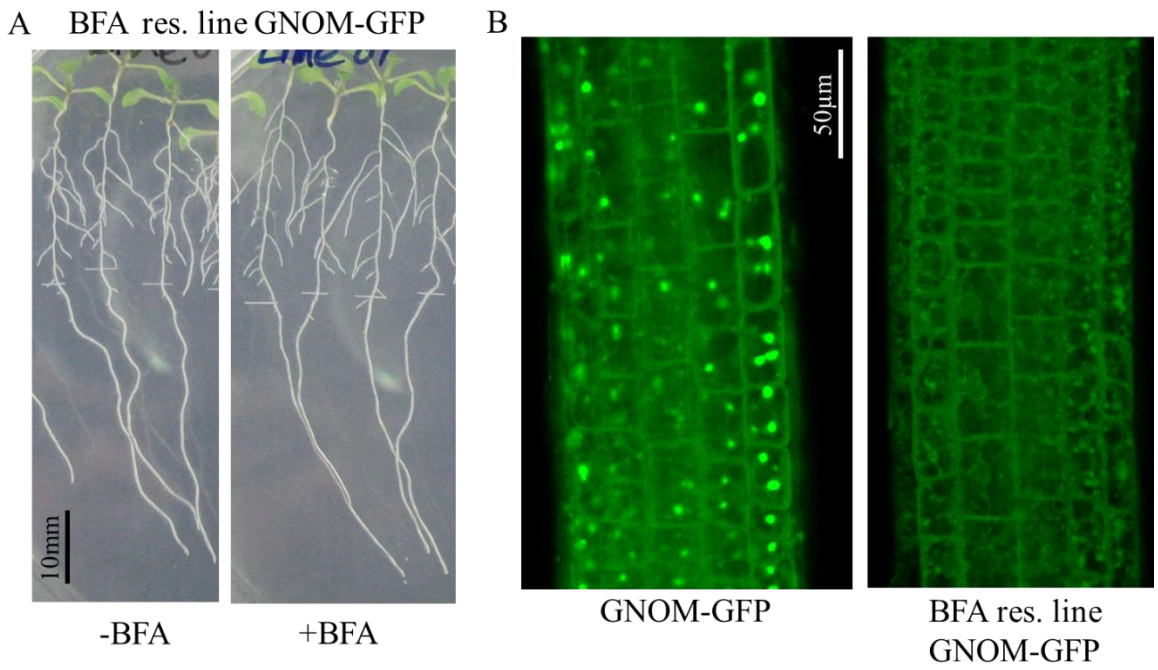

Figure 19. Response of BFA res. line GNOM-GFP in the presence of BFA for root growth and BFA bodies formation

(A) Phenotype of BFA res. line GNOM-GFP in presence of DMSO (-BFA) and 10µM BFA (+BFA). Four-day-old light grown seedlings were transferred to DMSO (-BFA) and 10µM BFA (+BFA) plates and incubated for three days. Scale bar = 10mm.

Five-day-old seedlings were transferred to 20µM BFA liquid solution and incubated for 40 minutes prior to confocal imaging.

(B) represents GNOM-GFP and BFA res. line GNOM-GFP in presence of 20µM BFA and incubated for 40 minutes. Scale bars = 50µm.

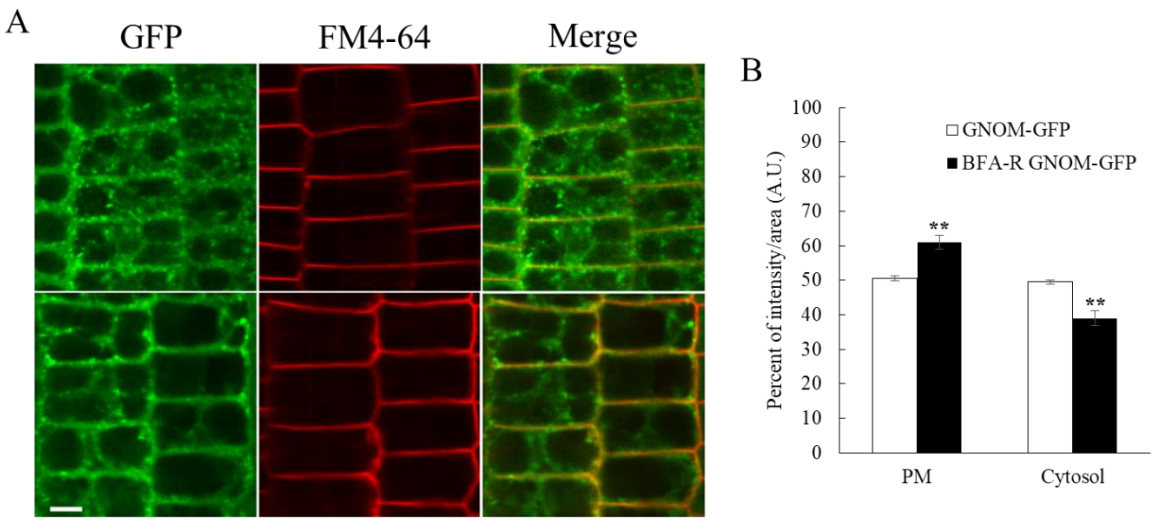

Figure 20. Sub-cellular localization of GNOM is altered in GNOM-engineered BFA res. line

Five-day-old light grown GNOM-GFP and BFA res. GNOM-GFP seedlings were used for confocal imaging. (A) Sub-cellular localization of GNOM-GFP and BFA res. GNOM-GFP line. Scale bar = 50µm. (B) GFP quantification of plasma membrane and cytosol for GNOM-GFP and BFA res. GNOM-GFP line. Data are average of more than 45 individual cells for cytosolic and plasma membrane regions obtained from three independent experiments with at least 15 cells observed per experiment.

Asterisks represent the statistical significance between the means for each treatment. **$P < 0.01$. Vertical bars in the graph represent mean ±SE.

2.3.6. Altered cellular localization of GNOM affects the localization of auxin efflux carrier PIN2

The recycling of PIN2 from cytosol to plasma membrane has been shown to be an important factor for optimal PIN2 activity, which is partially regulated by GNOM activity and subjected to BFA regulation (Geldner et al., 2003; Shibasaki et al., 2009; Rahman et al., 2010). Cold stress selectively inhibits this trafficking, which results in altered intracellular auxin homeostasis leading to root growth inhibition (Shibasaki et al., 2009; Shibasaki and Rahman, 2013). To understand whether the predominant membrane localization of GNOM in BFA res. line also alters PIN2 trafficking under cold stress, I compared endocytic trafficking of PIN2 in wild-type and BFA res. line using PIN2-GFP. Consistent with previous report, we also found that 4°C 12h treatment drastically reduces the intracellular trafficking of PIN2 (Figure 21A and 21B) (Shibasaki et al., 2009). Interestingly, cold stress-induced inhibition of PIN2 trafficking was only slightly affected in BFA res. line (Figure 21A and 21B). Taken together, these results suggest that the predominant plasma membrane localization of GNOM in BFA res. line possibly helps the plant to retain its PIN2 trafficking activity under cold stress that results in cold stress resistant root growth phenotype.

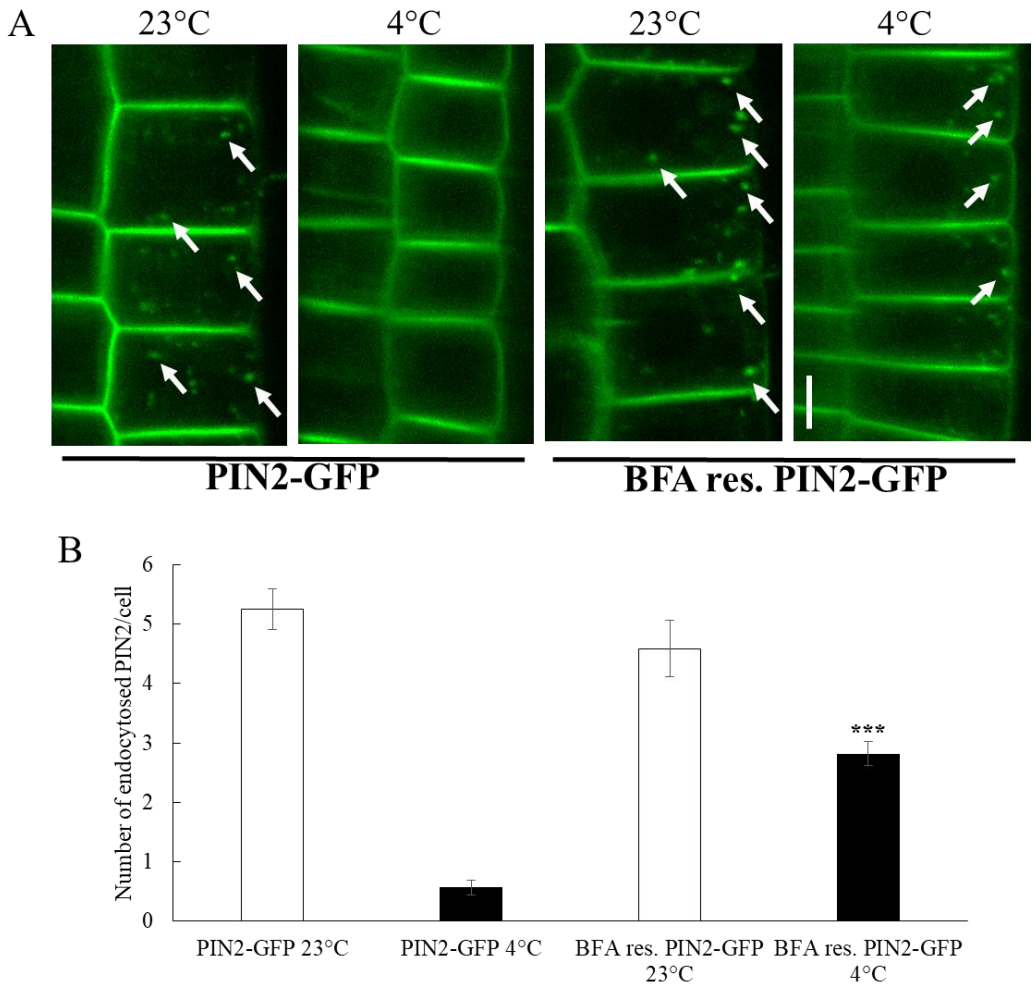

Figure 21. GNOM-mediated PIN2 trafficking persists in BFA res. line background at 4°C

(A) Cellular imaging of PIN2-GFP and BFA res. PIN2-GFP at 23°C and 4°C after 12h. (B) Quantification of endocytosed PIN2 in PIN2-GFP and BFA res. PIN2-GFP at 23°C and 4°C after 12h. Endocytosed PIN2-GFP signal was counted from 100 individual cells for each treatment and genotype.

Five-day-old light grown PIN2-GFP and BFA res. PIN2-GFP seedlings were transferred to new agar plates and incubated at 23°C and 4°C for 12h. The images were captured using same confocal setting and are representative of three independent experiments with 5 seedlings and 35 cells observed per experiment. Scale bar = 10µm.

Asterisks represent the statistical significance between the means for genotype specific treatment. ***P < 0.001. Vertical bars in the graph represent mean ±SE.

2.3.7. Resistance of BFA res. line to cold stress is linked to increased cell division

Decreased cell division attributes the decreased root growth in wild-type under cold stress (Figures 1, 2, 4, 5, 6). Since BFA res. line shows resistance to cold stress-induced inhibition of root growth, one would assume that this resistance phenotype may be linked to increased cell division under cold stress. To test this hypothesis, I compared CYCB1;1 expression in wild-type and BFA res. line (Figure 22). Although 24 h 4°C treatment results in severe reduction of CYCB1;1 expression in wildtype, the BFA res. line retains a considerable amount of CYCB1;1 expression (Figure 22A). Quantitative analysis of *CycB1;1-GUS* signal from the root images revealed a significant difference in cell cycle activity in BFA res. line roots compared with the wild type roots under cold stress (Figure 22B). Collectively, these results confirm that the regulation of cell cycle activity is an important determinant of root growth under cold stress and GNOM is a modulator of this activity.

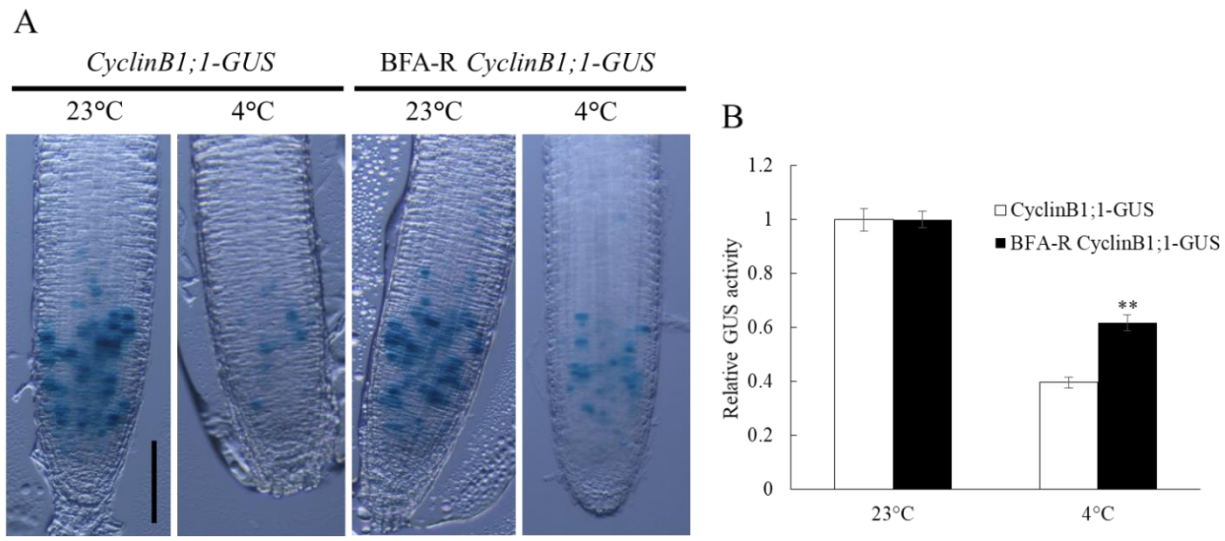

Figure 22. Increased root growth resistance of BFA res.line to cold stress is linked to increased cell division

(A) 5-day-old CyclinB1;1-GUSand BFA-R CyclinB1;1-GUSseedlings were treated at both 23°C and 4°C for 24h. After the treatment, seedlings were incubated with GUS staining buffer for 3h at 37°C.The images are representative of three independent experiments with at least 5 seedlings observed per experiment. (Scale bar = 100µm.)

(B) Quantification of GUS activity from (A). Asterisks represent the statistical significance between the means for genotype specific treatment. ** $P < 0.01$. Vertical bars inthe graph represent mean ±SE.

2.3.8. Intracellular trafficking of PIN2 and normal auxin homeostasis are retained under cold stress in BFA res. line

The recycling of PIN2 from cytosol to plasma membrane has been shown to be an important factor for optimal PIN2 activity, which is partially regulated by GNOM activity and subjected to BFA regulation (Geldner et al., 2003; Rahman et al., 2010; Shibasaki et al., 2009). Cold stress selectively inhibits this trafficking, which results in altered intracellular auxin homeostasis leading to root growth inhibition (Shibasaki and Rahman, 2013; Shibasaki et al., 2009). To understand whether the predominant membrane localization of GNOM in BFA res. line also alters PIN2 trafficking under cold stress, I compared endocytic trafficking of PIN2 in wild-type and BFA res. line using PIN2-GFP. Consistent with previous report, I also found that 4°C 12 h treatment drastically reduced the intracellular trafficking of PIN2 (Figure 21A, Shibasaki et al., 2009). Interestingly, cold stress-induced inhibition of PIN2 trafficking was only slightly affected in BFA res. line (Figure 21A). To check whether the increased PIN2 trafficking under cold stress in BFA res. line also affects the intracellular auxin homeostasis, I monitored the intracellular auxin response using two auxin responsive marker lines *IAA2-GUS* (Luschnig et al., 1998; Swarup et al., 2001) and DII-Venus (Brunoud et al., 2012). Consistent with previous results, I observed an increase in GUS activity in the peripheral cells including epidermis and cortex (Shibasaki et al., 2009; Figure 23) and a decrease in DII-VENUS signal (Figure 24) in wild-type roots under cold stress, which confirms the altered shootward transport activity and increased accumulation of auxin in root meristem. In contrast, cold stress-induced accumulation of GUS signal in root meristem was comparatively less in BFA res. line (Figure 23). Consistently, compared with the wildtype, more DII-Venus signal was observed in BFA res. line under cold stress (Figure 24). Taken together, these results suggest that the predominant plasma membrane localization of GNOM in BFA res. line helps the plant to retain its PIN2 trafficking activity under cold stress that facilitates the shootward auxin transport and maintenance of proper intracellular auxin gradient in meristem resulting in cold stress resistant root growth phenotype (Figure 25).

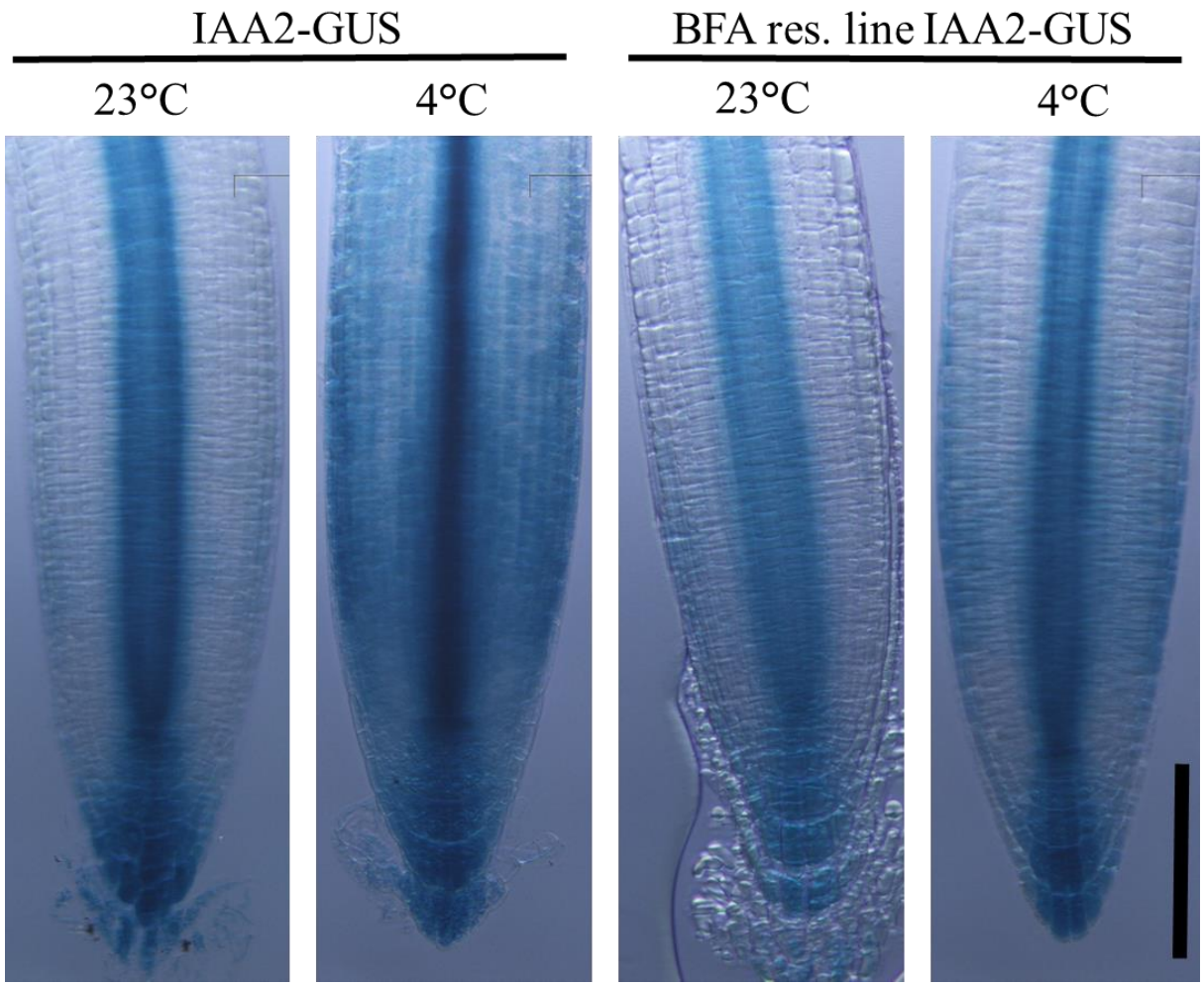

Figure 23. BFA res. line maintains auxin homeostasis at 4°C

5-day-old IAA2-GUS and BFA res. IAA2-GUS seedlings were treated at both 23°C and 4°C for 12h. After the treatment, seedlings were incubated with GUS staining buffer for 1h at 37°C. The images are representative of three independent experiments with at least 5 seedlings observed per experiment. (Scale bar = 100μm.)

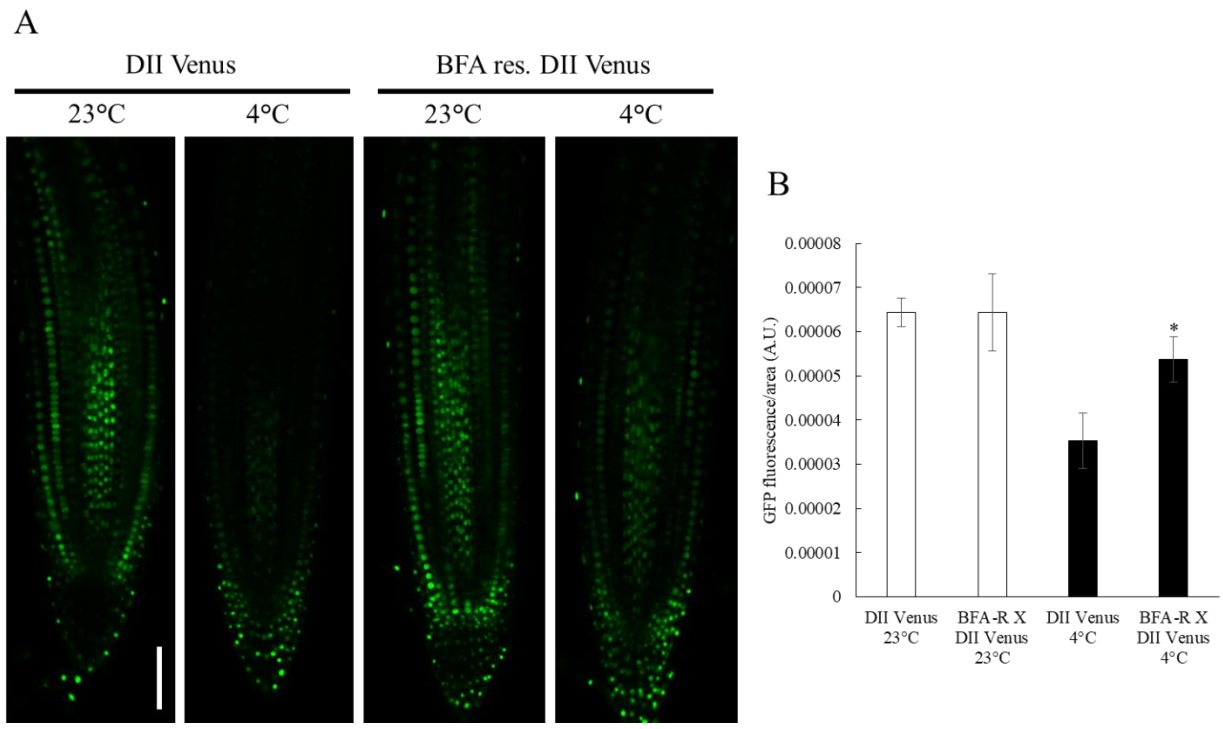

Figure 24. Overexpression of BFA alters the intracellular auxin homeostasis under cold stress

(A) 5-day-old DII-Venus and BFA res. DII-Venus seedlings were incubated at both 23°C and 4°C for 12h. Confocal images were taken using the same setting after corresponding treatment. The images are representative of three independent experiments with at least 5 seedlings observed per experiment. Scale bar = 50µm.

(B) represents the quantification from (A). Asterisks represent the statistical significance between the means for genotype specific treatment. *P < 0.01. Vertical bars in the graph represent mean ±SE.

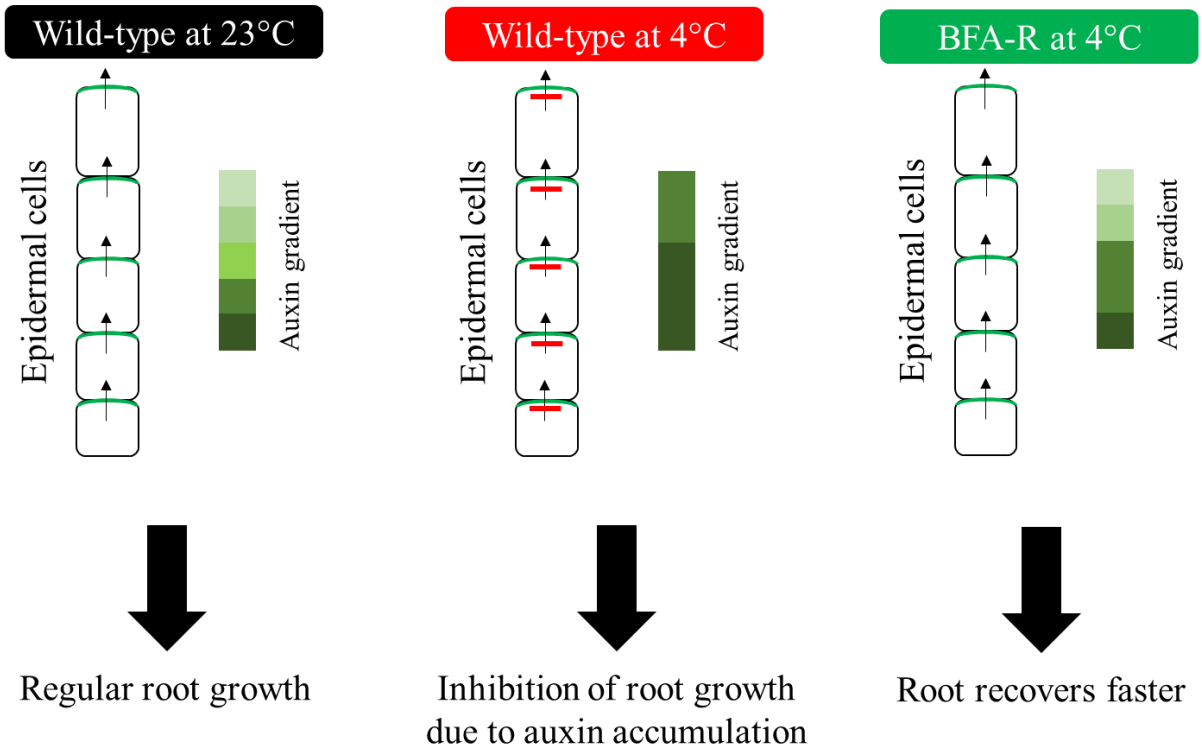

Figure 25. Proposed model from the study

(Left) Auxin gradient is required for proper root growth. (Middle) Inhibition of endosomal protein trafficking of auxin transporter alters auxin gradient in the root and slows down root growth as well. (Right) BFA res. line maintains proper auxin flow and gradient to confer faster cold stress recovery of root.

2.3.9. GNOM-mediated cold stress tolerance is beyond root

GNOM is ubiquitously expressed in Arabidopsis and plays important role from the development from the embryo stage (Steinmann et al., 1999; Geldner et al., 2004), supporting a universal instead of localized role of GNOM. To test whether GNOM functions at the whole plant level for regulating cold response, I took two different approaches; 1) performed electrolyte leakage analysis using leaves and 2) tested the ability of wild-type, *gnom*$^{B/E}$ and BFA res. line to grow under continuous cold stress. Electrolyte leakage analysis is a standard test to understand the plant response to cold stress. In Arabidopsis, cold-acclimated plants, which acquire more cold resistance, show a typical resistance to electrolyte leakage (Uemura et al., 1995). The comparative analyses of electrolyte leakage in wild-type, *gnom*$^{B/E}$ and BFA res. line show a distinct response pattern that is consistent with their cold responses. *gnom*$^{B/E}$, which shows slower recovery of root growth after cold stress, is more susceptible to ion leakage, while the BFA res line, which shows opposite response in root growth assay, shows less ion leakage at all freezing temperatures we tested (Figure 26).

Consistently, when Col-0, *gnom*$^{B/E}$, and BFA res. line were grown under 4°C continuously, they showed distinct phenotypic responses at whole plant level. As expected, *gnom*$^{B/E}$ shows a severe growth phenotype all along. Compared with wild-type, *gnom*$^{B/E}$ growth was extremely retarded. Leaves of both wild-type and *gnom*$^{B/E}$ accumulated visible amount of anthocyanin (Figure 27). On the other hand, BFA res. line showed a better growth phenomenon with faster growth of the leaves and production of inflorescence. Very less amount of anthocyanin accumulated in the leaves of BFA res. line (Figure 27 and 28). Interestingly, we also observed flowering in BFA res. line around 8 week time point, which is a rare event in plants grown under continuous cold temperature. Collectively, these results convincingly demonstrate that GNOM regulates cold stress response at all developmental stages and is a universal regulator of cold stress.

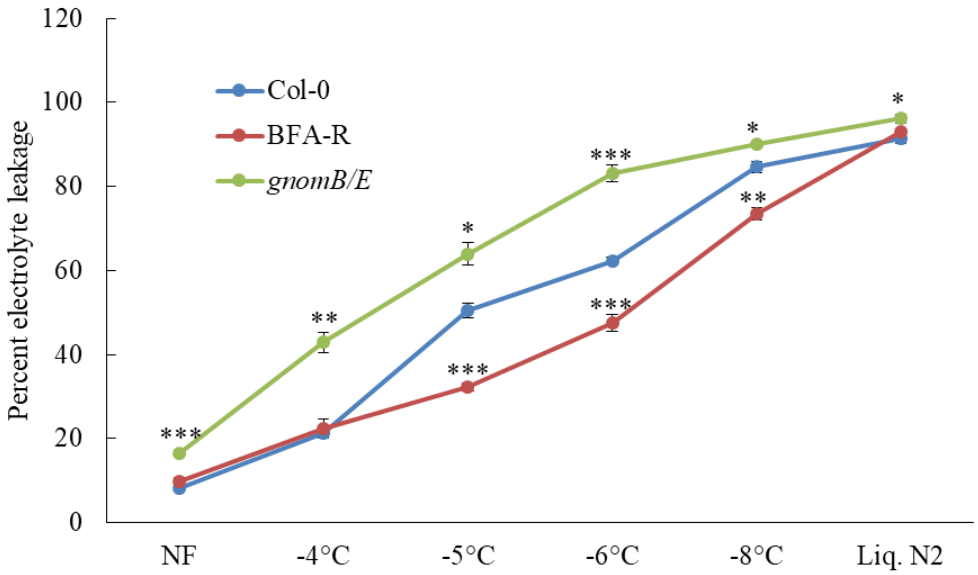

Figure 26. Overexpression of GNOM in BFA res. line provides membrane intactness

Electrolyte leakage assay for Col-0, BFA res. line and *gnom*$^{B/E}$ from 14-day-old leaves. NF indicates non-freezing sample and liquid nitrogen treated samples are considered as positive control. The data are representative of three biological independent experiments with 3 technical replicates observed per experiment.

Asterisks represent the statistical significance between the means for genotype specific treatment. *P < 0.05, **P < 0.01 and ***P < 0.001. Vertical bars in the graph represent mean ±SE.

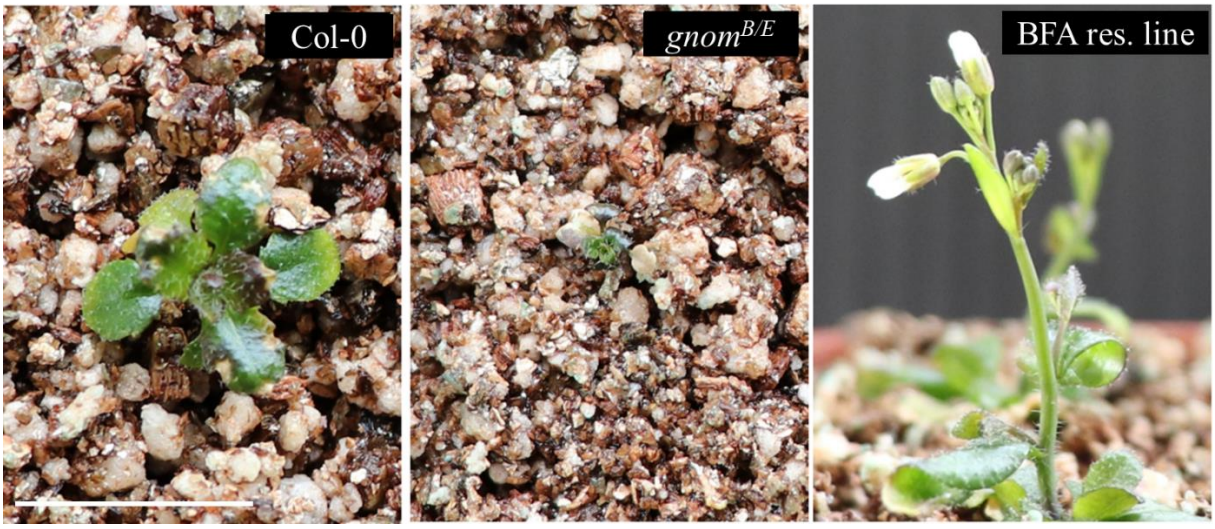

Figure 27. Alteration of GNOM expression affects cold response at whole plant level

Phenotype of seven-week-old Col-0, BFA res. line and *gnom*$^{B/E}$ plant on soil at 4°C under continuous light condition. Scale bar = 1cm.

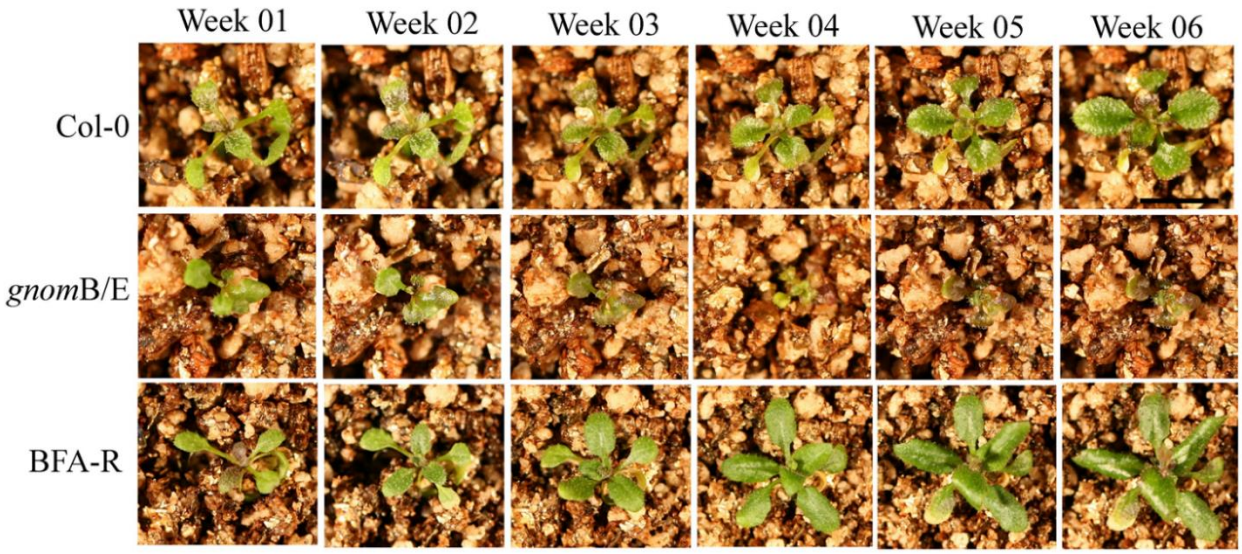

Figure 28. Phenotype of Col-0, BFA res. line and *gnom*$^{B/E}$ plant at 4°C

Ten-day-old seedlings were transferred to soil. Week 1 indicates the 7 days from the transfer to soil and so on. Phenotype of Col-0, BFA res. line and *gnom*$^{B/E}$ plant on soil from week 1 to week 6 at 4°C under continuous light condition. Scale bars = 1cm.

2.4. Discussion

Plants encounter various environmental stresses during its growth and development. One of the major factors that limit plant/crop productivity world-wide is cold stress. For instance, in 2009, chilling temperature alone resulted in crop damage equivalent to 158 billion yen in Japan. Similarly, early and late frosts result in damaging the vegetable and fruit productions equivalent to 5-6 billion yen per year in Japan (Rahman, 2013; Shibasaki and Rahman, 2013). In quest of making cold resistant plants, here I demonstrate that 1) GNOM is an important component of cold stress response pathway, and 2) overexpression and altered membrane localization of GNOM confer cold resistance in Arabidopsis through modulating intracellular auxin homeostasis.

Effect of cold stress on plant development varies with the temperature range. 4°C stress drastically inhibits the growth and development of plants (Figure 1) (Hong et al., 2017), while plants grown at 10-15°C stress show milder inhibitory phenotypes (Zhu et al., 2015; Yang et al., 2017). The cold stress-induced inhibition of growth may result from the inhibitory effect on both the cell division and cell elongation, or either of this one. Zhu et al. (2015) suggested that in Arabidopsis, the root growth inhibition at 16°C treatment results from the inhibition of cell division, although they did not measure the cell length (Zhu et al., 2015). In maize root, cell length pattern was found to be unchanged between 29 and 19°C (Silk, 1992) and for maize leaves, a temperature-invariant profile of cell length and proportion of dividing cells was observed for a wide range of temperature (13°C to 34°C) (Ben-Haj-Salah and Tardieu, 1995). Recently, Yang et al., (2017) showed an invariable final cell flux in Arabidopsis root across 15°C-25°C temperature range (Yang et al., 2017). The mature cell (elongation zone) length was also shown to be unaffected by low temperature, although the elongation of young cells showed a positive correlation with the increase in temperature (Yang et al., 2017). In this experimental condition, although 4°C treatment drastically inhibited the root elongation, it did not change the mature cell length (Figures 2, 3). The growth inhibition and reduced meristem size were found to be solely dependent on the cold stress-induced inhibition of cell division (Figure 2). Consistently, the resistance of the BFA res. line to cold stress was found to be linked to increased cell division (Figure 22). The present results demonstrate that cold stress directly affects the progression of cell cycle (Figures 4, 5). More cells were found to be stuck in the gap (G1/G2)

phase under 4°C treatment, resulting in less number of cells in S and M phases (Figure 5). The finding that low temperature increases progression of cell cycle time, or retains the cells in specific phases is consistent with the findings in other model organisms. For instance, in nematodes, embryonic cell division slows down from 5 min to 50 min during a shift in the temperature from 25°C to 5°C (Begasse et al., 2015). Multiple cold sensitive cell cycle mutants have been identified from for *E. coli* and *Saccharomyces cerevisiae* (Kudo et al., 1977; Moir et al., 1982). In hypothermic condition, chicken embryonic cells, epithelial and muscle cells of newborn rats stuck mostly at G2 phase (Levedeva and Zavarzin, 1966; Kruman et al., 1988). Even in rapid proliferating cancerous mouse leukemic (L5178Y) cells, cell cycle time delays up to 7 fold for a temperature shift from 37°C to 28°C (Rieder and Cole, 2002). Taken together, these results indicate the presence of cold-responsive cell cycle components in a wide range of model organisms, including Arabidopsis.

Cold stress response regulation in Arabidopsis is GNOM and SEC7 specific. Several lines of evidence support this idea; 1) the GNOM like1(GNL1) mutants (*gnl1-1,1-2,1-3*) show wild-type like response to cold stress, 2) different mutations in SEC7 domain of GNOM (*gnomB/E* and BFA res. line) result in contrasting response to cold stress, 3) mutation in SEC7 domain resulting in overexpression and altered endocytic/membrane localization ratio of GNOM contributes in conferring cold resistance, and 4) cold-induced inhibition of trafficking of auxin efflux carrier PIN2 and the alteration in intracellular auxin homeostasis is absent in BFA res. line.

GNOM, which encodes a GDP/GTP exchange factor for small G proteins of the large ARF-GEF class protein, is involved in activation of GTPases that cause bound GDP to dissociate from the GTPases, leading to its association with GTP (Gillingham and Munro, 2007; Anders et al., 2008). The ARF binding and GDP/GTP exchange are facilitated by the highly conserved SEC7 domain of ARF-GEFs, which helps in recruiting effector proteins through membrane trafficking (Anders et al., 2008). Further, large ARF-GEFs are sensitive to BFA, which also involves the SEC7 domain. BFA binds to the interface between the ARF-GDP and SEC7 domain and traps the ARF-GDP/SEC7 complex at the membrane resulting in inhibition of ARF-GEF-mediated protein trafficking (Casanova, 2007; Anders and Jürgens, 2008). The binding of the BFA to ARF-GEFs depends on the 40 amino acid residues of the SEC7 domain, and

manipulation of characteristic residues can make the protein resistant to BFA (Peyroche et al., 1999; Sata et al., 1999; Geldner et al., 2003). Consistently, it was shown that mutation in SEC7 domain of GNOM results in strong mutant phenotype; and a single point mutation at 696 position (M→L) of SEC7 domain makes the GNOM resistant to BFA (Mayer et al., 1993; Busch et al., 1996; Geldner et al., 2003). I also found that *gnom* alleles that have mutations in SEC7 domain show contrasting response to cold stress in both long and short term assays. Interestingly, partial loss of function $gnom^{B/E}$ shows hypersensitive response to cold stress, while the BFA res. GNOM line shows strong resistance (Figures 9, 10, 11). These results along with the wild-type sensitivity of the *gnom* alleles that have mutations outside the SEC7 domain to cold stress (Figure 9) confirm the importance of SEC7 domain and BFA sensitive trafficking process in Arabidopsis cold perception.

GNOM has two closest homologues GNOM LIKE 1 and 2 (GNL1 and GNL2). GNL1 has 61% homology to GNOM and shows an ubiquitous expression pattern, while GNL2 expression is pollen specific (Richter et al., 2007). In contrast to GNOM, mutations inside or outside of the SEC7 domain (in *gnl1-1* and *gnl1-3* mutations are outside of SEC7 domain, and in *gnl1-2* mutation is inside the SEC7 domain) of GNL1 had no effect on plant cold stress response, confirming that GNOM but not GNL1 regulates cold stress response (Figure 2B). This is consistent with the findings that GNOM and GNL1 function in two distinct trafficking pathways; while GNOM functions predominantly in recycling endosomal pathway, the GNL1 functions in Glogi and selective endocytosis, and *gn1l-1* knock-out leads to minor defects in development (Richter et al., 2007; Teh and Moore, 2007). Further, the promoter swap experiment with GNOM and GNL1 revealed that GNL1 cannot substitute GNOM functions, but GNOM can substitute GNL1 functions (Richter et al., 2007).

Intriguingly, the point mutation in the BFA res. line results in overexpression of GNOM both at transcriptional and translational levels (Figure 14). This is a unique and surprising finding but not inconsistent as point mutation may result in creating gain of function mutant, where the gene or protein overexpresses (Soppe et al., 2000; Shirano et al., 2002; Weigel and Glazebrook, 2002; Zhong and Ye, 2004; Ito and Gray, 2006). The overexpression also results in alteration of GNOM localization. Typical cytosolic/membrane localization ratio of GNOM is replaced by increasing membrane/cytosolic localization ratio in BFA res. line. In addition, the cold stress-

induced inhibition of GNOM expression is also absent in this line (Figure 18). The activation of ARF GTPases solely depends on their and ARF-GEFs membrane association (Anders and Jürgens, 2008). I suspect that the membrane localized GNOM in BFA res. line activates ARF-GTPases to recruit the effector proteins that provide resistance to cold stress, while in wild-type this process completely inhibited by cold. The auxin efflux carrier PIN2 trafficking results support this idea. Cold stress almost shuts down the intracellular trafficking of PIN2 and inhibits the agglomeration of PIN2 in BFA endosomal bodies (Shibasaki et al., 2009). This phenomenon was not observed in the BFA res. line under cold stress treatment. The PIN2 trafficking was found to be active in the BFA res. seedlings even after 12 h 4°C treatment (this study). Interestingly, increased GTPase activity has been shown to be associated with chilling tolerance in rice in another recent publication. Overexpression of *COLD1*, which functions as a GTPase-accelerating factor on rice G-protein α subunit 1 (RGA1), significantly enhances chilling tolerance, while downregulation of *COLD1* results in chilling sensitivity in rice (Ma et al., 2015). Taken together, these results indicate that the membrane localized GTPase activity of GNOM may play an important role in conferring cold resistance.

GNOM has been shown to be a master regulator of polar transport of auxin, which literally controls every aspect of plant growth and development (Davies, 1995; Steinmann et al., 1999; Geldner et al., 2003). The BFA sensitive polar localization of the auxin efflux carriers is fully or partially dependent on GNOM (Geldner et al., 2003; Rahman et al., 2010). The uninterrupted polar localization of PIN1 in presence of BFA in BFA res. line further confirms the importance of GNOM as in vivo mediator of auxin efflux (Geldner et al., 2003). Not surprisingly, auxin has also been shown to be an important regulator in cold-stress mediated plant growth. Cold-induced inhibition of root growth has been attributed to the altered intracellular auxin homeostasis resulted from inhibition of BFA sensitive PIN2 trafficking (Shibasaki et al., 2009; Rahman, 2013; Shibasaki and Rahman, 2013). In addition, a re-establishment of the auxin maximum in the quiescent center has been shown to be required for functional stem cell niche activity, which contributes in improving the roots ability to withstand cold stress (Hong et al., 2017). The findings that the PIN2 trafficking activity retains in the BFA res. line even after cold stress, and resistance of this line to cold stress-mediated inhibition of root growth (Figure 10 and 21) confirm that GNOM-regulated auxin transport plays an important role in Arabidopsis root cold stress response. This is consistent with previous findings showing

that compared with wild-type, BFA res. line shows much larger radioactive auxin peak in auxin transport assay and also shows complete resistance to BFA-induced inhibition of transport (Geldner et al., 2003). Collectively, these results suggest that GNOM-regulated BFA sensitive protein trafficking plays an important role in regulating plants cold stress response.

The most striking phenotype of BFA res. line is its strong resistance to long term cold stress and capability of flowering, although the plant growth remains to be recovered like wild-type (Figure 27). Consistently, the partial loss of function *gnom*$^{B/E}$ shows hypersensitive response to long term cold stress. This indicates that the observed contrasting phenotypes in these two lines under cold stress are solely due to GNOM. These results are in agreement with the observations in yeast system where GNOM has been shown to be linked to temperature response (Jones et al., 1999; Chantalat et al., 2004). Taken together, these findings establish GNOM as a general modulator of cold streess response across species.

Although the overexpression and altered cellular localization of GNOM along with GNOM-mediated trafficking of auxin transport proteins and appropriate intracellular auxin homeostasis provide a plausible explanation for long term resistance of BFA res. line to cold, the additional factors that are regulated by GNOM trafficking remain obscure. Future studies aiming to comprehensively identify and characterize all the proteins that are trafficked by GNOM will help in engineering the plants capable of growing and producing fruits/grains under severe cold stress.

Chapter 3

ATP Binding Cassette Proteins ABCG37 and ABCG33 function as cesium uptake carriers in *Arabidopsis thaliana*

3.1. Introduction

One of the most dangerous contaminants generated in a nuclear accident is cesium (Cs^+), which shares similar chemical properties with potassium (K^+). The stable isotope of cesium ^{133}Cs is present at a very low concentration (less than 25 µg/g) in the soil and does not possess any major environmental concern (Cooghtrey et al., 1983) . However, two radioisotopes of Cs (^{134}Cs and ^{137}Cs) are of environmental concerns due to their emission of harmful β and γ radiation, relatively long half-lives, and rapid incorporation into biological systems (White and Broadley, 2000; Kinoshita et al., 2011). In fact, consumption of agriculture products contaminated with radiocesium is the principal route of human exposure to this radionucleotide (Shaw and Bell, 1991), which has been shown to be related to increased risk of cancer. Trials of nuclear weapons, discharges from nuclear plants, and nuclear accidents such as the Chernobyl (Cooghtrey et al., 1983) and Fukushima (Isaure et al., 2006) can result in large accumulation of radioactive Cs^+ in the ground. This radioactive Cs^+ is expected to be transmitted to the crops grown in the contaminated fields and cause serious health hazard for the population (Zhu and Smolders, 2000). For public health safety, the Japanese government restricted agricultural crop production on the soil containing more than 5000 Bq/kg (Yamaki et al., 2017). Hence, decontamination of the soil is one of the major priorities to keep the crop fields clean from radio cesium for producing crops free of contamination.

Radiocesium mostly accumulates on the surface of the soil (Fujiwara, 2013). Removal of top soil and transport to dedicated sites is one of the potential solutions for cleaning radioactive Cs^+ contaminated field. Unfortunately, removal of soil from the surface, transportation and management is not an economic solution. Another technique is to use potassium fertilizer to reduce radiocesium toxicity (Zhu and Smolders, 2000). The classic work since 1940 suggests that Cs^+ uptake is regulated through both K^+ transporters and channels (Collander, 1941). Till today, most of the identified transporters that transport Cs^+ are already reported as K^+ transporters. For instance,

rice OsHAK1 (HIGH AFFINITY K^+ TRANSPORTER 1) and OsHAK5 which are known K^+ transporters can also function as cesium transporters (Nieves‐Cordones et al., 2017; Rai et al., 2017). AtKUP/HAK/KT9 also functions as uptake carrier for potassium and cesium (Kobayashi et al., 2010). Hence, the symptoms of Cs^+ intoxification can be reversed by supplying more K^+ in the soil (Shaw and Bell, 1991). However, this strategy has major drawbacks; 1) the K^+ transporter functioning at low external potassium concentration shows little discrimination against Cs^+, while the K^+ channel is dominant at high external K^+ concentration with high discrimination against Cs^+ (Zhu and Smolders, 2000), 2) high concentration of potassium itself is toxic to plants regardless of cesium concentration (Hampton et al., 2004) and 3) it is also economically impractical to provide large amount of potassium to soil. Further, it is a general consensus among the scientists that the mechanism by which Cs^+ is taken up by plant roots is not completely understood. K^+ transporters and channels are only partially responsible for Cs^+ uptake and translocation (Zhu and Smolders, 2000). Taken together, these results suggest that there are alternative routes for Cs^+ transport in plant which needs to be explored to understand the molecular mechanism of Cs^+ uptake.

One of the major pathways for plant to detoxify toxic metals is through transporting to sequestering them in the vacuole. The ATP binding cassette (ABC) transporters, also called multidrug resistance proteins, are ubiquitous in plant and animal kingdom and play an important role in transporting various substances, including metals. For instance, tonoplast-localized AtABCC1 and AtABCC2 transport As (Song et al., 2010), Cd, and Hg (Park et al., 2012) inside vacuole. AtATM3/AtABCB25 is involved in cadmium transport (Kim et al., 2006). Plasma membrane-localized AtABCG36/AtPDR8 functions as efflux carrier of Cd (Kim et al., 2007). AtABCG40 has been shown to be linked to lead transport (Lee et al., 2005b). These results suggest that ABC transporters have broader substrate specificity and can transport metals efficiently.

Although Cs^+ has been suggested to compete with K^+ for translocation, transcriptome analysis revealed that distinct set of genes show altered expression in Cs^+ intoxicated plants compared with K^+ starved plants (Hampton et al., 2004), confirming that Cs^+ intoxication symptom in plants is not solely linked to K^+. Interestingly, in Cs^+ intoxicated plants, genes encoding ABC proteins show altered expression pattern. At least 4 genes belong to this family showed 2.5-3 folds upregulation in response to Cs^+ application but were not altered in K^+ starvation (Hampton et al., 2004). In addition, a recent study using rice-transporter-enriched yeast expression library screening

for Cs^+ carrier identified one ABC transporter and one NRAMP transporter as functional Cs^+ transporter in yeast (Yamaki et al., 2017). Taken together, these results suggest the possible existence of K^+ independent transport system of Cs^+ in plant and also identify ABC proteins as potential targets functioning as Cs^+ transporters.

In the present work, we focused on ABC transporter proteins to understand their roles in Cs^+ transport. In plants, there are 8 subfamilies of ABC transporter proteins, namely ABCA-ABCH (Verrier et al., 2008). The *Arabidopsis* ABC superfamily comprises of 130 full molecular transporters containing at least two membrane spanning domains and two nucleotide binding folds. Among the ABC protein subfamilies, subfamilies B, C, and G have already been shown to possess metal transport activity (Lee et al., 2005b; Kim et al., 2006; Kim et al., 2007; Song et al., 2010; Park et al., 2012). ABCC proteins are exclusively tonoplast localized and ABCB and ABCG are predominantly plasma membrane localized (Verrier et al., 2008). Since I am interested in Cs^+ transport from soil, I focused on plasma membrane localized subfamilies (ABCB and ABCG). Through screening of 37 available ABCB and ABCG mutants root growth against a concentarion of Cs^+ (1.5mM) which inhibits 50 percent root growth in wild-type, I identified ABCG33 and ABCG37 as potential Cs^+ transporters. The gain of function mutant of ABCG37 (*abcg37-1*) shows hypersensitive response to Cs-induced root growth inhibition, while the double knock out mutant of ABCG33 and ABCG37 (*abcg33-1abcg37-2*) shows resistance. Single loss of function mutant of ABCG33 and ABCG37 (*abcg33-1*; *abcg37-2*) did not show any alteration in Cs^+ response. Short term uptake experiment with radioactive Cs^+ revealed reduced cesium uptake by *abcg33-1abgc37-2* compared with wild-type. Potassium response and content were unaffected in the double mutant background confirming that Cs^+ transport by ABCG33 and ABCG37 is independent of K^+. Collectively, this work identified two ABC proteins as new Cs^+ influx transporters, which act redundantly and independent of K^+ transport pathway.

3.2. Materials and Methods

3.2.1. Plant materials

All lines are in the Columbia background of *Arabidopsis thaliana*. *abcb1*/*mdr1*, *abcb2*/*mdr2*, *abcb3*/*mdr3*, *abcb4*/*mdr4*, *abcb5*/*mdr5*, *abcb6*/*mdr5*, *abcb6*/*mdr6*, *abcb7*/*mdr7*, *abcb9*/*mdr9*, *abcb10*/*mdr10*, *abcb11*/*mdr8*, *abcb12*/*mdr16*, *abcb13*/*mdr15*, *abcb14*/*mdr12*, *abcb15*/*mdr13*, *abcb16*/*mdr18*, *abcb17*/*mdr19*, *abcb18*/*mdr20*, *abcb19*/*mdr11*, *abcb20*/*mdr14*, *abcb22*/*mdr21* were provided by Edgar Spalding, Department of Botany, University of Wisconsin-Madison and *abcg37-1*/*pdr9-1* was provided by Willian M. Gray, Department of Plant Biology, University of Minnesota. Other T-DNA insertion mutants were obtained from ABRC (Arabidopsis Biological Resource Center).

ABCG37-GFP (Růžička et al., 2010), ABCG33-GFP (Schuetz et al., 2014), PIN2-GFP (Xu and Scheres, 2005), EGFP-LTI6b (Kurup et al., 2005) and pCyclinB1;1-GUS were described elsewhere (Colón‐Carmona et al., 1999).

Three independent double knockout mutants (*abgc37-2 abcg33-1*) were generated by crossing and the homozygous lines were selected through genotyping.

3.2.2. Growth conditions

Surface-sterilized seeds were placed in round, 9-cm Petri plates on modified Hoagland medium (Baskin and Wilson, 1997) containing 1% (w/v) Sucrose and 0.8% (w/v) agar (Difco Bacto agar; BD Laboratories). Two days after stratification at 4°C in the dark, plates were transferred to a growth chamber (NK System; LH-70CCFL-CT) at 23°C under continuous white light (at an irradiance of ~100 µmol $m^{-2}s^{-1}$). The seedlings were grown vertically for 3 days. For cesium chloride treatment, 3-days-old seedlings were transferred to cesium chloride containing plates of various concentrations and incubate for various time points. To measure the root elongation, photographs of plates were taken using a digital camera (Power Shot A640, Canon, http://canon.jp) and analyzed by an image analyzing software ImageJ (http://rsb.info.nih.gov/ij/).

3.2.3. Chemicals

Cesium chloride was purchased from Sigma Chemical Co (Canada). Propidium idodide was purchased from Invitrogen (USA). The carrier-free ^{137}Cs solution (3.7 MBq mL^{-1}) was

purchased from Eckert & Ziegler (California, USA). Other chemicals were purchased from Wako, Japan.

3.2.4. Kinematic analysis

Seedlings were grown vertically for 4 days after stratification. On day 4, seedlings were transferred to plates supplemented with or without and 1.5 mM cesium chloride and grown vertically for another 3 days. Root elongation was measured by scoring the position of the root tip on the back of the Petri plate once per day. After the end of the incubation, cortical cell length was measured using light microscope (Nikon Diaphot) equipped with a digital camera control unit (Digital Sight [DS-L2]; Nikon, Japan). To ensure newly matured cells were scored, cells were measured for the root zone, where root hair length was roughly half maximal. The length of 10 mature cortical cells was measured from each root, with 8 roots used per treatment. The cell production rate was calculated by taking the ratio of root elongation rate and average cell length and average cell length for each individual and averaging over all roots in the treatment. The data were obtained from three independent biological replicates.

3.2.5. GUS staining

GUS staining was performed based on previously described method (Okamoto et al., 2008). In brief, 3-d-old seedlings were transferred to 1.5 mM cesium chloride containing agar plate and grown vertically at 23°C under continuous white light. After three days incubation, seedlings were transferred to GUS staining buffer (100 mM sodium phosphate, pH 7.0, 10 mM EDTA, 0.5 mM potassium ferricyanide, 0.5 mM potassium ferrocyanide, and 0.1% Triton X-100) containing 1 mM X-gluc and incubated at 37°C in the dark for 1 h. The roots were imaged with a light microscope (Nikon Diaphot) equipped with a digital camera control unit (Digital Sight [DS-L2]; Nikon, Japan).

3.2.6. Gene expression analysis

3-d-old vertically grown *Arabidopsis thaliana* seedlings were transferred to 1.5 mM cesium chloride containing agar plate and incubated at 23°C for three days. After the treatment, RNA was extracted from the root tissue using RNA Extraction Kit (APRO Science, Japan) with on-column DNA digestion to remove residual genomic DNA using RNase-free DNase according to manufacturer's protocol. Extracted RNA was tested for quality and quantity. Each RNA

concentration was normalized with RNase free water. 500 ng RNA was used to synthesize cDNA using Rever Tra Ace qPCR RT master mix (Toyobo, Japan). Quantitative PCR reactions were performed using the Takara TP-850 thermal cycler (Takara Bio, Japan) and SsoAdvanced™ Universal SYBR® Green Supermix (BIO-RAD, USA).The reaction was performed as per manufacturer's instruction. For quantification of *ABCG37* and *ABCG33* expression, we used the 2-ΔΔCT (cycle threshold) method with a normalization to the ef1α expression (Hanzawa et al., 2013). Data were obtained from three biological replicates.

3.2.7. Live-Cell imaging

To image GFP, the 3-day-old seedlings were transferred to 1.5 mM cesium chloride containing plates and incubated at 23°C under continuous light for three days. Images were taken in every 24 h time interval up to 72 h. After mounting on a large cover glass, the roots were imaged using a Nikon laser scanning microscope (Eclipse Ti equipped with Nikon C2 Si laser scanning unit) with a X20 objective. Same confocal settings were used for each group of experiments. Fluorescence intensities were measured by drawing a region of interest (ROI) in the images obtained from live-cell imaging using Image J software.

3.2.8. Cesium transport assay

4-day-old light grown seedlings were incubated in 0.1 µM, 10 µM, 1.5 mM and 15 mM $^{137}Cs^{+}$ containing liquid Hoagland solution for 2 h both in presence (6 mM K^{+}) and absence (0 mM K^{+}) of potassium, transferred over Nylon mesh and briefly washed with liquid Hoagland solution three times. 10mm root tip from 10 seedlings were collected for each sample and inserted into the scintillation vial with 500µL MicroScint 40 (PerkinElmer, Inc., USA). The uptake of $^{137}Cs^{+}$ was determined with a NaI scintillation counter (ARC-300, Aloka, Japan).

3.2.9. Measurements of ion contents

Three-day-old Col-0 and double knockout mutant seedlings were transferred to control and 1.5mM cesium containing plates in presence of 0, 100 µM, 1 mM and 6 mM potassium and incubated for three days at 23°C under continuous white light. Whole seedlings were collected, washed three times with ultrapure water, soaked in the paper towel and measured the fresh weight. Samples were dried at 65°C and digested using ultrapure nitric acid (Kanto Chemical, Japan) at

95°C for 600 min. Ion contents were determined using an inductive coupled plasma mass spectrometer (ICP-MS, NexION 350S, Perkin Elmer, Japan).

3.2.10. Bioinformatics analysis

Mutational information of ABCG37 mutants were collected from SALK T-DNA repository (http://signal.salk.edu/cgi-bin/tdnaexpress) and schematic diagram of mutants were drawn based on Exon-Intron Graphic maker (http://wormweb.org/exonintron).

Protein sequences of ABCG transporters were collected from TAIR database (https://www.arabidopsis.org/index.jsp) and phylogenetic tree was constructed using online Clustal Omega (https://www.ebi.ac.uk/Tools/msa/clustalo/) tool.

3.2.11. Statistical Analysis

Results are expressed as the means of ±SE from appropriate of experiments as described in the figure legends. A two-tailed Student's *t*-test was used to analyze statistical significance.

3.3. Results

3.3.1. Cesium inhibits *Arabidopsis* primary root growth elongation

Metal stress or toxicity in plants is sensed via plant root and subsequently transported to other parts of the plant. To understand the effect of Cs^+ on primary root growth, I performed both dose response and time course assay of cesium chloride using Arabidopsis wild-type (Col-0) seedlings. The time course and dose response data indicate that 1 mM and 1.5 mM cesium inhibits root growth approximately 50% after 5 day and 3 day incubation, respectively (Figure 29). Because 1.5 mM Cs^+ can inhibit ~50% root growth in a shorter incubation period, we decided to use 1.5 mM cesium and three days incubation as an assay system for further experiments. This treatment affects the growth of whole seedling including root and leaf. After 3 day incubation in 1.5 mM Cs^+, root growth is inhibited and leaf chlorosis becomes apparent (Figures 30 and 31). Although root growth is severely inhibited and root phenotype is drastically changed after 3 day Cs^+ incubation, the meristematic cells remain active as I did not observe any cell death by Propidium Iodide (PI) staining (Figure 31).

The growth of primary root is a combination of cell division and elongation, which is further extended through differentiation (Rahman et al., 2007). Cesium-induced inhibition of primary root growth could be the consequence of either decreased cell number or shorter cell length or both. To answer this question, Cs^+ treated seedlings were subjected to kinematic analysis (Rahman et al., 2007), which revealed that Cs^+ inhibits both cell elongation and cell production (Figures 30B and 30C). The Cs^+ effect on cell production rate was further confirmed by using G2-M phase cell cycle marker *CyclinB1;1::GUS*, where only few cells were found to be mitotically active compared with wild-type (Figure 26D). The reduced cell division also affected the meristem growth as the reduction of meristem size was observed in Cs^+ treated seedlings (Figures 30D and 31). Taken together, these results suggest that cesium affects both cell division and elongation to inhibit the overall primary root elongation.

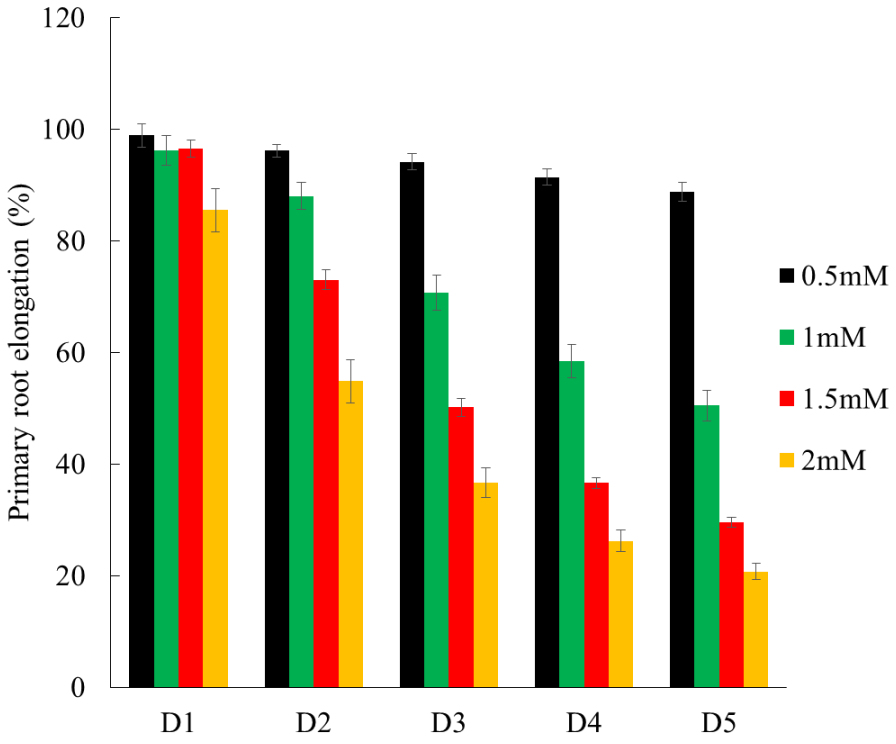

Figure 29. Cesium dose response and time course experiment of *Arabidopsis thaliana*

Primary root growth elongation of wild-type (Col-0) in presence of Cs^+. Three-day-old light grown wild-type (Col-0) seedlings were transferred to new agar plates with and without cesium (0.5, 1, 1.5 and 2 mM) and incubated at 23°C for five days.

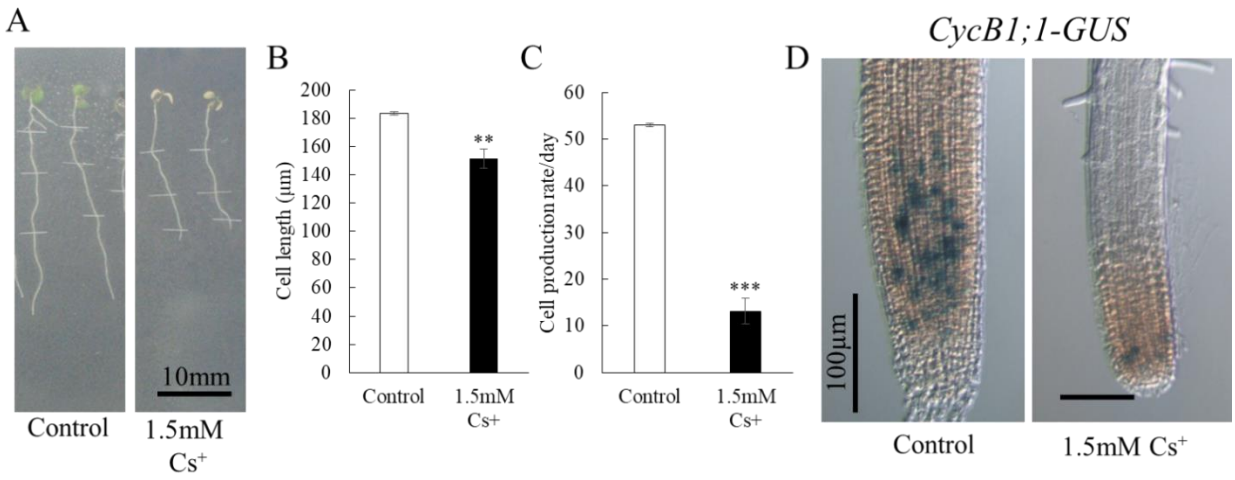

Figure 30. Cesium affects both cell division and cell elongation of *Arabidopsis thaliana* root

(A) Root phenotype of wild-type (Col-0) after three days incubation in control and 1.5mM Cs^+ plates. (B) Cortical cell length of wild-type (Col-0) after three days incubation in control and 1.5mM Cs^+ plates. (C) Cell production rate of wild-type (Col-0) after three days incubation in control and 1.5mM Cs^+ plates. (D) Effect of cesium on expression of *CycB1;1-GUS* in the primary root tip.

Vertical bars mean ±SE from three independent experiments with 8 seedlings observed per experiment (B, C). Asterisks represent the statistical significance between treatments as judged by student's *t*-test: **P < 0.01 and ***P < 0.001. Images are representative of at least three independent experiments with 5-8 seedlings observed per experiment (A, D). Bars = 10 mm for A and 100 μm for D.

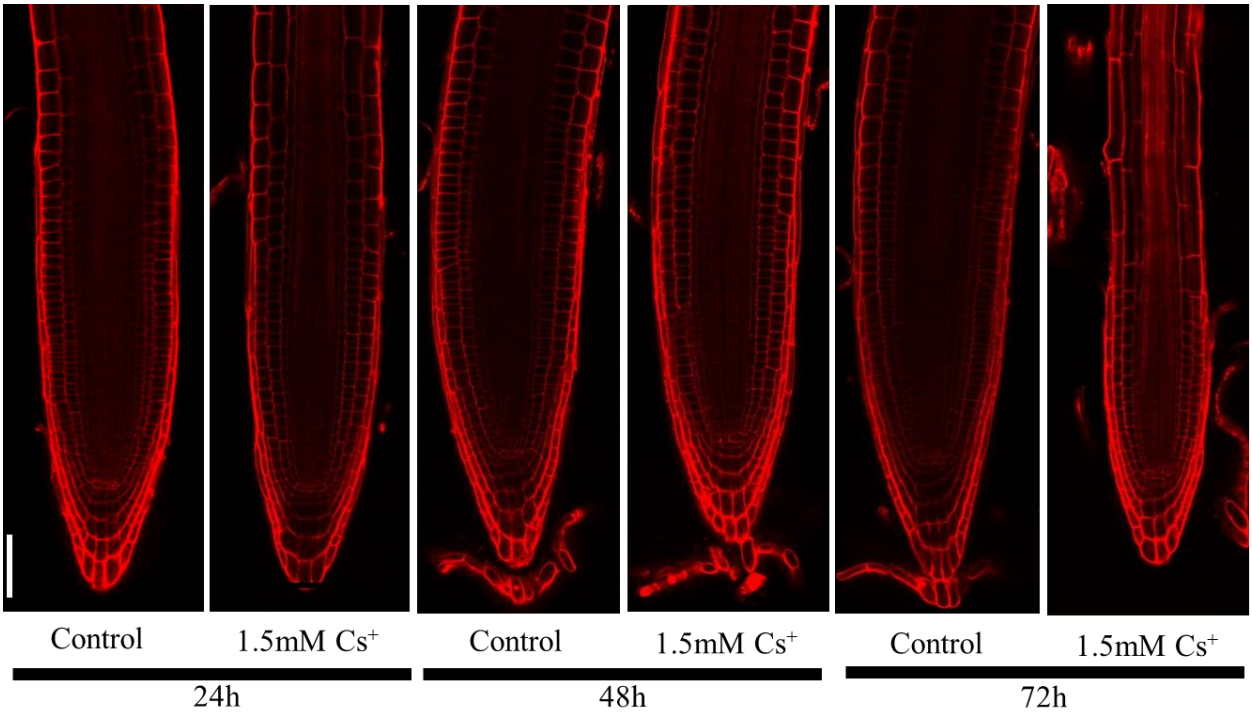

Figure 31. Meristematic growth of *Arabidopsis thaliana* root in presence of cesium

Propidium idodide staining of wild-type (Col-0). Three-day-old light grown wild-type (Col-0) seedlings were transferred to new agar plates with and without 1.5mM Cs^+ and observed under confocal microscope at 24, 48 and 72h time point. Images are representative of at least three independent experiments with 5-8 seedlings observed per experiment. Bars = 50 µm.

3.3.2. Gain-of-function mutant *abcg37-1* is hypersensitive to cesium

In quest of finding new transporters for Cs^+, I focused on ABC transporters as they have already been reported to transport metals such as As, Cd, Hg, Pb (Lee et al., 2005b; Kim et al., 2006; Kim et al., 2007; Song et al., 2010; Park et al., 2012). The broader substrate specificity along with the altered expression pattern of some of the ABC family proteins under Cs^+ intoxicated condition (Hampton et al., 2004) makes them potential candidates for Cs^+ transporter. To elucidate the roles of ABC proteins in Cs^+ transport, I focused on plasma membrane localized subfamilies of ABC proteins ABCB and ABCG and screened available 20 ABCB and 17 ABCG mutants against 1.5 mM cesium for root growth response, which inhibits around 50% root growth in wild-type (Figures 32 and 33). The screening revealed four mutants (*abcb15-1*, *abcg36-1*, *abcg37-1*, *abcg42*) showing altered response to Cs^+. Among these mutants, I selected *abcg37-1* (also known as *pdr9-1*) for further studies as it is the most sensitive to Cs^+ among these four mutants and also a gain-of-function mutant (Ito and Gray, 2006). Time course and dose response analyses revealed that *abcg37-1* shows hypersensitive response to root growth at all concentrations and all incubation periods that I tested (Figure 36). The Cs^+ hypersensitivity in the gain of function mutant suggests that ABCG37 is possibly facilitating the uptake of Cs^+, which results in increased root growth inhibition and leaf chlorosis (Figures 34B and 35). If this is the case, then one would expect that the loss of function mutant will show opposite response. To validate this, I used several alleles of loss-of-function mutant of ABCG37 (*abcg37-2*, *abcg37-3*, *and abcg37-4*) (Figures 34A, 34B and 35). Unfortunately, loss-of-function mutants did not show cesium resistant phenotype.

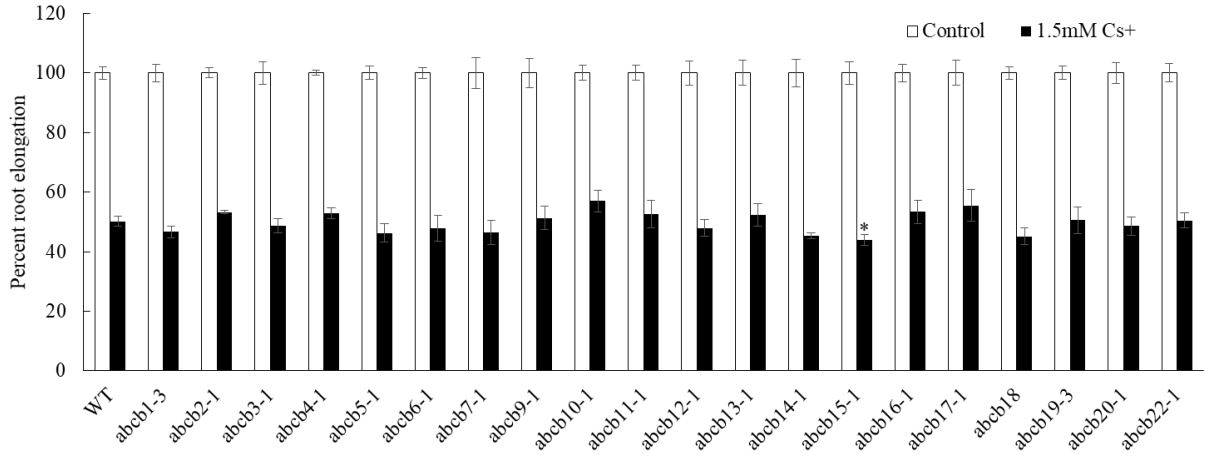

Figure 32. Screening of *abcb* mutants against cesium chloride

Primary root growth elongation of *abcb* mutants in presence of 1.5mM cesium was compared with wild-type (Col-0) seedlings. Three-day-old light grown seedlings were transferred to new agar plates with and without 1.5mM cesium and incubated at 23°C for three days. Vertical bars mean ±SE from three independent experiments with 8 seedlings observed per experiment. Asterisks represent the statistical significance between treatments as judged by student's *t*-test: *P < 0.05.

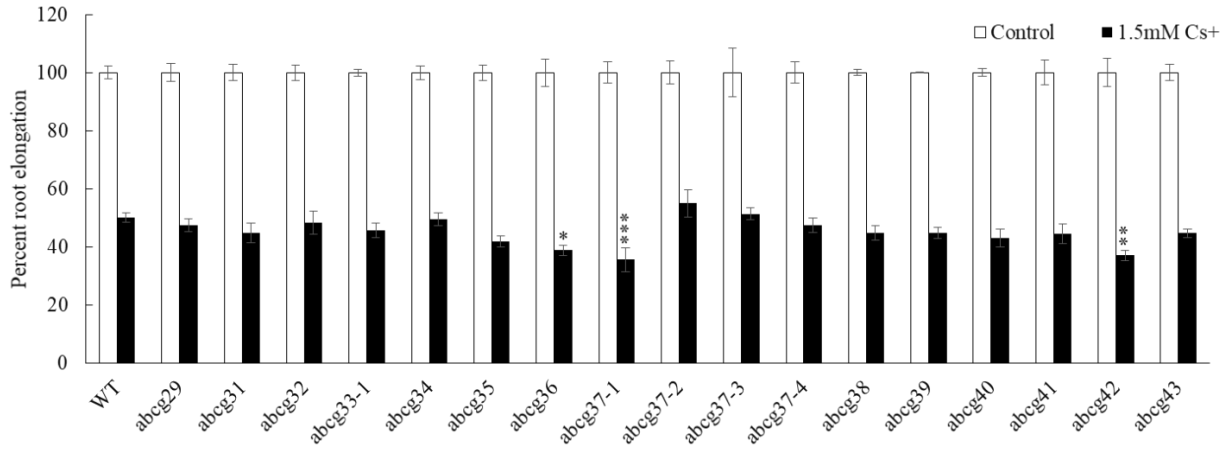

Figure 33. Screening of *abcg* mutants against cesium chloride

Primary root growth elongation of *abcg* mutants in presence of 1.5mM cesium was compared with wild-type (Col-0) seedlings. Three-day-old light grown seedlings were transferred to new agar plates with and without 1.5mM cesium and incubated at 23°C for three days. Vertical bars mean ±SE from three independent experiments with 8 seedlings observed per experiment. Asterisks represent the statistical significance between treatments as judged by student's *t*-test: *P < 0.05 and ***P < 0.001.

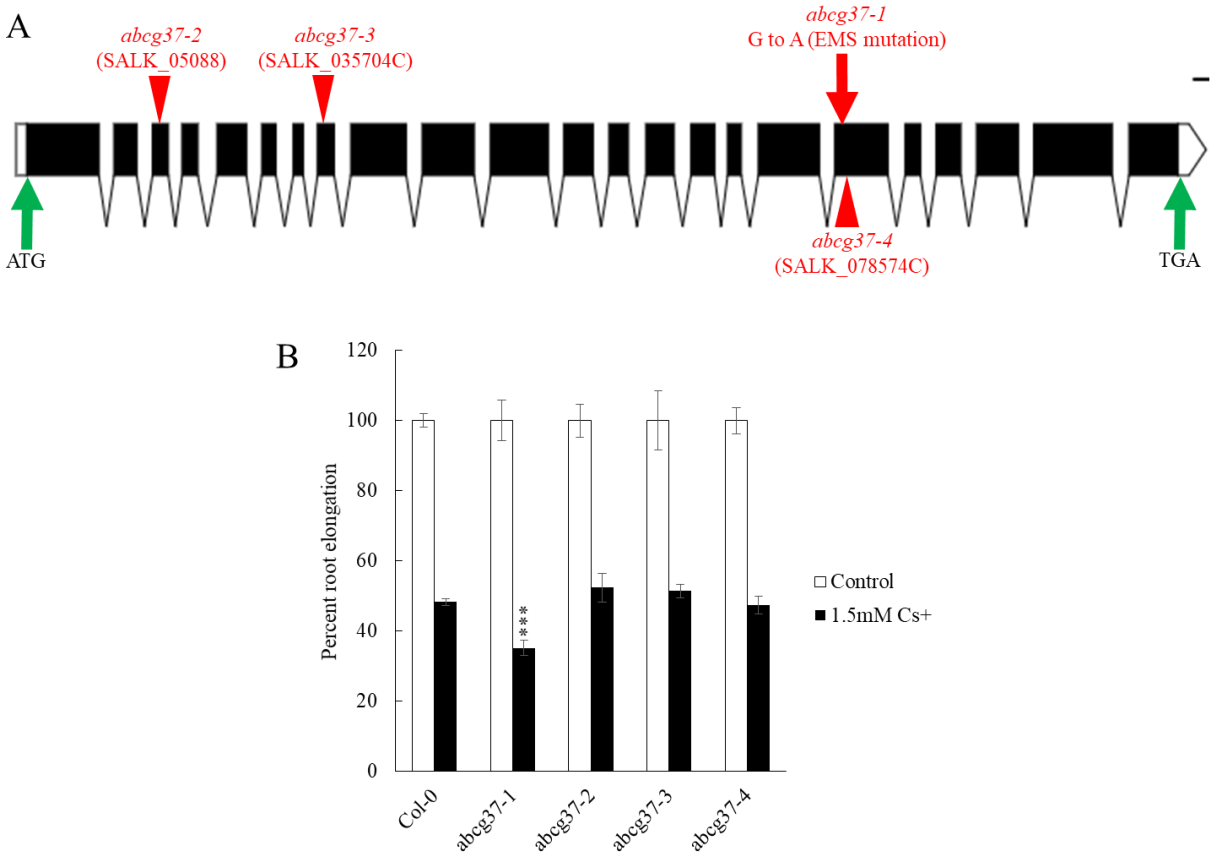

Figure 34. Gain-of-function mutant, *abcg37-1* shows hypersensitive response to cesium

(A) Representative diagram for *ABCG37* mutants used in this study. Solid black box and interrupted black line indicate exon and intron, respectively. (B) Primary root growth elongation of Col-0, *abcb37-1*, *abcg37-2*, *abcg37-3* and *abcg37-4* in presence of 1.5mM Cs^+. Three-day-old light grown seedlings were transferred to new agar plates with and without 1.5mM Cs^+ and incubated at 23°C for three days. Vertical bars mean ±SE from three independent experiments with 8 seedlings observed per experiment. Asterisks represent the statistical significance between treatments as judged by student's *t*-test: ***P < 0.001. Bar =10mm.

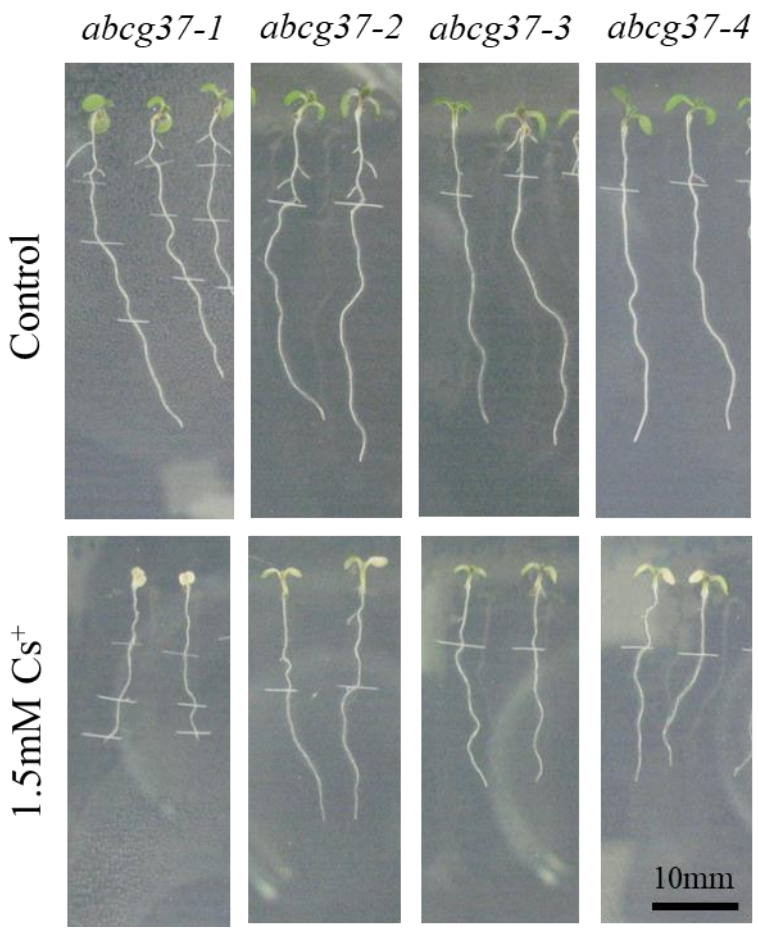

Figure 35. Root phenotype of *abcg37* mutants in presence of cesium

Three-day-old light grown seedlings were transferred to new agar plates with and without 1.5mM Cs^+ and incubated at 23°C for three days.

Root phenotype of wild-type (Col-0), *abcb37-1*, *abcg37-2*, *abcg37-3* and *abcg37-4* after three days incubation in control and 1.5mM Cs^+ plates. Images are representative of at least three independent experiments with 8 seedlings observed per experiment. Bar =10mm.

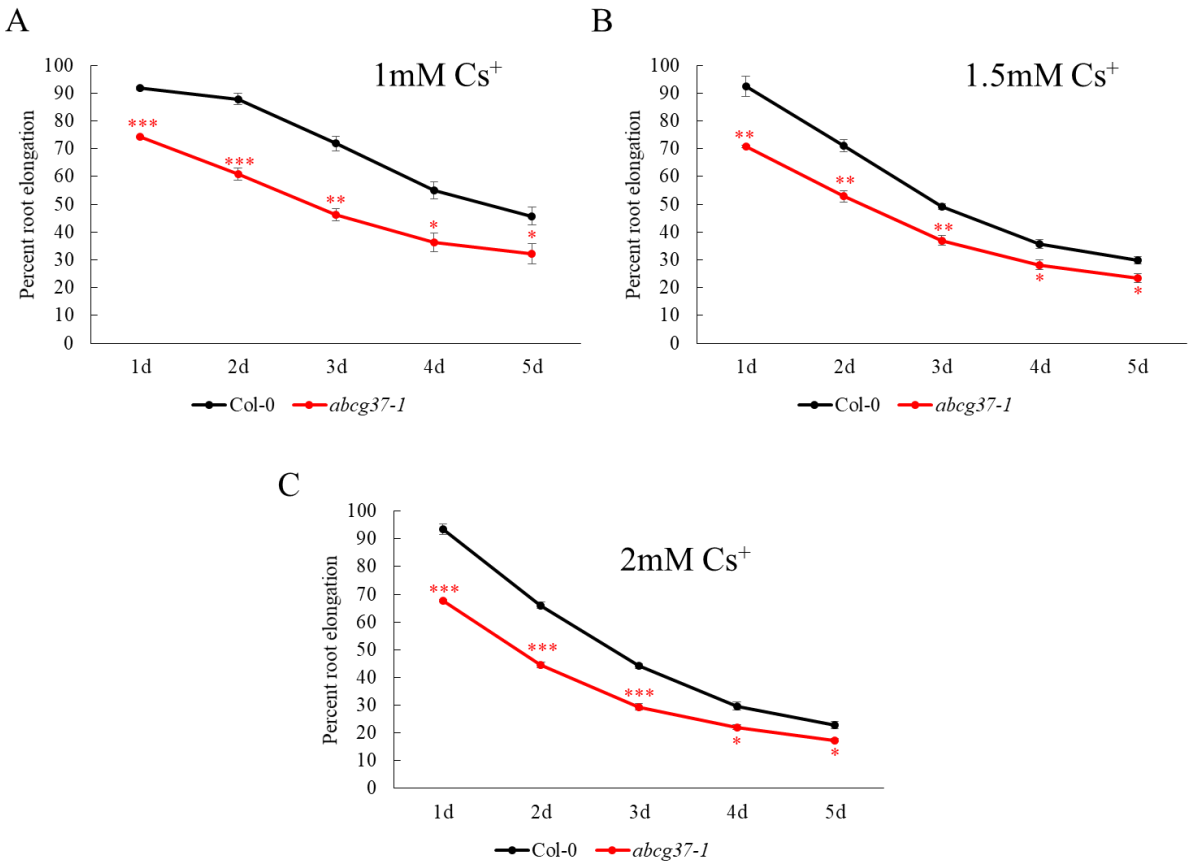

Figure 36. Time course and dose response of Col-0 and *abcg37-1* in cesium

Percentage of primary root growth elongation of Col-0 and *abcb37-1* in presence of 1mM (A), 1.5mM (B) and 2mM (C) Cs^+. Three-day-old light grown seedlings were transferred to new agar plates and incubated at 23°C for five days. Vertical bars mean ±SE from three independent experiments with 8 seedlings observed per experiment. Asterisks represent the statistical significance between treatments as judged by student's *t*-test: *P < 0.05, **P < 0.01 and ***P < 0.001.

3.3.3. ABCG37 and ABCG33 function redundantly as cesium transporter

The unexpected wild-type like response of the loss-of-function ABCG37 mutants to cesium (Figures 34B and 35) prompted us to hypothesize that loss of ABCG37 may be compensated by another ABC protein. For tonoplast localized arsenic transporter, *abcc1 abcc2* double mutant showed severe phenotype compared to individual single mutants, suggesting the existence of redundant function of the ABC proteins (Song et al., 2010). To support the redundancy hypothesis, I searched the close homolog of ABCG37 based on phylogenetic analysis of 43 *Arabidopsis thaliana* ABCG proteins. ABCG33 turned out to be the closest homolog of ABCG37, residing in the same clade (Figure 37). They show ~80% identity at protein level (Figure 38).

Double knockout homozygous *abcg33-1 abcg37-2* mutant was generated to test the redundant functional hypothesis (Figure 49). Consistent with my hypothesis, I found that *abcg33-1 abcg37-2*-11, *abcg33-1 abcg37-2*-21 and *abcg33-1 abcg37-2-23* (three independent double mutant lines obtained from three independent crossing) show resistance to cesium for both root growth inhibition and leaf chlorosis (Figures 39 and 40). The time course and dose response assay revealed that the double mutants show strong resistance to lower concentration of Cs^+ -induced root growth inhibition at all incubation period. The resistant phenotype becomes weaker with progressively higher concentration of Cs^+ (Figure 41). However, at early incubation time point (like 2 days incubation in Cs^+), the double mutants showed strong resistance to Cs^+ irrespective of the concentration (Figure 41). Collectively, these results confirm that ABCG33 and ABC37 act redundantly to transport Cs^+, and possibly function as Cs^+ uptake carriers.

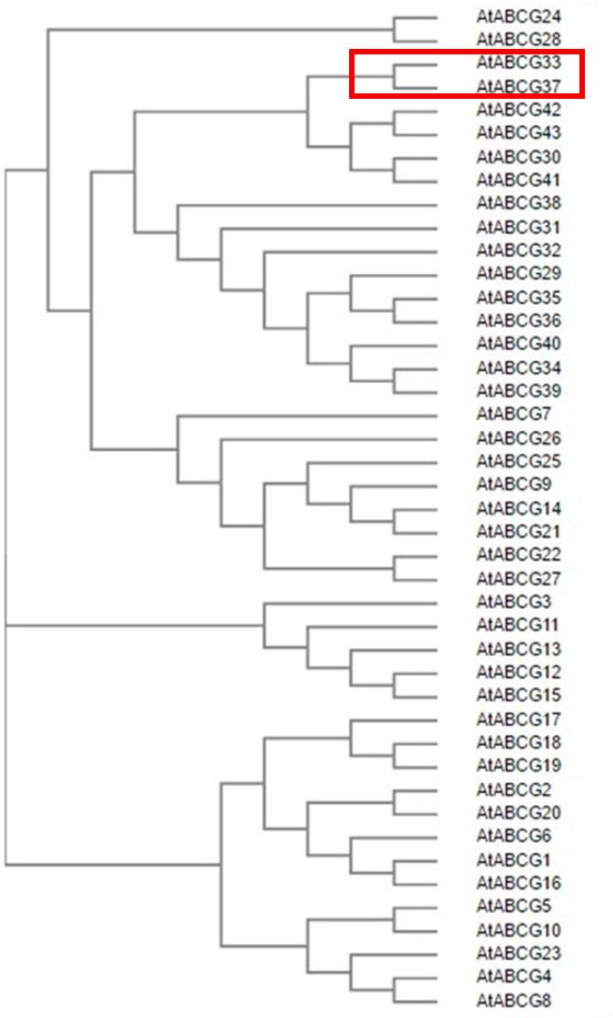

Figure 37. ABCG37 and ABCG33 reside in the same clade

Phylogenetic analysis of 43 ABCG proteins of *Arabidopsis thaliana*. Red marked box indicates the corresponding clade of ABCG37 and ABCG33.

Figure 38. ABCG37 and ABCG33 have higher homology in protein level

Protein sequence homology of ABCG37 and ABCG33. Amino acid residues are colored and perfectly matched positions are indicated by asterisk sign based on Clustal Omega (https://www.ebi.ac.uk/Tools/msa/clustalo/)

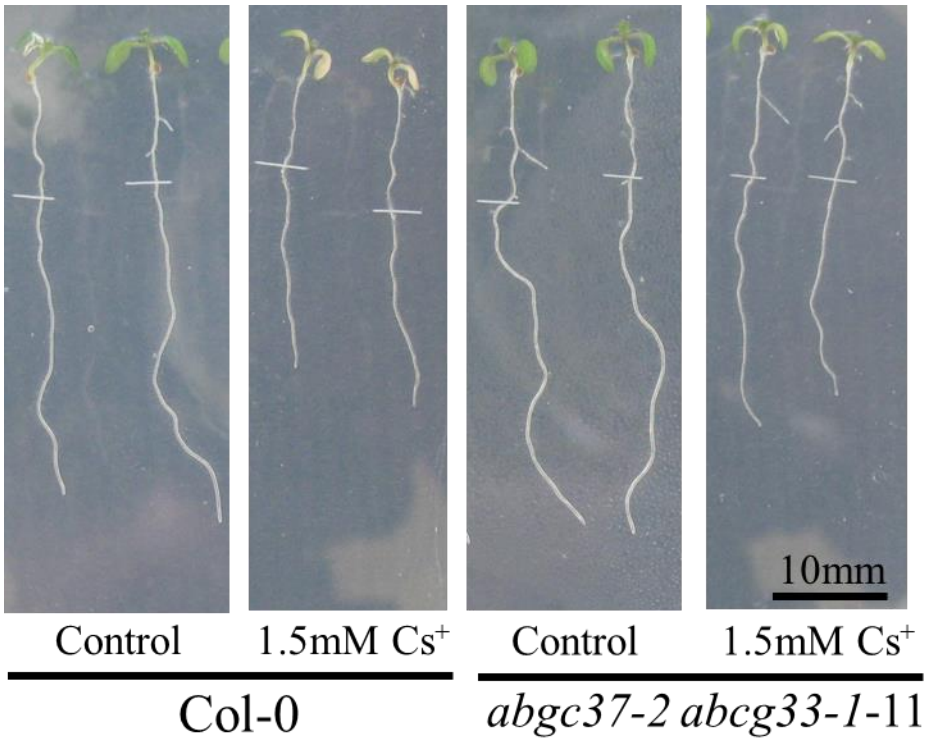

Figure 39. Phenotype of wild-type and *abcg37-2 abcg33-1* double mutant in presence of cesium

Root phenotype of wild-type (Col-0) and *abcg37-2 abcg33-1*-11 after three days incubation in control and 1.5mM Cs^+ plates. Images are representative of at least three independent experiments with 8 seedlings observed per experiment. Bar =10mm.

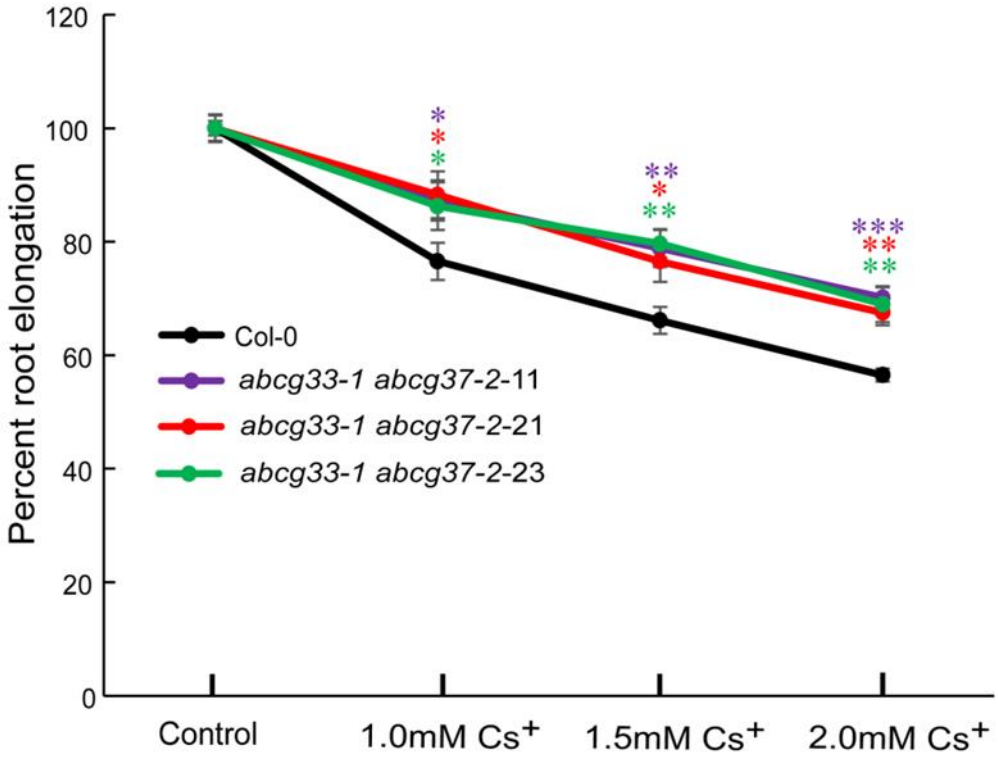

Figure 40. ABCG37 and ABCG33 work redundantly as cesium transporter

Primary root growth elongation of Col-0, *abcb37-2 abcg33-1*-11, *abcb37-2 abcg33-1*-21 and *abcb37-2 abcg33-1*-23 in presence of 1, 1.5 and 2 mM Cs^+. Three-day-old light grown seedlings were transferred to new agar plates and incubated at 23°C for two days. Vertical bars mean ±SE from three independent experiments with 8 seedlings observed per experiment. Asterisks represent the statistical significance between treatments as judged by student's *t*-test: *P < 0.05, **P < 0.01 and ***P < 0.001.

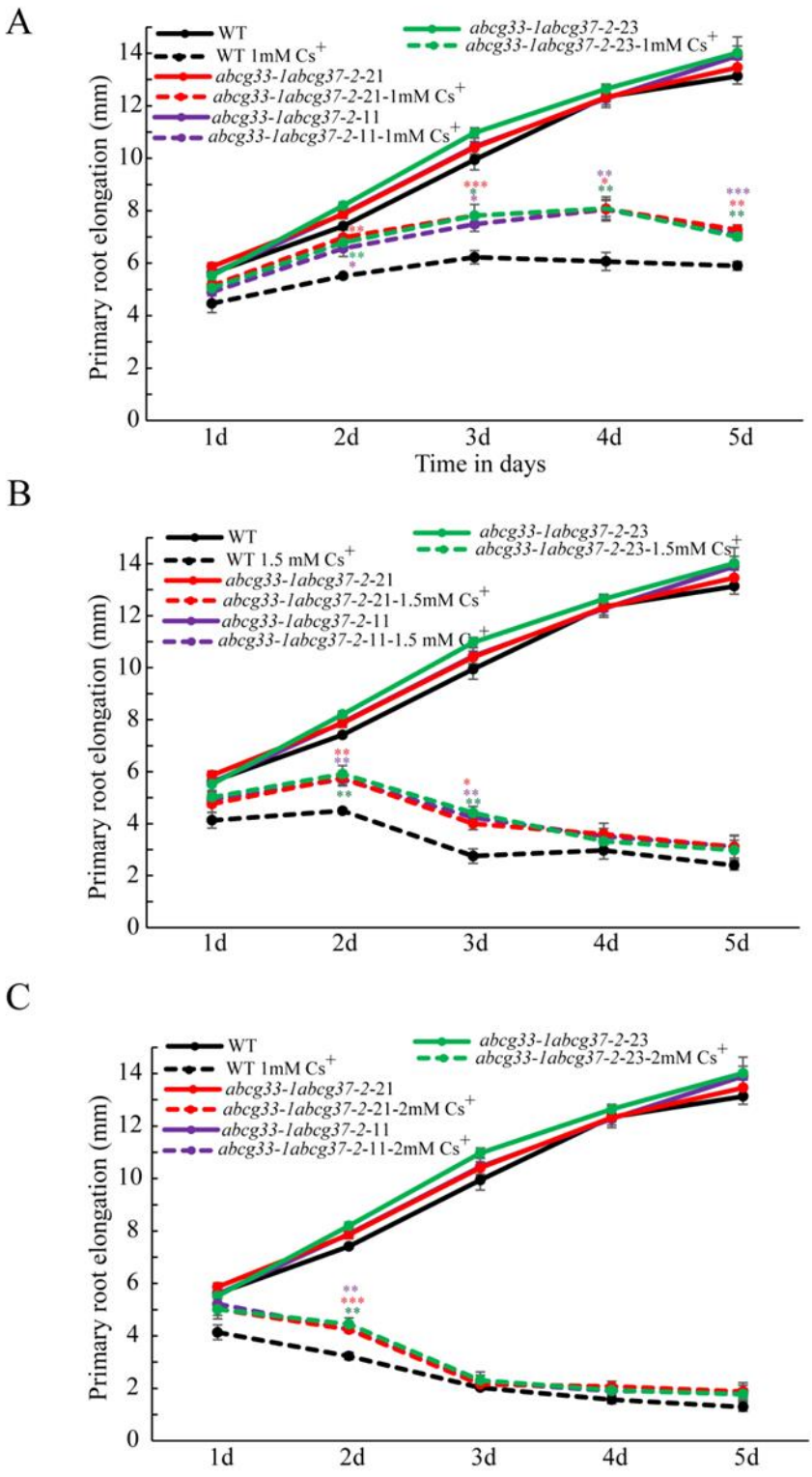

Figure 41. Time course and dose response of abcg33 *abcg37* double mutants in cesium

Primary root growth elongation of Col-0, *abcg37-2 abcg33-1*-11, *abcg37-2 abcg33-1*-21 and *abcg37-2 abcg33-1*-23 in presence of 1 mM (A), 1.5 mM (B) and 2 mM (C) Cs^{+}. Three-day-old light grown seedlings were transferred to new agar plates and incubated at 23°C for five days. Vertical bars mean ±SE from three independent experiments with 8 seedlings observed per experiment. Asterisks represent the statistical significance between treatments as judged by student's *t*-test: *P < 0.05, **P < 0.01 and ***P < 0.001.

3.3.4. Cesium regulates the expression of ABCG37 and ABCG33 at translational level

Many of the metals (Cd^{2+}, Pb^{2+}) regulate the gene expression of their corresponding ABC transporters (*AtABCG36*, *AtABCB25*, and *AtABCG40*) (Lee et al., 2005b; Kim et al., 2006; Kim et al., 2007). Furthermore, differential expression of a group of Arabidopsis genes, including ABC proteins was observed in cesium intoxicated plants (Hampton et al., 2004). To test whether cesium regulates the expression of *ABCG37* and *ABCG33*, I used quantitative real time PCR. However, compared with wild-type, I did not observe any significant changes in the transcripts of *ABCG37* and *ABCG33* in Cs^+ treated plants (Figure 42). This observation is not inconsistent as in few cases it has been shown that transporters' transcriptions are not affected by the application of the substrate. For instance, arsenite has no effect on expression of *AtABCC1* and *AtABCC2* (Song et al., 2010); rice cesium transporters are not transcriptionally altered by cesium (Yamaki et al., 2017).

The quantitative real-time PCR analyses of *ABCG37* and *ABCG33* indicate that ABCG37 and ABCG33 are not under direct transcriptional regulation of cesium. To understand whether Cs^+ regulates ABCG33 and ABCG37 at translational level, I monitored the cellular expression of these proteins using GFP tagged lines. Interestingly, I found that both ABCG37-GFP and ABCG33-GFP intracellular expressions are severely reduced by 1.5 mM cesium treatment in a time dependent manner. The reduction of the GFP signal is maximum on day three but the Cs^+ effect on these proteins are apparent from day 2 (Figures 43 and 45). To clarify the specificity of Cs^+ effect on ABCG33 and ABCG37, I used two root specific membrane proteins, PIN2-GFP (Xu and Scheres, 2005) and EGFP-LTI6b (Kurup et al., 2005) as markers. Cs^+ slightly reduced PIN2-GFP signal but did not affect the LTI6b expression (Figures 44 and 45). These results nullify the possibility that the Cs^+-induced inhibition of ABCG33 and ABCG37 expression is due to toxicity, rather it suggests that Cs^+ selectively inhibits a subset of membrane proteins or accelerates proteolysis.

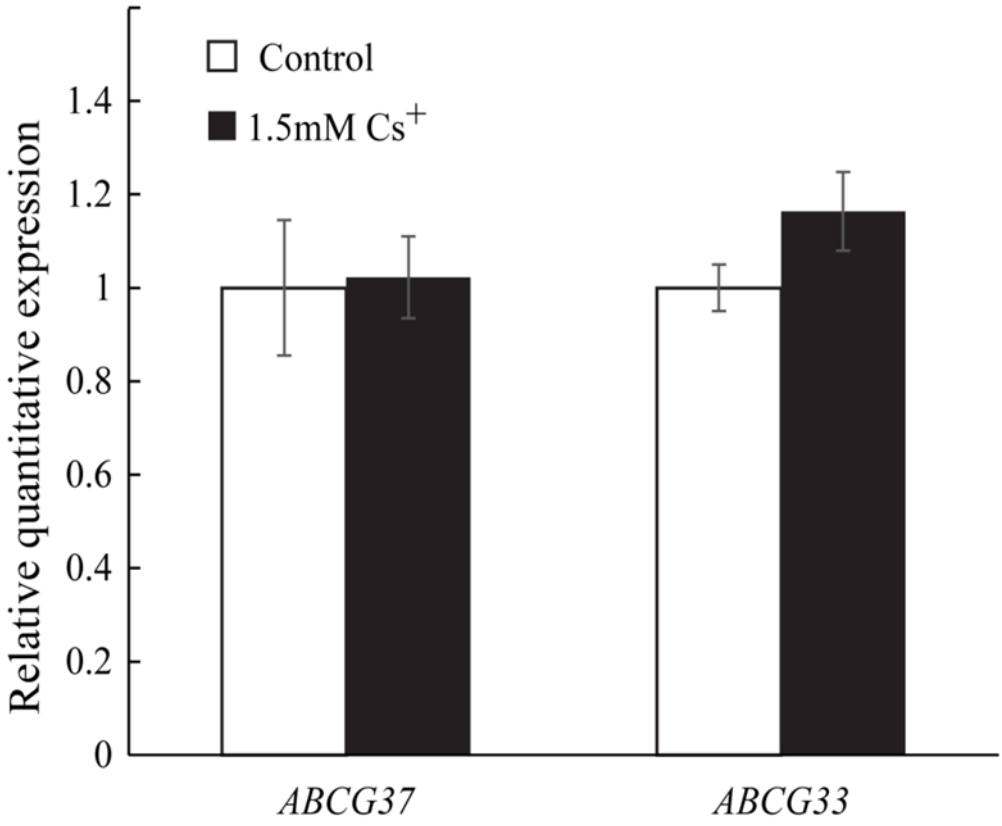

Figure 42. Cesium does not alter the expression of *ABCG33* and *ABCG37*

Relative quantification of *ABCG37* and *ABCG33*in wild-type. Three-day-old light grown Col-0 seedlings were transferred to control and 1.5mM Cs^+ containing plates and incubated for three days. After the treatment, root samples were collected for RNA isolation, cDNA preparation and qRT-PCR analysis. All the data were normalized against EF1α. The data were obtained from three independent biological replicates and show no significant difference between treatments as judged by the student's *t*-test.

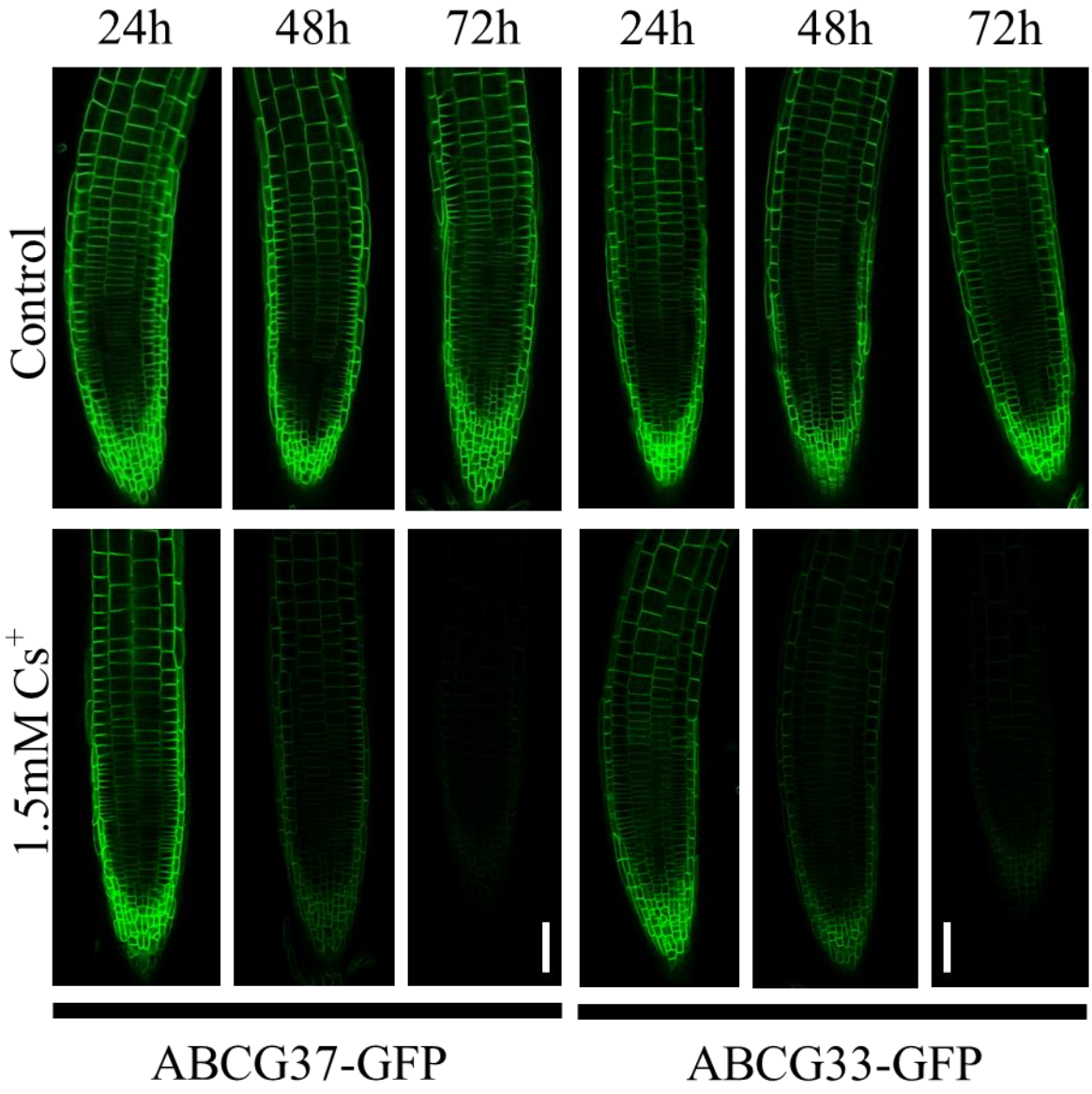

Figure 43. Translational regulation of ABCG37 and ABCG33 in presence of cesium

Three-day-old light grown ABCG37-GFP and ABCG33-GFP seedlings were transferred to control and 1.5mM Cs^+ containing plates. GFP fluorescence of ABCG37-GFP and ABCG33-GFP were observed at 24, 48 and 72h time point. The images are single confocal sections representative of three independent experiments with 5 seedlings observed per treatment for each experiment. Bars = 50µm.

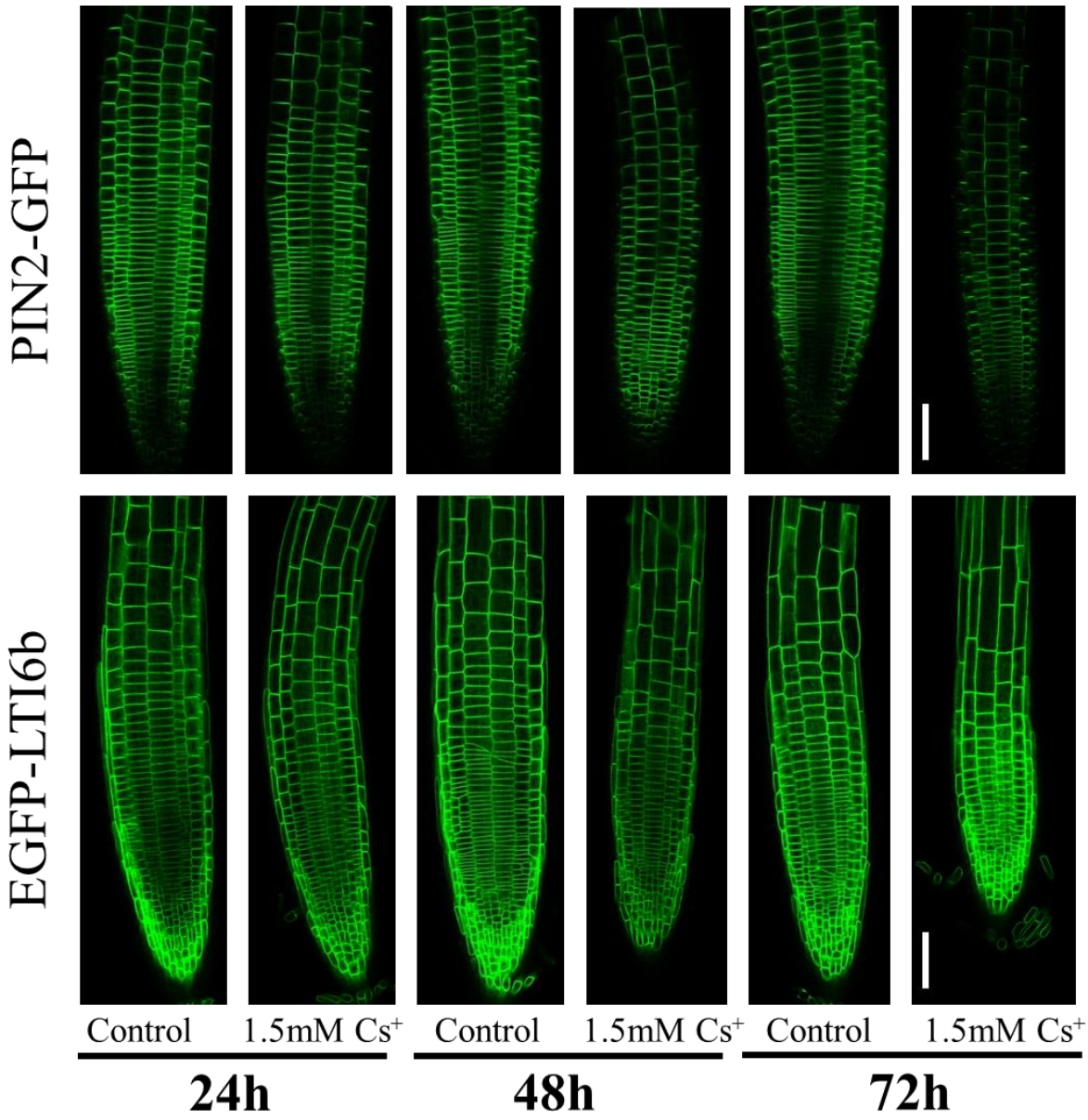

Figure 44. Expression of PIN2-GFP and EGFP-LTI6b in presence of cesium

Three-day-old light grown PIN2-GFP and EGFP-LTI6b seedlings were transferred to control and 1.5mM cesium containing plates. GFP fluorescence of PIN2-GFP and EGFP-LTI6b were observed at 24, 48 and 72h time point under confocal microscope. The images are representative of three independent experiments with 5 seedlings observed per experiment. The seedlings were imaged with same confocal settings for each genotype. Scale bars = 50µm.

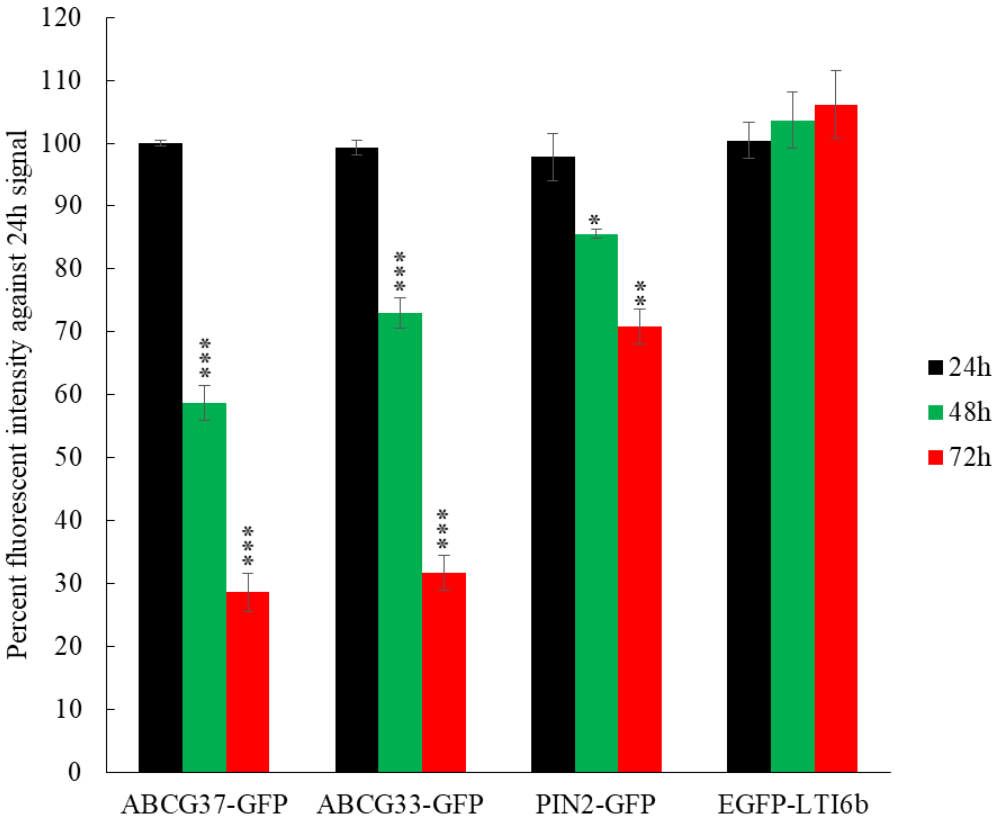

Figure 45. Cesium inhibits the expression of ABCG33 and ABCG37

Quantification of GFP signal in ABCG37-GFP, ABCG33-GFP, PIN2-GFP and EGFP-LTI6b from control and 1.5mM Cs^+ containing plates at 24, 48 and 72h time point. Quantification was performed from three independent experiments with 5 seedlings observed per treatment for each experiment. Vertical bars mean ±SE. Asterisks represent the statistical significance between treatments as judged by student's *t*-test: *P < 0.05 and ***P < 0.001.

3.3.5. ABCG37 and ABCG33 are functionally redundant cesium influx carriers

The physiological, molecular and cellular analyses identified ABCG33 and ABCG37 as potential Cs^+ transporters. However, evidence for direct transport activity is still lacking. To confirm the potential role of ABCG33 and ABCG37 in Cs^+ uptake, I performed a short term uptake assay in Arabidopsis seedlings using different concentration of (0.1 µM, 10 µM, 1.5 mM, and 15 mM) radio labeled cesium (^{137}Cs) in presence (6 mM K^+) and absence (0 mM K^+) of potassium.

Cs^+ uptake capacity of Col-0, *abcg37-2*, *abcg33-1*, *abcg37-2 abcg33-1* (DM21 and DM 23) was measured through scintillation counting. In both presence and absence of potassium, I have observed the reduction of cesium uptake by double mutants (Figure 46). In addition, ICP-MS based measurement Cs^+ and K^+ further confirms the role of ABCG33 and ABCG37 as Cs^+ transport at various potassium concentration (0 mM, 100 µM, 1 mM and, 6 mM). The double mutants contains significantly reduced amount of Cs^+ compared with wild-type (Figure 47A), whereas K+ content remains unaltered (Figure 47B). The short term uptake data along with ICP-MS data suggest that ABCG37 and ABCG33 function as cesium influx carriers.

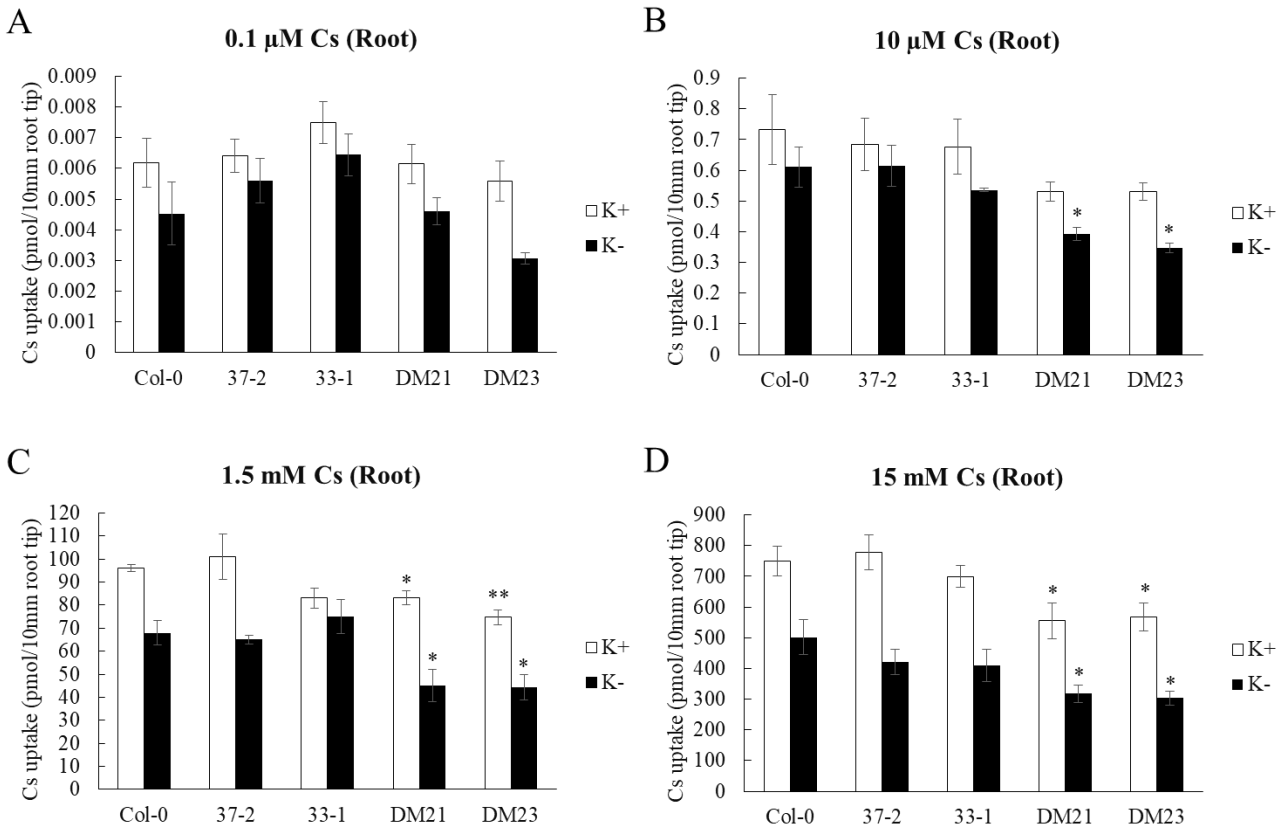

Figure 46. ABCG33 and ABCG37 function as cesium influx carrier

Liquid scintillation count of $^{137}Cs^{+}$ in Col-0, *abcg37-2*, *abcg33-1*, *abcg37-2 abcg33-1* (21) and *abcg37-2 abcg33-1* (23) at 0.1µM (A), 10µM (B), 1.5mM (C), and 15mM (D) Cs^{+} in presence and absence of potassium.

Four-day-old light grown Col-0, single and double mutant seedlings were incubated for 2h at 0.1µM, 10µM, 1.5mM, and 15mM Cs^{+} in presence (6mM) and absence (0mM) of potassium. Incubated seedlings were washed three times thoroughly with or without potassium containing liquid Hoagland solution. For each sample, 10 mm root tip from 10 seedlings were collected. The data were obtained from three independent experiments. Vertical bars mean ±SE. Asterisks represent the statistical significance between treatments as judged by student's *t*-test: **P < 0.01 and *P < 0.05.

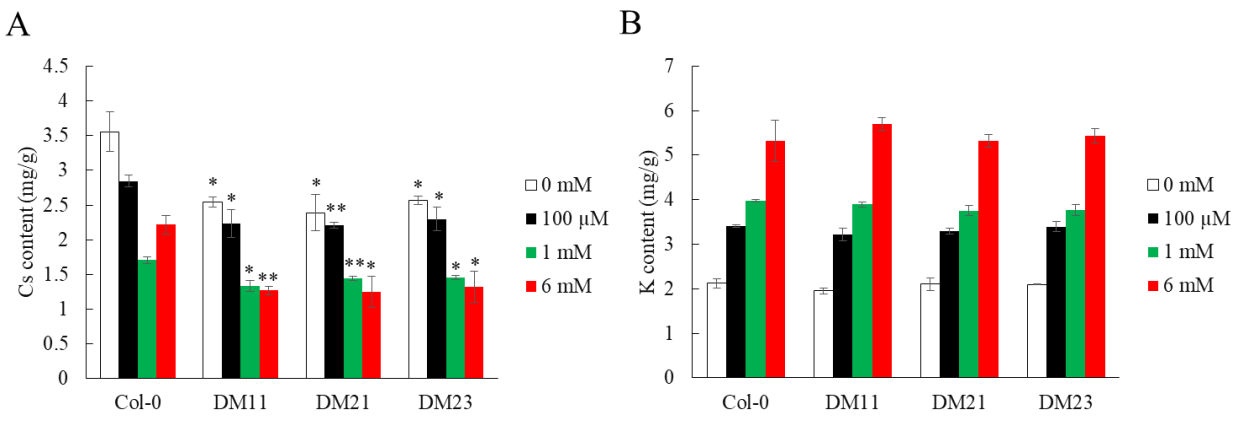

Figure 47. Cesium, not potassium, content is reduced in *abcg37-2 abcg33-1* double mutant

Cesium (A) and potassium (B) content in Col-0 and *abcg37-2 abcg33-1* double mutants. Three-day-old light grown Col-0 and double mutant seedlings were transferred to 1.5mM Cs^+ plates with 0 mM, 100 µM, 1mM and 6 mM potassium and incubated for three days. Cs^+ content of whole seedling was measured by ICP-MS. The data were obtained from three independent experiments. Vertical bars mean ±SE. Asterisks represent the statistical significance between treatments as judged by student's *t*-test: *P < 0.05 and **P < 0.01.

3.3.6. ABCG37 and ABCG33 act as potassium-independent cesium transporter

Because of the structural similarity of Cs^+ with K^+, most of the Cs^+ transporters found today also transport K^+. Here we identified two ABCG proteins functioning as Cs^+ influx transporters. To verify that these proteins solely uptake Cs^+ but not K^+, I measured the endogenous K^+ content in wild-type and double mutants using ICP-MS and also compared the root growth response to a concentration of K^+ that inhibits 50% root growth in wild-type. ICP-MS data revealed no significant difference in K^+ content between wild-type and double mutants (Figure 47B). Consistently, the double mutants respond to exogenous K^+ for root growth like wild-type (Figure 48). These results provide strong evidence in support of the hypothesis that ABCG33 and ABCG37 are Cs^+ specific transporter and act independent of K^+.

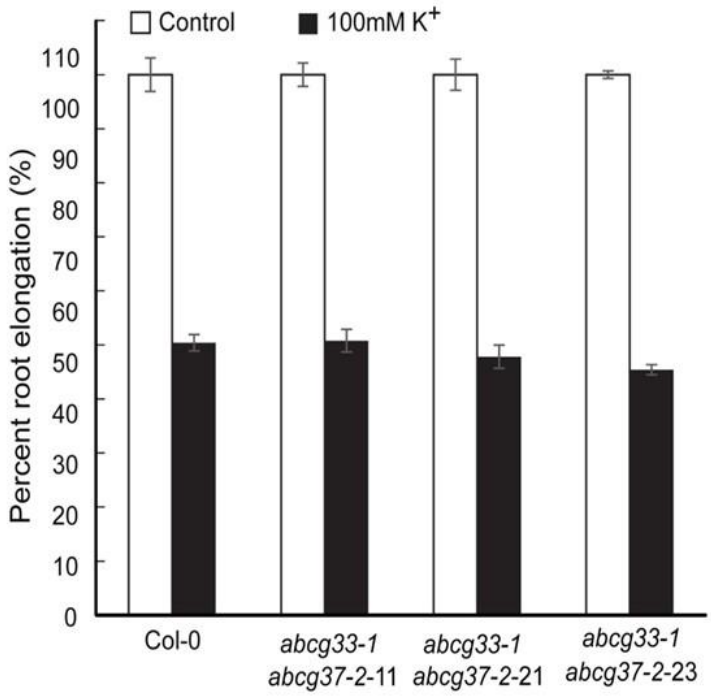

Figure 48. ABCG33 and ABCG37 are potassium-independent cesium transporters

Primary root elongation response of Col-0, *abcg37-2 abcg33-1*-11, *abcg37-2 abcg33-1*-21 and *abcg37-2 abcg33-1*-23 in presence of 100 mM potassium chloride. Four-day-old light grown Col-0 and double mutant seedlings were transferred to 100 mM potassium chloride containing plates and incubated for three days.

Vertical bars mean ±SE from three independent experiments with 8 seedlings observed per experiment. The percent root elongation in double mutant is statistically non-significant compared with wild-type as judged by the student's *t*-test.

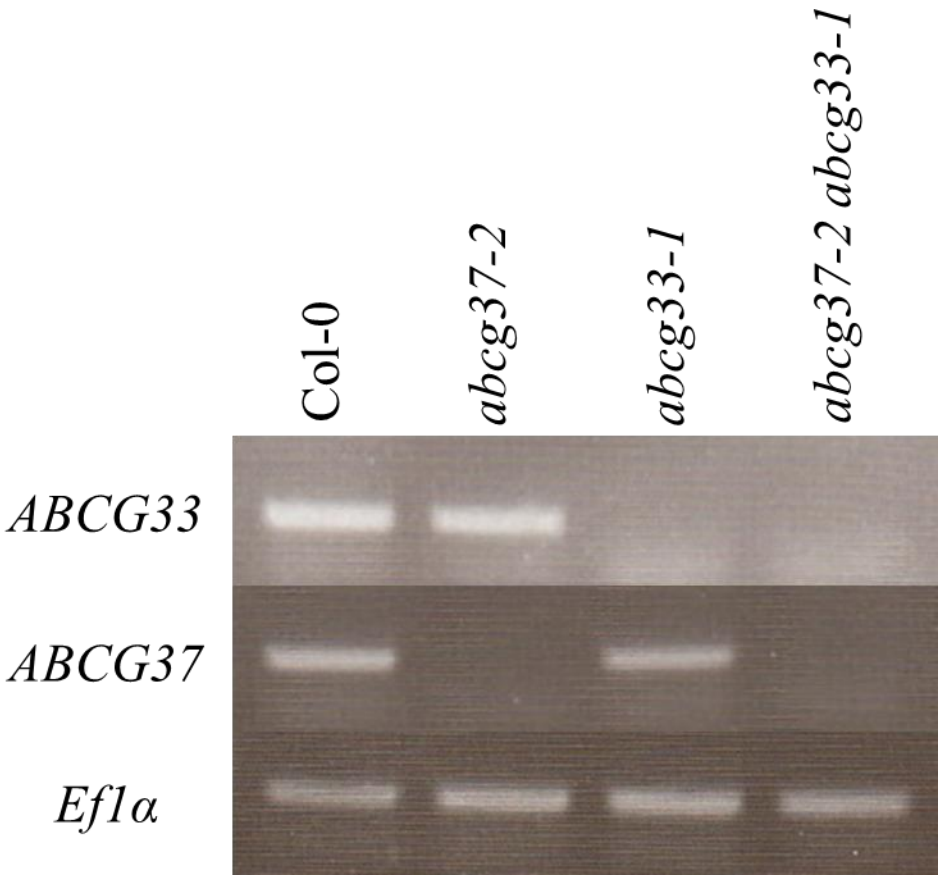

Figure 49. *abcg37-2* and *abcg33-1* are null allele

Seven-day-old light grown Col-0, *abcg37-2*, *abcg33-1* and *abcg37-2 abcg33-1-11* seedlings were collected for RNA extraction and cDNA preparation. *ABCG37* and *ABCG33* specific primers were used to analyze the expression from Col-0, *abcg37-2*, *abcg33-1* and *abcg37-2 abcg33-1*.

3.4. Discussion

Cesium belongs to group I alkali metal with chemical properties similar to K^+. Not surprisingly, the transport and translocation of Cs^+ in plant is tightly linked to K^+. Most of the transporters that had been characterized to date as Cs^+ transporters are directly or indirectly linked to K^+. Recently identified cesium transporters from Arabidopsis, rice, tomato and other system are mostly well studied potassium transporters, such as *OsHAK1* (Nieves‐Cordones et al., 2017; Rai et al., 2017), *AtKUP/HAK/KT9* (Kobayashi et al., 2010), *OsHAK5*, *OsHAK17* (Yamaki et al., 2017), and *SlHAK5* (Ródenas et al., 2017). Even the ecotype screening for cesium transporters pointed out *AtCNGC1* (*CYCLIC-NUCLEOTIDE-GATED CHANNEL 1*) as potential causal gene, which is the close homolog of *AtCNGC2*, a known K^+ transporter (Kanter et al., 2010). In another study, *OsSOS2* had been shown to transport Cs^+ (Ishikawa et al., 2017). However, *OsSOS2* was found to indirectly link to K^+ as in *OsSOS2* mutant, K^+ and Na^+ transporter genes (*OsHAK1*, *OsHAK5*, *OsAKT1*, *OsHKT2;1*) are downregulated at low K^+/Na^+ (Ishikawa et al., 2017). It is predicted that Cs^+ uptake is reduced due to the lower expression of these transporters in presence of the K^+/Na^+ imbalance (Ishikawa et al., 2017). Altogether, these results suggest a possible single pathway of Cs+ transport in plants. However, this idea is partially correct as all the recently identified low cesium concentration mutants function only under low K^+ content (Qi et al., 2008; Ishikawa et al., 2017; Nieves‐Cordones et al., 2017; Rai et al., 2017). At higher K^+ concentrations, the selectivity for K^+ strongly increase and this selective discrimination indicates the existence of alternate route of Cs^+ transport in planta.

In the present study, I identified two ABC proteins (ABCG33 and ABCG37) as cesium specific transporters. The broader specificity of ABC proteins make them excellent transporter of many metals, hormones and chemical compounds. The same ABC transporter can transport many different substrates (Lee et al., 2005b; Kim et al., 2006; Kim et al., 2007; Song et al., 2010; Park et al., 2012). For instance, ABCG37 has been shown to play an important role in transporting auxin, synthetic auxin, iron and coumarin (Ito and Gray, 2006; Růžička et al., 2010; Fourcroy et al., 2014). In contrast, the functional role ABCG33 is yet undefined although it may function in transporting monolignol (Schuetz et al., 2014). These physiological, genetic, cell biological and direct transport assay data indicated that ABCG33 and ABCG37 function redundantly in uptaking Cs^+. Additionally, the reduction in Cs^+ uptake in *abcg33 abcg37* double mutant is not linked to low K^+

availability as all the experiments were performed using standard K^+ concentration. The specificity of these proteins to transport only Cs^+ but not K^+ was also confirmed by measuring the endogenous K^+ concentration and root growth response to high concentration of exogenous K^+ in the double mutant lines. The finding that ABC proteins function as Cs^+ specific influx carriers is supported by the recent identification of cesium transporters from the screening of rice-transporter-enriched yeast expression library. Rice OsABCG45 is functionally active as cesium transporter in yeast (Yamaki et al., 2017), and shows ~50% homology with both ABCG33 and ABCG37 from Arabidopsis. Cs^+ intoxication results in upregulation of *AtABCG16*, *AtABCA7* and *AtNAP5* in Arabidopsis (Hampton et al., 2004). In addition, during screening in the present study, I found additional three loss of function ABC mutants; *abcb15, abcg36* and *abcg42* showing hypersensitive response to Cs^+-induced inhibition of root growth. Collectively, these results suggest that beside ABCG33 and ABCG37, other ABC transporters may function as cesium transporters.

Although it has been shown that both low and high Cs^+ can alter the gene expression in Arabidopsis (Hampton et al., 2004; Sahr et al., 2005b; Sahr et al., 2005a), ABCG33 and ABCG37 are not under the transcriptional regulation of Cs^+. Cesium alters the expression of ABCG33 and ABCG37 protein in a time dependent manner. Since ABCG33 and ABCG37 function as Cs^+ influx carriers, one plausible explanation is plants shut off the transporters to protect it from long term toxicity. This process is possibly regulated by the cesium-mediated post-translational regulation of transporters. However, the mechanism of this regulation is still unclear. Similar observation was reported for BRASSINOSTEROID INSENSITIVE 1(BRI1) receptor regulation at prolonged ambient temperature. Although 26°C incubation did not alter the transcript of *BRI1*, the protein expression was shown to be decreased in a time dependent manner (Martins et al., 2017). Polyubiquitin-dependent endocytosis and degradation have been suggested to regulate this process (Martins et al., 2017). Cesium toxicity has already been reported to induce proteolytic degradation of AGO1 possibly through autophagy (Jung et al., 2015). Recent studies on ethylene signaling provided further insight about translational regulation. C-terminal end of EIN2 (EIN2-CEND) interacts with 3'UTR of EBF1/2 and represses the translation of EBF1/2 by directing them towards P body for RNA decay. As a result, EBF1/2 become unable to degrade EIN3/EIL1, major transcription factors for ethylene-mediated response (Li et al., 2015; Merchante et al., 2015). These results indicate the existence of various mechanisms for post translational regulation of proteins.

Future research focusing on understanding the cesium-mediated translational regulation will shed light on intracellular Cs^+ signaling events.

The present work identified the long sought K^+-independent transport pathway of Cs^+. ABCG protein mediated transport facilitates the Cs^+ transport along with known K^+ transporters. Based on the results, I developed a working model where cesium uptake and transport inside the cell are mediated by potassium transporters, ABC transporters (ABCG37 and ABCG33) and other unknown transporters (Figure 53). Hence, in the double knockout mutant I did not observe complete resistance to cesium. Bio remediation of the contaminated soil is a clever and affordable technology, which is largely unused for Cs^+ removal because of the similarity in chemical properties of Cs^+ to K^+, which is a major macronutrient for plant growth. Removal of K^+ transporters affects the plant growth and also low K^+ content soil is also a common requirement to transport contaminated Cs^+ (Nieves‐Cordones et al., 2017; Rai et al., 2017; Ródenas et al., 2017; Yamaki et al., 2017). Future research aiming in generating new transgenic plants manipulating both K^+ transport pathway and the newly identified ABC protein mediated Cs^+ transport pathway will facilitate the efficient removal of Cs^+ from the contaminated soil.

Chapter 4

General Discussion

Plasma membrane functions as the boundary of cell and membrane-localized/associated proteins are responsible for the perception, signal transduction and protection from abiotic stress. Although the role of membrane proteins in abiotic stress regulation has been started to emerge, to develop stress resistant crop varieties is still elusive due to the lack of our understanding related to abiotic stress response mechanism. The model plant *Arabidopsis thaliana* provides an amazing system to decipher the molecular mechanism of abiotic stress regulation. In this thesis work, I have used *Arabidopsis thaliana* as a working system to understand the role of membrane proteins during cold (Chapter 2) and cesium stress (Chapter 3). Understanding the molecular mechanism from the model plant will help us to translate this knowledge to engineer crop plants for developing abiotic stress tolerant varieties. To meet the challenge of global food crisis, one of the major issues is to combat the abiotic stress in terms of crop productivity.

In the chapter 2, I have focused on the endosomal trafficking pathways and proteins associated with corresponding pathways to dissect their role in the cold stress regulation. Prior knowledge suggests that PIN2 trafficking is inhibited due to cold stress (Shibasaki et al., 2009; Rahman, 2013; Shibasaki and Rahman, 2013) and PIN2 proteins are continuously endocytosed inside the cell (Dhonukshe et al., 2007). In the cold stress screening, I have identified GNOM as a cold stress response regulator (Figure 50). Interestingly, the role of *GNOM* as temperature responsive gene had been reported from the study of yeast (Steinmann et al., 1999). How does GNOM integrate cold signaling and cellular response, is still unknown. One of the major integration points is the membrane-associated GTPase activity of GNOM and subsequent cellular events. Recent studies have shown that COLD1-mediated induction of GTPase activity increases cold stress tolerance (Ma et al., 2015). Investigating the GTPase activity of GNOM during cold stress and downstream molecules activated through the process will provide insights regarding GNOM-mediated cold responsive pathway.

GNOM participates in the recycling endosomal pathway and involves in PIN2 trafficking. Inhibition of protein trafficking inside the cell via fungal toxin Brefeldin A (BFA) helps to demonstrate the co-localization of GNOM and PIN2 both in the same characteristic BFA bodies

(Dhonukshe et al., 2007). As a result, the cold-mediated targeting of GNOM (this study) impairs the PIN2 trafficking (Shibasaki et al., 2009; Rahman, 2013; Shibasaki and Rahman, 2013). Inducible repression of GNOM shows the disruption of shoot-ward auxin flow in the epidermal cells, which is mediated by PIN2 and required for gravitropism (Guo et al., 2014). Cellular events are orchestrated through the coordinated regulation of multiple trafficking proteins. Cold-mediated targeting of GNOM – PIN2 pathway is one of them, and the role of rest of trafficking system under cold stress is still obscure. Two potential future endeavors are: 1) identification of interacting GNOM proteins and 2) isolation of GNOM and PIN2 containing BFA bodies to decipher unknown proteins. We already have some substantial, not comprehensive, idea about GNOM interacting proteins Cyclophilin 5 (Grebe et al., 2000) and AHK4 (Dortay et al., 2008). The latter approach, isolation of BFA bodies, is more specific strategy, but experimentally challenging to accomplish till date.

In this study, using GNOM-engineered or BFA resistant line, I have shown that point mutation in the catalytically conversed SEC7 domain causes over-expression of GNOM and results in cold stress tolerance (Figure 50). Previous studies demonstrated that BFA treatment alters root gravitropism, but the root gravitropism of BFA res. line remains same with or without BFA treatment (Geldner et al., 2003). It clearly suggests the perfectly maintained auxin homeostasis in the BFA resistant line, which is required for root gravitropism. Interestingly, cold stress affects root gravitropism by altering auxin homeostasis (Shibasaki et al., 2009). My finding provides the mechanistic explanation of point mutation induced GNOM over-expression for maintaining auxin homeostasis under cold stress and subsequently shows cold resistant phenotype. Interestingly, same kind of mutation is observed in GNL1 (Geldner et al., 2003), but knockout mutants do not show cold sensitive phenotype. It suggests that point mutation based cold stress regulation is GNOM-specific.

Although the mutation in the SEC7 was artificially induced, this point mutation or single nucleotide polymorphisms (SNPs) is reminiscing about the natural variation or ecotypes (Figure 51). Till date, approximately 300 ecotypes have been identified around the globe and the whole genome was sequenced. Among these ecotypes, few of them are adapted from cold regions. It would be interesting to observe the role of this particular amino acid to act as a pivotal point for

cold stress tolerance from natural variation and cold acclimated varieties (Figure 52). This will help us to develop point mutation-based cold tolerant model from natural variation.

In the chapter 3, I tried to understand the transport mechanism of cesium. Cesium is chemically similar to essential nutrient potassium. Potassium is the most abundant ion inside the plant cell and participates for a wide range of biological functions such as maintenance of electrical potential gradients across the membrane, generation of turgor pressure, activation of enzymes (Britto and Kronzucker, 2008). Due to the chemical similarity, cesium exploits the potassium transport system at plasma membrane. But, the long sought question was whether cesium has potassium-independent transport system? In this study, I have identified two potassium-independent cesium transporters (ABCG37 and ABCG33) and double knockout mutant (*abcg37-2 abcg33-1*) has resistant phenotype against cesium. Unfortunately, the double knockout mutant from my study is not completely resistant to cesium, which suggests the existing role of potassium transporters and a set of unknown cesium transporters (Figure 53). As a result, even in the double knockout, plants experience cellular toxicity and consequent inhibition of growth.

The cellular detoxification process is mediated through cysteine-rich oligomers, also known as Phytochelatins (PCs) (Pochodylo and Aristilde, 2017). This PC-based sequestration helps to reduce toxicity inside the cell. Trapped components are transported from cytosol to the vacuole and entered into the vacuole through tonoplast transporters. Vacuolar sequestration process is mediated by ATP-dependent vacuolar pumps (V-ATPase and V-PPase), ABC transporters, zinc iron permeases (ZIPs) and natural resistance-associated macrophage proteins (NRAMPs) (Sharma et al., 2016). Future research should be focused on understanding the cellular detoxification process for cesium and tonoplast localized cesium transporter. For this purpose, screening of tonoplast localized ABCC transporters for cesium response will be the most rational approach. Because, two ABCC transporters, ABCC1 and ABCC2, have already been reported as vacuolar metal-PC complex transporter in both *Schizosaccharomyces pombe* (Mendoza-Cózatl et al., 2011) and *Arabidopsis* (Park et al., 2012). Combining these two characterized cesium transporters (this study) with the identification of tonoplast localized cesium transporter will help to map the entire cesium-related pathway and develop plant which has minimal effect due to cesium (Figure 54).

In this study, I have found that cesium degrades its own influx carriers (ABCG37-GFP and ABCG33-GFP) in a time dependent manner. The logic behind degrading its own transporter is enigmatic. Based on the current knowledge, protein degradation in plants occurs through either ubiquitin proteasome system (UPS) (Lyzenga and Stone, 2011) or by autophagosomes induction (Liu and Bassham, 2012). Ubiquitination is employed to degrade unwanted proteins and autophagy delivers damaged proteins to vacuoles. Metal stresses have been reported to involve in proteolysis. For instance, cadmium induces the expression of ubiquitin proteasome pathway in yeast (Jungmann et al., 1993). In the same way, Cd induces ubiquitin expression in both root and shoot of rice plant (Oono et al., 2016). Similar to ubiquitination, different metals (Cu, Ni, Zn, Cd and Mn) induce the expression of a group of ATG genes, required for the autophagy process (Zhang and Chen, 2010; Zheng et al., 2012). Further investigation will reveal whether cesium-induced degradation of ABCG37 and ABCG33 is ubiquitin or autophagy dependent.

Additionally, the role of post-translational regulation is unexplored for metal transportation. Recently, it has been demonstrated that phosphorylation-mediated regulation of ABCC1 (Ser^{846}) activity is essential for vacuolar sequestration of As. From the phosphomimic mutant study, they have demonstrated that phosphorylation of Ser^{846} plays pivotal role for the As resistance function of ABCC1 (Zhang et al., 2017). Future research on the post-translational modification of identified cesium influx carriers (ABCG37 and ABCG33) may lead to different dimension of metal stress regulation.

Considering the both abiotic stresses from this thesis work, it helps me to conclude that membrane proteins play vital role as transporter and signal transducing intracellular trafficking components during abiotic stress. Alteration or manipulation of membrane proteins has potentiality to bring changes at cellular and whole plant architecture against abiotic stress. For instance, GNOM provides agronomically important function under cold stress and translating this knowledge to crop plants will help to develop cold resistant varieties. In the same way, double knockout mutant (*abcg37-2 abcg33-1*) demonstrates low cesium uptake phenotype without affecting regular growth of plants. Combining this strategy with existing low cesium containing plants will help to produce crops in cesium containing soil in near future. The discoveries from this work: point mutation based cold stress tolerance and potassium-independent cesium

transporter are mechanistically unique approaches and proposed for the first time. Findings of this research will help to develop crop varieties to fight the global food crisis.

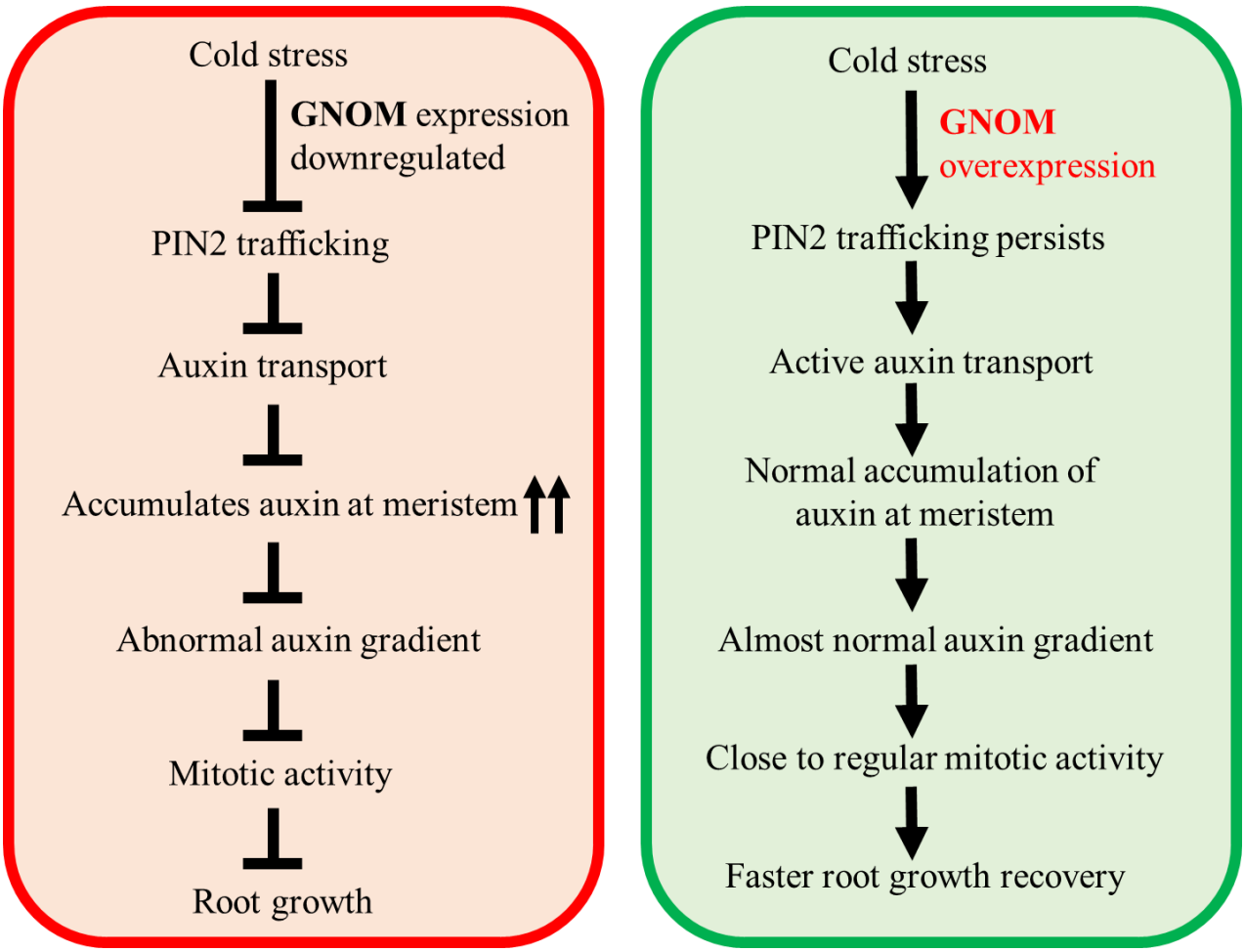

Figure 50. Graphical model of GNOM-mediated cold stress response

Schematic representation of current working model of GNOM-mediated cold response in Arabidopsis. Left panel demonstrates the typical wild-type GNOM and the right panel demonstrates GNOM-engineered BFA res. line or GNOM overexpression under cold stress. GNOM-engineered BFA res. line or GNOM overexpression facilitates the PIN2 endocytosis after low temperature treatment and consequently maintain active auxin transport and auxin gradient in root as well as. Proper maintenance of auxin gradient helps mitotic activity to keep going and maintain the root growth recovery even after cold stress.

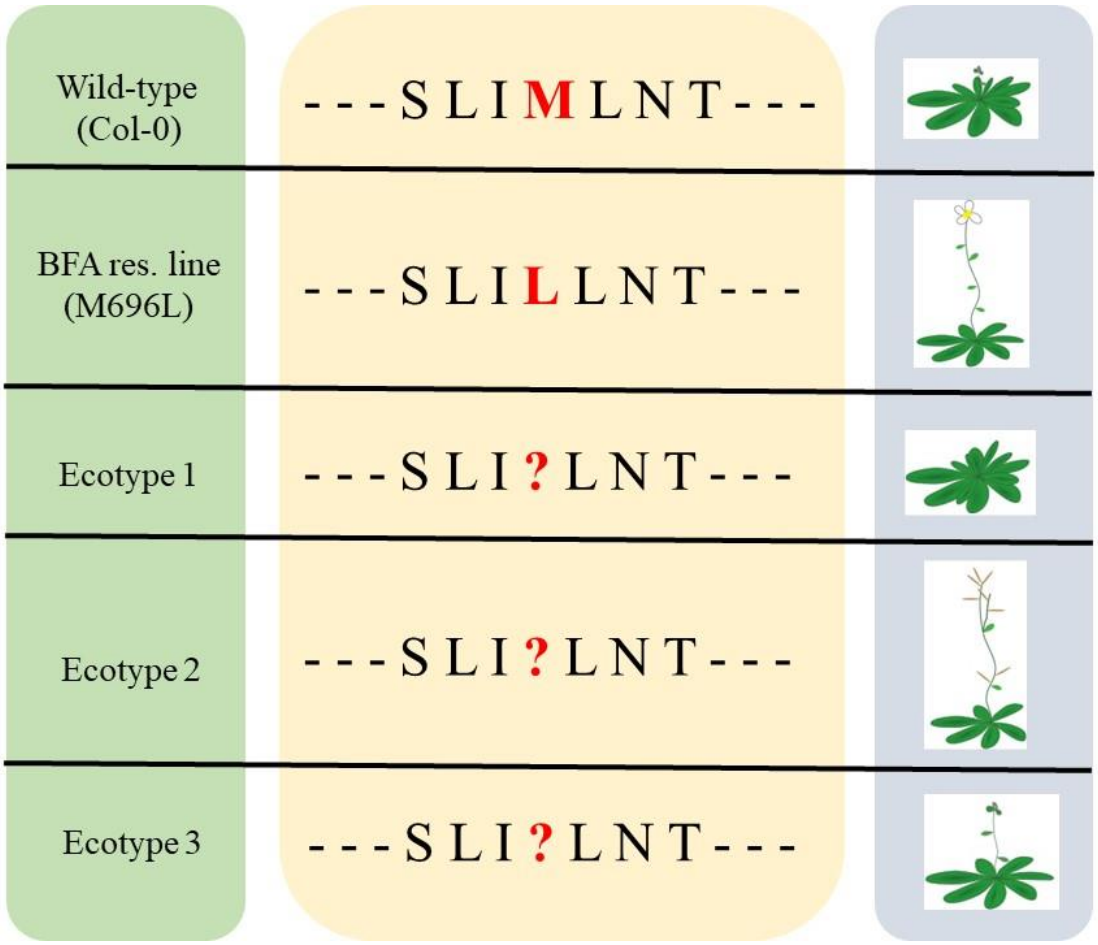

Figure 51. Point mutation based cold tolerance model

Point mutation at conserved SEC7 domain confers cold resistance. Alteration of this amino acid may have different degree of cold resistance based on the replace amino acids.

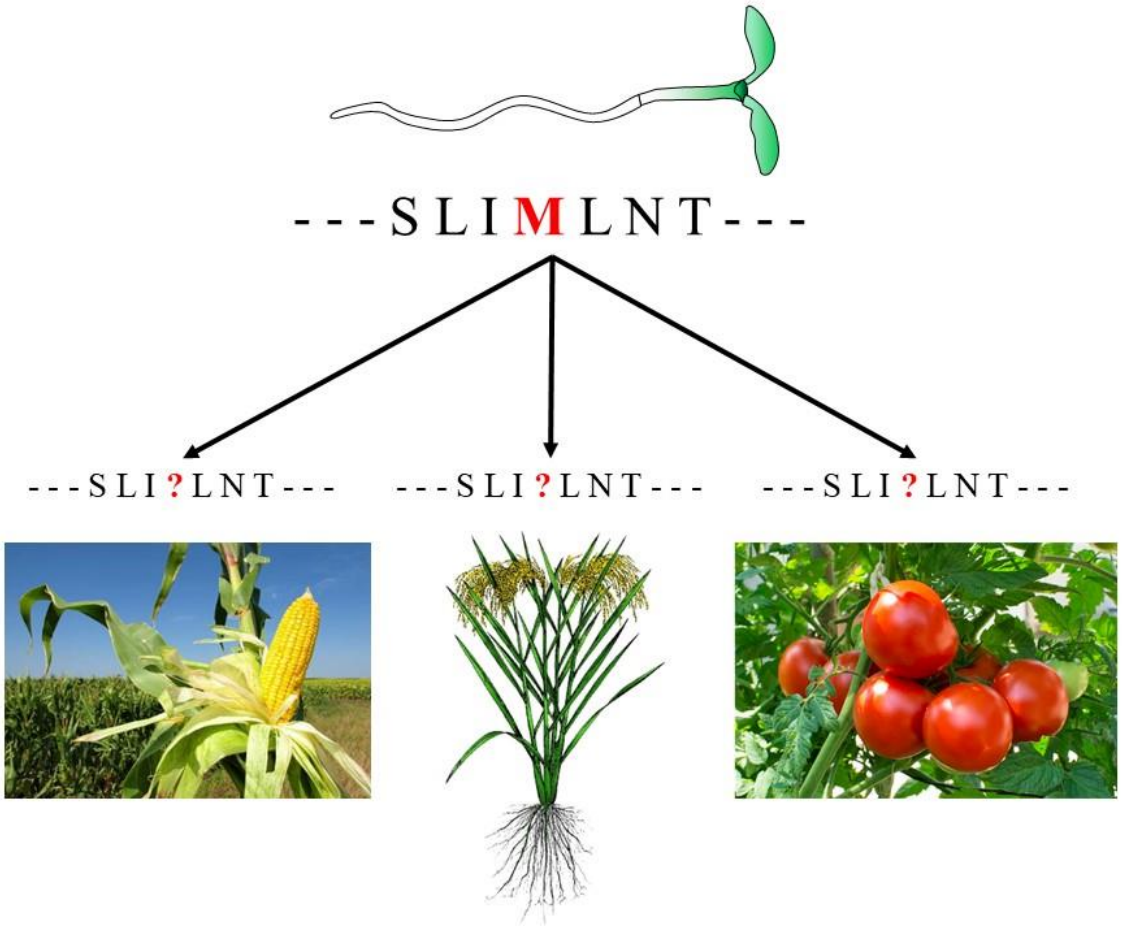

Figure 52. Predictable cold tolerance mechanism based on the knowledge of the model plant

GNOM, as well as SEC7 domain, is conserved around the kingdom, from plant to animal system. Identification of mutation in the SEC7 domain of GNOM in the crop plant varieties may help to characterize cold tolerant plant.

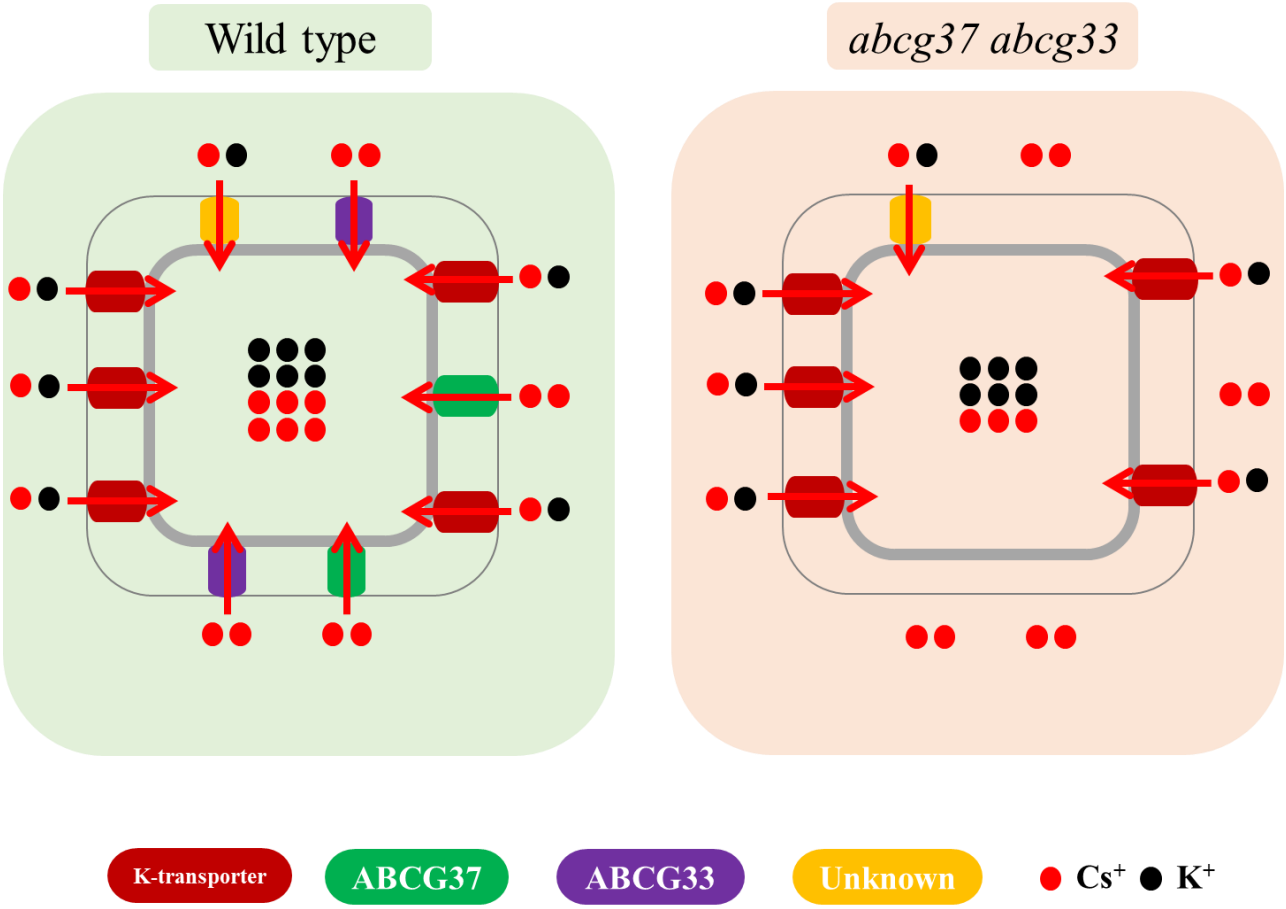

Figure 53. Graphical model of cesium uptake

Schematic representation of current working model of Cs^+ uptake in Arabidopsis. Left panel demonstrates the typical Cs^+ uptake inside wild-type (Col-0) cell using various transporters, including ABC proteins. Right panel shows the loss of ABCG33 and ABCG37 in double knockout mutant resulting in reduced Cs^+ uptake. K^+ transporters are presented in red, ABCG33 in purple, ABCG37 in green and yet unidentified Cs^+ transporters are in yellow.

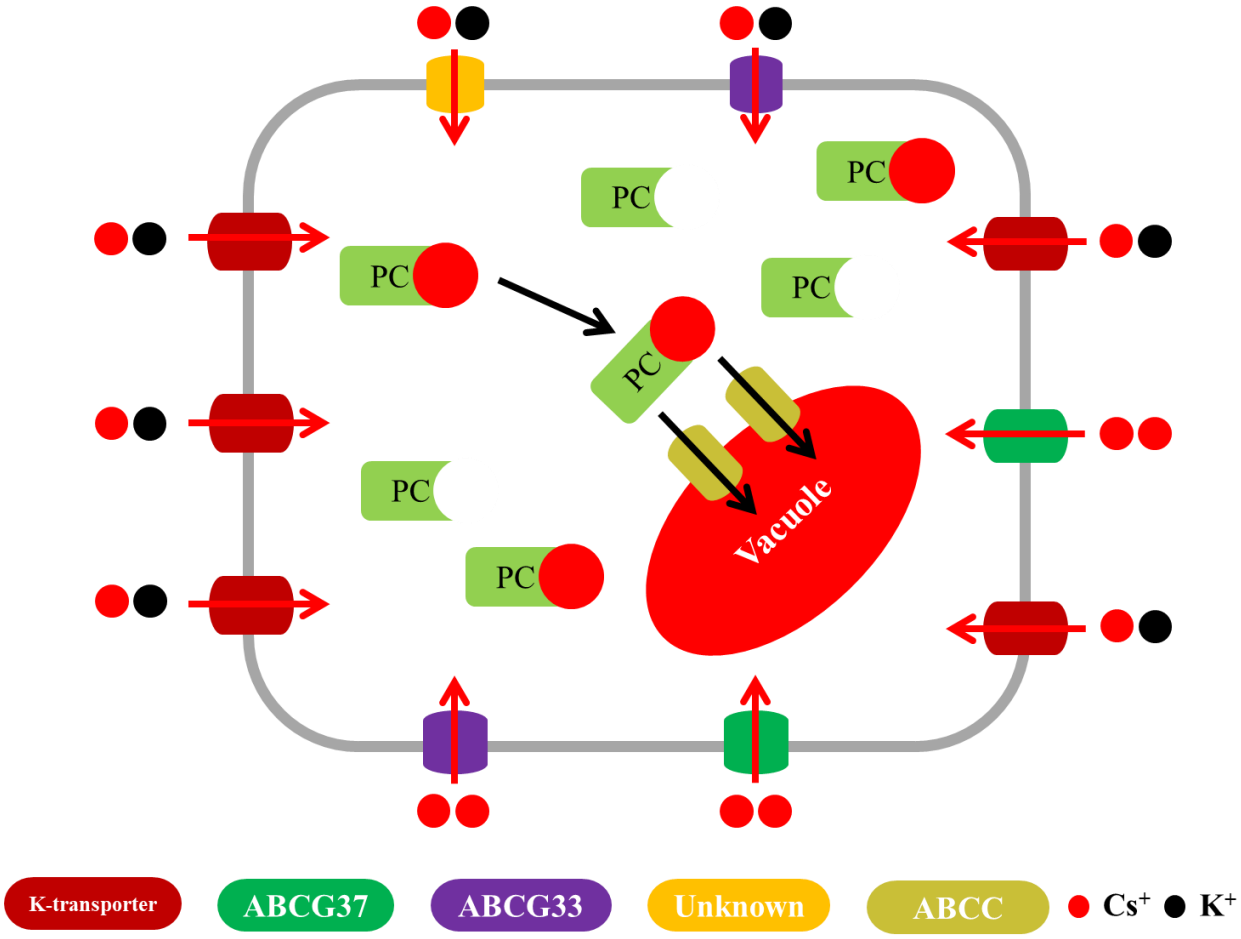

Figure 54. Intracellular cesium detoxification model

Probable model for intracellular detoxification is mediated through firstly binding with phytochelatins (PCs) and eventually sequestered inside the vacuole.

Acknowledgement

I would like to thank my supervisor Dr. Abidur Rahman for his guidelines, discussion and critical review of the experimental data and manuscripts. I am grateful to Dr. Matsuo Uemura of Iwate University, Dr. Wataru Mitsuhashi of Yamagata University and Dr. Michiko Sasabe, Hirosaki University for their support and suggestions throughout the both research projects.

I am grateful to our collaborator Dr. Keitaro Tanoi and Dr. Ryuhei Sugita from The University of Tokyo for their endless support to carry out transport assay of cesium and ICP-MS experiment.

I would like to thank Takashi Ueda (National Institute of Basic Biology, Japan), Nobuharu Fujii (Tohoku University, Japan), Satoshi Naramoto (Tohoku University, Japan), Wu Shuang (Fujian Agriculture and Forestry University, China), Hidehiro Fukaki (Kobe University, Japan), Peter Mergaert (French National Center for Scientific Research, France), Sachihiro Matsunaga (Tokyo University of Science, Japan), Ben Scheres (University of Utrecht, The Netherlands), Gloria Muday (Wake Forest University, Winston-Salem, NC, USA), Edgar Spalding (Department of Botany, University of Wisconsin Madison, WI, USA), William M. Gray (University of Minnesota, Saint Paul, MN, USA), Angus Murphy (University of Maryland, College Park, MD, USA), Lacey Samuels (University of British Columbia, Canada) for sharing the study materials.

The cold stress project was supported in part by the Iwate University grant for high level research (Abidur Rahman). The cesium transporter identification work was partially funded by Iwate University President Fund (Abidur Rahman), and UGAS, IU Research fund 2017 (Mohammad Arif Ashraf). Thanks to Japanese government to support my Ph.D. program through MEXT scholarship.

Finally, I want to thank all the past and current members of Abidur Lab for their relentless support and discussion to improve these projects. I appreciate the help from Dr. Matsuo Uemura, Dr. Yukio Kawamura and their lab members.

References

Alonso, A., Queiroz, C.S., and Magalhães, A.C. (1997). Chilling stress leads to increased cell membrane rigidity in roots of coffee (Coffea arabica L.) seedlings. Biochimica et Biophysica Acta (BBA)-Biomembranes **1323,** 75-84.

Amme, S., Matros, A., Schlesier, B., and Mock, H.-P. (2006). Proteome analysis of cold stress response in Arabidopsis thaliana using DIGE-technology. Journal of Experimental Botany **57,** 1537-1546.

Anders, N., and Jürgens, G. (2008). Large ARF guanine nucleotide exchange factors in membrane trafficking. Cellular and Molecular Life Sciences **65,** 3433-3445.

Anders, N., Nielsen, M., Keicher, J., Stierhof, Y.-D., Furutani, M., Tasaka, M., Skriver, K., and Jürgens, G. (2008). Membrane association of the Arabidopsis ARF exchange factor GNOM involves interaction of conserved domains. The Plant Cell **20,** 142-151.

Barrero-Gil, J., and Salinas, J. (2017). CBFs at the Crossroads of Plant Hormone Signaling in Cold Stress Response. Molecular Plant **10,** 542-544.

Baskin, T.I., and Wilson, J.E. (1997). Inhibitors of protein kinases and phosphatases alter root morphology and disorganize cortical microtubules. Plant Physiology **113,** 493-502.

Begasse, M.L., Leaver, M., Vazquez, F., Grill, S.W., and Hyman, A.A. (2015). Temperature dependence of cell division timing accounts for a shift in the thermal limits of C. elegans and C. briggsae. Cell Reports **10,** 647-653.

Ben-Haj-Salah, H., and Tardieu, F. (1995). Temperature affects expansion rate of maize leaves without change in spatial distribution of cell length (analysis of the coordination between cell division and cell expansion). Plant Physiology **109,** 861-870.

Bielach, A., Hrtyan, M., and Tognetti, V.B. (2017). Plants under stress: Involvement of auxin and cytokinin. International Journal of Molecular Sciences **18,** 1427.

Britto, D.T., and Kronzucker, H.J. (2008). Cellular mechanisms of potassium transport in plants. Physiologia Plantarum **133,** 637-650.

Brunoud, G., Wells, D.M., Oliva, M., Larrieu, A., Mirabet, V., Burrow, A.H., Beeckman, T., Kepinski, S., Traas, J., and Bennett, M.J. (2012). A novel sensor to map auxin response and distribution at high spatio-temporal resolution. Nature **482,** 103.

Busch, M., Mayer, U., and Jürgens, G. (1996). Molecular analysis of the Arabidopsis pattern formation gene GNOM: gene structure and intragenic complementation. Molecular and General Genetics MGG **250,** 681-691.

Casanova, J.E. (2007). Regulation of Arf activation: the Sec7 family of guanine nucleotide exchange factors. Traffic **8,** 1476-1485.

Chantalat, S., Park, S.-K., Hua, Z., Liu, K., Gobin, R., Peyroche, A., Rambourg, A., Graham, T.R., and Jackson, C.L. (2004). The Arf activator Gea2p and the P-type ATPase Drs2p interact at the Golgi in Saccharomyces cerevisiae. Journal of Cell Science **117,** 711-722.

Collander, R. (1941). Selective absorption of cations by higher plants. Plant Physiology **16,** 691.

Collins, N.C., Thordal-Christensen, H., Lipka, V., Bau, S., Kombrink, E., Qiu, J.-L., Hückelhoven, R., Stein, M., Freialdenhoven, A., and Somerville, S.C. (2003). SNARE-protein-mediated disease resistance at the plant cell wall. Nature **425,** 973.

Colón-Carmona, A., You, R., Haimovitch-Gal, T., and Doerner, P. (1999). Spatio-temporal analysis of mitotic activity with a labile cyclin–GUS fusion protein. The Plant Journal **20,** 503-508.

Cooghtrey, P., Jackson, D., and Thorne, M. (1983). Radionuclide distribution and transport in terrestrial and aquatic ecosystems: A critical review of data. (eds: P.J. Coughtrey, D. Jackson, M.C. Thorne) CRC press.

Davies, P.J. (1995). The plant hormone concept: concentration, sensitivity and transport. (Springer, Dordrecht).

Dhonukshe, P., Aniento, F., Hwang, I., Robinson, D.G., Mravec, J., Stierhof, Y.-D., and Friml, J. (2007). Clathrin-mediated constitutive endocytosis of PIN auxin efflux carriers in Arabidopsis. Current Biology **17,** 520-527.

Dortay, H., Gruhn, N., Pfeifer, A., Schwerdtner, M., Schmülling, T., and Heyl, A. (2008). Toward an interaction map of the two-component signaling pathway of Arabidopsis thaliana. Journal of Proteome Research **7,** 3649-3660.

Ebine, K., Okatani, Y., Uemura, T., Goh, T., Shoda, K., Niihama, M., Morita, M.T., Spitzer, C., Otegui, M.S., and Nakano, A. (2008). A SNARE complex unique to seed plants is required for protein storage vacuole biogenesis and seed development of Arabidopsis thaliana. The Plant Cell **20,** 3006-3021.

Ebine, K., Fujimoto, M., Okatani, Y., Nishiyama, T., Goh, T., Ito, E., Dainobu, T., Nishitani, A., Uemura, T., and Sato, M.H. (2011). A membrane trafficking pathway regulated by the plant-specific RAB GTPase ARA6. Nature Cell Biology **13,** 853-859.

Eckardt, N.A. (2014). The Plant Cell Reviews Aspects of Photobiology: It's a Matter of Stop'n Go. Plant Cell 26, 1.

Einset, J., Nielsen, E., Connolly, E.L., Bones, A., Sparstad, T., Winge, P., and Zhu, J.K. (2007). Membrane-trafficking RabA4c involved in the effect of glycine betaine on recovery from chilling stress in Arabidopsis. Physiologia Plantarum **130,** 511-518.

Ellinger, D., Glöckner, A., Koch, J., Naumann, M., Stürtz, V., Schütt, K., Manisseri, C., Somerville, S.C., and Voigt, C.A. (2014). Interaction of the Arabidopsis GTPase RabA4c with its effector PMR4 results in complete penetration resistance to powdery mildew. The Plant Cell **26,** 3185-3200.

Feyder, S., De Craene, J.-O., Bär, S., Bertazzi, D.L., and Friant, S. (2015). Membrane trafficking in the yeast Saccharomyces cerevisiae model. International Journal of Molecular Sciences **16,** 1509-1525.

Fourcroy, P., Sisó-Terraza, P., Sudre, D., Savirón, M., Reyt, G., Gaymard, F., Abadía, A., Abadia, J., Álvarez-Fernández, A., and Briat, J.F. (2014). Involvement of the ABCG37 transporter in secretion of scopoletin and derivatives by Arabidopsis roots in response to iron deficiency. New Phytologist **201,** 155-167.

Franklin, K.A., Lee, S.H., Patel, D., Kumar, S.V., Spartz, A.K., Gu, C., Ye, S., Yu, P., Breen, G., and Cohen, J.D. (2011). Phytochrome-interacting factor 4 (PIF4) regulates auxin biosynthesis at high temperature. Proceedings of the National Academy of Sciences **108,** 20231-20235.

Fujiwara, T. (2013). Cesium uptake in rice: possible transporter, distribution, and variation. In Agricultural Implications of the Fukushima Nuclear Accident. (eds: Tomoko M. Nakanish, Keitaro Tanoi) (Springer), pp. 29-35.

Geldner, N., Richter, S., Vieten, A., Marquardt, S., Torres-Ruiz, R.A., Mayer, U., and Jürgens, G. (2004). Partial loss-of-function alleles reveal a role for GNOM in auxin transport-related, post-embryonic development of Arabidopsis. Development **131,** 389-400.

Geldner, N., Anders, N., Wolters, H., Keicher, J., Kornberger, W., Muller, P., Delbarre, A., Ueda, T., Nakano, A., and Jürgens, G. (2003). The Arabidopsis GNOM ARF-GEF mediates endosomal recycling, auxin transport, and auxin-dependent plant growth. Cell **112,** 219-230.

Gillingham, A.K., and Munro, S. (2007). The small G proteins of the Arf family and their regulators. Annual Review of Cell and Developmental Biology **23,** 579-611.

Goh, T., Uchida, W., Arakawa, S., Ito, E., Dainobu, T., Ebine, K., Takeuchi, M., Sato, K., Ueda, T., and Nakano, A. (2007). VPS9a, the common activator for two distinct types of Rab5 GTPases, is essential for the development of Arabidopsis thaliana. The Plant Cell **19,** 3504-3515.

Gray, W.M., Östin, A., Sandberg, G., Romano, C.P., and Estelle, M. (1998). High temperature promotes auxin-mediated hypocotyl elongation in Arabidopsis. Proceedings of the National Academy of Sciences the United States of America **95,** 7197-7202.

Grebe, M., Gadea, J., Steinmann, T., Kientz, M., Rahfeld, J.-U., Salchert, K., Koncz, C., and Jürgens, G. (2000). A conserved domain of the Arabidopsis GNOM protein mediates subunit interaction and cyclophilin 5 binding. The Plant Cell **12,** 343-356.

Grennan, A.K. (2009). Identification of genes involved in metal transport in plants. Plant Physiology **149,** 1623-1624.

Guo, J., Wei, J., Xu, J., and Sun, M.-X. (2014). Inducible knock-down of GNOM during root formation reveals tissue-specific response to auxin transport and its modulation of local auxin biosynthesis. Journal of Experimental Botany **65,** 1165-1179.

Hampton, C.R., Bowen, H.C., Broadley, M.R., Hammond, J.P., Mead, A., Payne, K.A., Pritchard, J., and White, P.J. (2004). Cesium toxicity in Arabidopsis. Plant Physiology **136,** 3824-3837.

Hannah, M.A., Heyer, A.G., and Hincha, D.K. (2005). A global survey of gene regulation during cold acclimation in Arabidopsis thaliana. PLoS Genetics **1,** e26.

Hanzawa, T., Shibasaki, K., Numata, T., Kawamura, Y., Gaude, T., and Rahman, A. (2013). Cellular auxin homeostasis under high temperature is regulated through a SORTING NEXIN1–dependent endosomal trafficking pathway. The Plant Cell **25,** 3424-3433.

Hong, J.H., Savina, M., Du, J., Devendran, A., Ramakanth, K.K., Tian, X., Sim, W.S., Mironova, V.V., and Xu, J. (2017). A sacrifice-for-survival mechanism protects root stem cell niche from chilling stress. Cell **170,** 102-113. e114.

Hosomi, A., Nakase, M., and Takegawa, K. (2011). Schizosaccharomyces pombe Pep12p is required for vacuolar protein transport and vacuolar homotypic fusion. Journal of Bioscience and Bioengineering **112,** 309-314.

Isaure, M.-P., Fraysse, A., Deves, G., Le Lay, P., Fayard, B., Susini, J., Bourguignon, J., and Ortega, R. (2006). Micro-chemical imaging of cesium distribution in Arabidopsis thaliana plant and its interaction with potassium and essential trace elements. Biochimie **88,** 1583-1590.

Ishikawa, S., Hayashi, S., Abe, T., Igura, M., Kuramata, M., Tanikawa, H., Iino, M., Saito, T., Ono, Y., and Ishikawa, T. (2017). Low-cesium rice: mutation in OsSOS2 reduces radiocesium in rice grains. Scientific Reports **7,** 2432.

Ito, H., and Gray, W.M. (2006). A gain-of-function mutation in the Arabidopsis pleiotropic drug resistance transporter PDR9 confers resistance to auxinic herbicides. Plant Physiology **142,** 63-74.

Jaillais, Y., Fobis-Loisy, I., Miege, C., Rollin, C., and Gaude, T. (2006). AtSNX1 defines an endosome for auxin-carrier trafficking in Arabidopsis. Nature **443,** 106.

Jones, S., Jedd, G., Kahn, R.A., Franzusoff, A., Bartolini, F., and Segev, N. (1999). Genetic interactions in yeast between Ypt GTPases and Arf guanine nucleotide exchangers. Genetics **152,** 1543-1556.

Jung, I.L., Ryu, M., Cho, S.K., Shah, P., Lee, J.H., Bae, H., Kim, I.G., and Yang, S.W. (2015). Cesium toxicity alters MicroRNA processing and AGO1 expressions in Arabidopsis thaliana. PloS One **10,** e0125514.

Jungmann, J., Reins, H.-A., Schobert, C., and Jentsch, S. (1993). Resistance to cadmium mediated by ubiquitin-dependent proteolysis. Nature **361,** 369.

Kamiya, T., Tanaka, M., Mitani, N., Ma, J.F., Maeshima, M., and Fujiwara, T. (2009). NIP1; 1, an aquaporin homolog, determines the arsenite sensitivity of Arabidopsis thaliana. Journal of Biological Chemistry **284,** 2114-2120.

Kandachar, V., and Roegiers, F. (2012). Endocytosis and control of Notch signaling. Current Opinion in Cell Biology **24,** 534-540.

Kanter, U., Hauser, A., Michalke, B., Dräxl, S., and Schäffner, A.R. (2010). Caesium and strontium accumulation in shoots of Arabidopsis thaliana: genetic and physiological aspects. Journal of Experimental Botany **61,** 3995-4009.

Kazemi-Shahandashti, S.-S., and Maali-Amiri, R. (2018). Global insights of protein responses to cold stress in plants: Signaling, defence, and degradation. Journal of Plant Physiology **226**, 123-135.

Kim, D.-Y., Bovet, L., Kushnir, S., Noh, E.W., Martinoia, E., and Lee, Y. (2006). AtATM3 is involved in heavy metal resistance in Arabidopsis. Plant Physiology **140,** 922-932.

Kim, D.Y., Bovet, L., Maeshima, M., Martinoia, E., and Lee, Y. (2007). The ABC transporter AtPDR8 is a cadmium extrusion pump conferring heavy metal resistance. The Plant Journal **50,** 207-218.

Kinoshita, N., Sueki, K., Sasa, K., Kitagawa, J.-i., Ikarashi, S., Nishimura, T., Wong, Y.-S., Satou, Y., Handa, K., and Takahashi, T. (2011). Assessment of individual radionuclide distributions from the Fukushima nuclear accident covering central-east Japan. Proceedings of the National Academy of Sciences, the United States of America **108,** 19526-19529.

Kobayashi, D., Uozumi, N., HISAMATSU, S.i., and Yamagami, M. (2010). AtKUP/HAK/KT9, a K+ transporter from Arabidopsis thaliana, mediates Cs^+ uptake in Escherichia coli. Bioscience, Biotechnology, and Biochemistry **74,** 203-205.

Koini, M.A., Alvey, L., Allen, T., Tilley, C.A., Harberd, N.P., Whitelam, G.C., and Franklin, K.A. (2009). High temperature-mediated adaptations in plant architecture require the bHLH transcription factor PIF4. Current Biology **19,** 408-413.

Kruman, I., Ilyasova, E., Rudchenko, S., and Khurkhulu, Z. (1988). The intestinal epithelial cells of ground squirrel (Citellus undulatus) accumulate at G2 phase of the cell cycle throughout a bout of hibernation. Comparative Biochemistry and Physiology. A, Comparative physiology **90,** 233-236.

Kudo, T., Nagai, K., and Tamura, G. (1977). Characteristics of cold-sensitive cell division mutant of Escherichia coli K-12. Agricultural and Biological Chemistry **41,** 97-107.

Kurup, S., Runions, J., Köhler, U., Laplaze, L., Hodge, S., and Haseloff, J. (2005). Marking cell lineages in living tissues. The Plant Journal **42,** 444-453.

Lee, B. H., Henderson, D.A., and Zhu, J.-K. (2005a). The Arabidopsis cold-responsive transcriptome and its regulation by ICE1. The Plant Cell **17,** 3155-3175.

Lee, M., Lee, K., Lee, J., Noh, E.W., and Lee, Y. (2005b). AtPDR12 contributes to lead resistance in Arabidopsis. Plant Physiology **138,** 827-836.

Levedeva, G., and Zavarzin, A. (1967). Differential sensitivity of the phase of the mitotic cycle to temperature effects in 2 types of cell populations in one day-old rats. Nature **214,** 110-111.

Levitt, J. (1972). Response of plants to environmental stresses. Academic Press (New York, USA)

Li, S., Liu, X., Wang, S., Hao, D., and Xi, J. (2014). Proteomics dissection of cold responsive proteins based on PEG fractionation in Arabidopsis. Chemical Research in Chinese Universities **30,** 272-278.

Li, W., Ma, M., Feng, Y., Li, H., Wang, Y., Ma, Y., Li, M., An, F., and Guo, H. (2015). EIN2-directed translational regulation of ethylene signaling in Arabidopsis. Cell **163,** 670-683.

Liu, Y., and Bassham, D.C. (2012). Autophagy: pathways for self-eating in plant cells. Annual Review of Plant Biology **63,** 215-237.

Liu, Z., Jia, Y., Ding, Y., Shi, Y., Li, Z., Guo, Y., Gong, Z., and Yang, S. (2017). Plasma membrane CRPK1-mediated phosphorylation of 14-3-3 proteins induces their nuclear import to fine-tune CBF signaling during cold response. Molecular Cell **66,** 117-128. e115.

Luschnig, C., Gaxiola, R.A., Grisafi, P., and Fink, G.R. (1998). EIR1, a root-specific protein involved in auxin transport, is required for gravitropism in Arabidopsis thaliana. Genes & Development **12,** 2175-2187.

Lyzenga, W.J., and Stone, S.L. (2011). Abiotic stress tolerance mediated by protein ubiquitination. Journal of Experimental Botany **63,** 599-616.

Ma, J.F., Yamaji, N., Mitani, N., Xu, X.-Y., Su, Y.-H., McGrath, S.P., and Zhao, F.-J. (2008). Transporters of arsenite in rice and their role in arsenic accumulation in rice grain. Proceedings of the National Academy of Sciences, the United States of America **105,** 9931-9935.

Ma, Y., Dai, X., Xu, Y., Luo, W., Zheng, X., Zeng, D., Pan, Y., Lin, X., Liu, H., and Zhang, D. (2015). COLD1 confers chilling tolerance in rice. Cell **160,** 1209-1221.

Mao, H., Aryal, B., Langenecker, T., Hagmann, J., Geisler, M., and Grebe, M. (2017). Arabidopsis BTB/POZ protein-dependent PENETRATION3 trafficking and disease susceptibility. Nature Plants**, 3**, 854–858.

Martins, S., Montiel-Jorda, A., Cayrel, A., Huguet, S., Paysant-Le Roux, C., Ljung, K., and Vert, G. (2017). Brassinosteroid signaling-dependent root responses to prolonged elevated ambient temperature. Nature Communications **8**, 30.

Mayer, U., Buttner, G., and Jurgens, G. (1993). Apical-basal pattern formation in the Arabidopsis embryo: studies on the role of the gnom gene. Development **117,** 149-162.

Mejía, R., Gómez-Eichelmann, M.C., and Fernández, M.S. (1995). Membrane fluidity of Escherichia coli during heat-shock. Biochimica et Biophysica Acta (BBA)-Biomembranes **1239,** 195-200.

Mendoza-Cózatl, D.G., Jobe, T.O., Hauser, F., and Schroeder, J.I. (2011). Long-distance transport, vacuolar sequestration, tolerance, and transcriptional responses induced by cadmium and arsenic. Current Opinion in Plant Biology **14,** 554-562.

Merchante, C., Brumos, J., Yun, J., Hu, Q., Spencer, K.R., Enríquez, P., Binder, B.M., Heber, S., Stepanova, A.N., and Alonso, J.M. (2015). Gene-specific translation regulation mediated by the hormone-signaling molecule EIN2. Cell **163,** 684-697.

Mittler, R. (2006). Abiotic stress, the field environment and stress combination. Trends in Plant Science **11,** 15-19.

Miura, K., and Furumoto, T. (2013). Cold signaling and cold response in plants. International Journal of Molecular Sciences **14,** 5312-5337.

Miyazawa, Y., Takahashi, A., Kobayashi, A., Kaneyasu, T., Fujii, N., and Takahashi, H. (2009). GNOM-mediated vesicular trafficking plays an essential role in hydrotropism of Arabidopsis roots. Plant Physiology **149,** 835-840.

Moir, D., Stewart, S.E., Osmond, B.C., and Botstein, D. (1982). Cold-sensitive cell-division-cycle mutants of yeast: isolation, properties, and pseudoreversion studies. Genetics **100,** 547-563.

Moriwaki, T., Miyazawa, Y., Fujii, N., and Takahashi, H. (2014). GNOM regulates root hydrotropism and phototropism independently of PIN-mediated auxin transport. Plant Science **215,** 141-149.

Nakanishi, H., Ogawa, I., Ishimaru, Y., Mori, S., and Nishizawa, N.K. (2006). Iron deficiency enhances cadmium uptake and translocation mediated by the Fe^{2+} transporters OsIRT1 and OsIRT2 in rice. Soil Science & Plant Nutrition **52,** 464-469.

Naramoto, S., Otegui, M.S., Kutsuna, N., De Rycke, R., Dainobu, T., Karampelias, M., Fujimoto, M., Feraru, E., Miki, D., and Fukuda, H. (2014). Insights into the localization and function of the membrane trafficking regulator GNOM ARF-GEF at the Golgi apparatus in Arabidopsis. The Plant Cell **26,** 3062-3076.

Nielsen, M.E., Jürgens, G., and Thordal-Christensen, H. (2017). VPS9a Activates the Rab5 GTPase ARA7 to Confer Distinct Pre-and Postinvasive Plant Innate Immunity. The Plant Cell **29,** 1927-1937.

Nielsen, M.E., Feechan, A., Böhlenius, H., Ueda, T., and Thordal-Christensen, H. (2012). Arabidopsis ARF-GTP exchange factor, GNOM, mediates transport required for innate immunity and focal accumulation of syntaxin PEN1. Proceedings of the National Academy of Sciences, the United States of America **109,** 11443-11448.

Nieves-Cordones, M., Mohamed, S., Tanoi, K., Kobayashi, N.I., Takagi, K., Vernet, A., Guiderdoni, E., Périn, C., Sentenac, H., and Véry, A.A. (2017). Production of low-Cs+ rice plants by inactivation of the K+ transporter OsHAK1 with the CRISPR-Cas system. The Plant Journal **92**, 43–56.

Okamoto, T., Tsurumi, S., Shibasaki, K., Obana, Y., Takaji, H., Oono, Y., and Rahman, A. (2008). Genetic dissection of hormonal responses in the roots of Arabidopsis grown under continuous mechanical impedance. Plant Physiology **146,** 1651-1662.

Okumura, K.-i., Goh, T., Toyokura, K., Kasahara, H., Takebayashi, Y., Mimura, T., Kamiya, Y., and Fukaki, H. (2013). GNOM/FEWER ROOTS is required for the establishment of an auxin response maximum for arabidopsis lateral root initiation. Plant and Cell Physiology **54,** 406-417.

Oliveira, G., and Peñuelas, J. (2005). Effects of winter cold stress on photosynthesis and photochemical efficiency of PSII of the Mediterranean Cistus albidus L. and Quercus ilex L. Plant Ecology **175,** 179-191.

Oono, Y., Yazawa, T., Kanamori, H., Sasaki, H., Mori, S., Handa, H., and Matsumoto, T. (2016). Genome-wide transcriptome analysis of cadmium stress in rice. BioMed Research International **2016**.

Pal, S., Lant, B., Yu, B., Tian, R., Tong, J., Krieger, J.R., Moran, M.F., Gingras, A.-C., and Derry, W.B. (2017). CCM-3 promotes C. elegans germline development by regulating vesicle trafficking cytokinesis and polarity. Current Biology **27,** 868-876.

Park, J., Song, W.Y., Ko, D., Eom, Y., Hansen, T.H., Schiller, M., Lee, T.G., Martinoia, E., and Lee, Y. (2012). The phytochelatin transporters AtABCC1 and AtABCC2 mediate tolerance to cadmium and mercury. The Plant Journal **69,** 278-288.

Peyroche, A., Antonny, B., Robineau, S., Acker, J., Cherfils, J., and Jackson, C.L. (1999). Brefeldin A acts to stabilize an abortive ARF–GDP–Sec7 domain protein complex: involvement of specific residues of the Sec7 domain. Molecular Cell **3,** 275-285.

Pochodylo, A.L., and Aristilde, L. (2017). Molecular dynamics of stability and structures in phytochelatin complexes with Zn, Cu, Fe, Mg, and Ca: Implications for metal detoxification. Environmental Chemistry Letters **15,** 495-500.

Prasad, P., Pisipati, S., Momčilović, I., and Ristic, Z. (2011). Independent and combined effects of high temperature and drought stress during grain filling on plant yield and chloroplast EF-Tu expression in spring wheat. Journal of Agronomy and Crop Science **197,** 430-441.

Qi, Z., Hampton, C.R., Shin, R., Barkla, B.J., White, P.J., and Schachtman, D.P. (2008). The high affinity K+ transporter AtHAK5 plays a physiological role in planta at very low K+ concentrations and provides a caesium uptake pathway in Arabidopsis. Journal of Experimental Botany **59,** 595-607.

Rahman, A. (2013). Auxin: a regulator of cold stress response. Physiologia Plantarum **147,** 28-35.

Rahman, A., Bannigan, A., Sulaman, W., Pechter, P., Blancaflor, E.B., and Baskin, T.I. (2007). Auxin, actin and growth of the Arabidopsis thaliana primary root. The Plant Journal **50,** 514-528.

Rahman, A., Takahashi, M., Shibasaki, K., Wu, S., Inaba, T., Tsurumi, S., and Baskin, T.I. (2010). Gravitropism of Arabidopsis thaliana roots requires the polarization of PIN2 toward the root tip in meristematic cortical cells. The Plant Cell **22,** 1762-1776.

Rai, H., Yokoyama, S., Satoh-Nagasawa, N., Furukawa, J., Nomi, T., Ito, Y., Fujimura, S., Takahashi, H., Suzuki, R., and Yousra, E. (2017). Cesium uptake by rice roots largely depends upon a single gene, HAK1, which encodes a potassium transporter. Plant and Cell Physiology **58,** 1486-1493.

Rai, V., Tuteja, N., and Takabe, T. (2012). Transporters and abiotic stress tolerance in plants. Improving Crop Resistance to Abiotic Stress. (eds: Narendra Tuteja, Sarvajeet Singh Gill, Antonio F. Tiburcio, Renu Tuteja) pp 507-522. Wiley-Blackwell.

Richter, S., Geldner, N., Schrader, J., Wolters, H., Stierhof, Y.-D., Rios, G., Koncz, C., Robinson, D.G., and Jürgens, G. (2007). Functional diversification of closely related ARF-GEFs in protein secretion and recycling. Nature **448,** 488-492.

Rieder, C.L., and Cole, R.W. (2002). Cold-shock and the Mammalian cell cycle. Cell Cycle **1,** 168-174.

Rizhsky, L., Davletova, S., Liang, H., and Mittler, R. (2004). The zinc finger protein Zat12 is required for cytosolic ascorbate peroxidase 1 expression during oxidative stress in Arabidopsis. Journal of Biological Chemistry **279,** 11736-11743.

Ródenas, R., Nieves-Cordones, M., Rivero, R.M., Martinez, V., and Rubio, F. (2017). Pharmacological and gene regulation properties point to the SlHAK5 K^+ transporter as a system for high-affinity Cs^+ uptake in tomato plants. Physiologia Plantarum **162**, 455-466.

Růžička, K., Strader, L.C., Bailly, A., Yang, H., Blakeslee, J., Łangowski, Ł., Nejedlá, E., Fujita, H., Itoh, H., and Syōno, K. (2010). Arabidopsis PIS1 encodes the ABCG37 transporter of auxinic compounds including the auxin precursor indole-3-butyric acid. Proceedings of the National Academy of Sciences, the United States of America **107,** 10749-10753.

Sahr, T., Voigt, G., Schimmack, W., Paretzke, H.G., and Ernst, D. (2005a). Low-level radiocaesium exposure alters gene expression in roots of Arabidopsis. New Phytologist **168,** 141-148.

Sahr, T., Voigt, G., Paretzke, H.G., Schramel, P., and Ernst, D. (2005b). Caesium-affected gene expression in Arabidopsis thaliana. New Phytologist **165,** 747-754.

Sakata, T., Oshino, T., Miura, S., Tomabechi, M., Tsunaga, Y., Higashitani, N., Miyazawa, Y., Takahashi, H., Watanabe, M., and Higashitani, A. (2010). Auxins reverse plant

male sterility caused by high temperatures. Proceedings of the National Academy of Sciences, the United States of America **107,** 8569-8574.

Sakurai, H.T., Inoue, T., Nakano, A., and Ueda, T. (2016). ENDOSOMAL RAB EFFECTOR WITH PX-DOMAIN, an interacting partner of RAB5 GTPases, regulates membrane trafficking to protein storage vacuoles in Arabidopsis. The Plant Cell **28,** 1490-1503.

Sata, M., Moss, J., and Vaughan, M. (1999). Structural basis for the inhibitory effect of brefeldin A on guanine nucleotide-exchange proteins for ADP-ribosylation factors. Proceedings of the National Academy of Sciences, the United States of America **96,** 2752-2757.

Schuetz, M., Benske, A., Smith, R.A., Watanabe, Y., Tobimatsu, Y., Ralph, J., Demura, T., Ellis, B., and Samuels, A.L. (2014). Laccases direct lignification in the discrete secondary cell wall domains of protoxylem. Plant Physiology **166,** 798-807.

Sharma, S.S., Dietz, K.J., and Mimura, T. (2016). Vacuolar compartmentalization as indispensable component of heavy metal detoxification in plants. Plant, Cell & Environment **39,** 1112-1126.

Shaw, G., and Bell, J. (1991). Competitive effects of potassium and ammonium on caesium uptake kinetics in wheat. Journal of Environmental Radioactivity **13,** 283-296.

Shi, Y., and Yang, S. (2014). ABA regulation of the cold stress response in plants. In Abscisic Acid: Metabolism, Transport and Signaling (ed: Da-Peng Zhang) pp 337-363. Springer.

Shibasaki, K., and Rahman, A. (2013). Auxin and temperature stress: molecular and cellular perspectives. In Polar Auxin Transport (eds: Chen, R and Baluska, F) (Springer), pp. 295-310.

Shibasaki, K., Uemura, M., Tsurumi, S., and Rahman, A. (2009). Auxin response in Arabidopsis under cold stress: underlying molecular mechanisms. The Plant Cell **21,** 3823-3838.

Shirano, Y., Kachroo, P., Shah, J., and Klessig, D.F. (2002). A gain-of-function mutation in an Arabidopsis Toll Interleukin1 Receptor–Nucleotide Binding Site–Leucine-Rich Repeat type R gene triggers defense responses and results in enhanced disease resistance. The Plant Cell **14,** 3149-3162.

Silk, W.K. (1992). Steady form from changing cells. International Journal of Plant Sciences **153,** S49-S58.

Smith, H.B. (1999). Vacuolar protein trafficking and vesicles: Continuing to sort it all out. The Plant Cell **11,** 1377-1379.

Song, W.-Y., Park, J., Mendoza-Cózatl, D.G., Suter-Grotemeyer, M., Shim, D., Hörtensteiner, S., Geisler, M., Weder, B., Rea, P.A., and Rentsch, D. (2010). Arsenic tolerance in Arabidopsis is mediated by two ABCC-type phytochelatin transporters. Proceedings of the National Academy of Sciences, the United States of America **107,** 21187-21192.

Soppe, W.J., Jacobsen, S.E., Alonso-Blanco, C., Jackson, J.P., Kakutani, T., Koornneef, M., and Peeters, A.J. (2000). The late flowering phenotype of fwa mutants is caused by gain-of-function epigenetic alleles of a homeodomain gene. Molecular Cell **6,** 791-802.

Steinmann, T., Geldner, N., Grebe, M., Mangold, S., Jackson, C.L., Paris, S., Gälweiler, L., Palme, K., and Jürgens, G. (1999). Coordinated polar localization of auxin efflux carrier PIN1 by GNOM ARF GEF. Science **286,** 316-318.

Stewart, B.A. (2002). Membrane trafficking in Drosophila wing and eye development. Seminars in Cell & Developmental Biology **13,** 91-97.

Sun, J., Qi, L., Li, Y., Chu, J., and Li, C. (2012). PIF4–mediated activation of YUCCA8 expression integrates temperature into the auxin pathway in regulating Arabidopsis hypocotyl growth. PLoS Genetics **8,** e1002594.

Suzuki, N., Rivero, R.M., Shulaev, V., Blumwald, E., and Mittler, R. (2014). Abiotic and biotic stress combinations. New Phytologist **203,** 32-43.

Swarup, R., Friml, J., Marchant, A., Ljung, K., Sandberg, G., Palme, K., and Bennett, M. (2001). Localization of the auxin permease AUX1 suggests two functionally distinct hormone transport pathways operate in the Arabidopsis root apex. Genes & development **15,** 2648-2653.

Tamang, B.G., and Fukao, T. (2015). Plant adaptation to multiple stresses during submergence and following desubmergence. International Journal of Molecular Sciences **16,** 30164-30180.

Teh, O. K., and Moore, I. (2007). An ARF-GEF acting at the Golgi and in selective endocytosis in polarized plant cells. Nature **448,** 493-496.

Thomashow, M.F. (1999). Plant cold acclimation: freezing tolerance genes and regulatory mechanisms. Annual Review of Plant Biology **50,** 571-599.

Uemura, M., Joseph, R.A., and Steponkus, P.L. (1995). Cold acclimation of Arabidopsis thaliana (effect on plasma membrane lipid composition and freeze-induced lesions). Plant Physiology **109,** 15-30.

Uemura, T., Kim, H., Saito, C., Ebine, K., Ueda, T., Schulze-Lefert, P., and Nakano, A. (2012). Qa-SNAREs localized to the trans-Golgi network regulate multiple transport pathways and extracellular disease resistance in plants. Proceedings of the National Academy of Sciences, the United States of America **109,** 1784-1789.

Vanstraelen, M., Baloban, M., Da Ines, O., Cultrone, A., Lammens, T., Boudolf, V., Brown, S.C., De Veylder, L., Mergaert, P., and Kondorosi, E. (2009). APC/CCCS52A complexes control meristem maintenance in the Arabidopsis root. Proceedings of the National Academy of Sciences, the United States of America **106,** 11806-11811.

Verrier, P.J., Bird, D., Burla, B., Dassa, E., Forestier, C., Geisler, M., Klein, M., Kolukisaoglu, Ü., Lee, Y., and Martinoia, E. (2008). Plant ABC proteins–a unified nomenclature and updated inventory. Trends in Plant Science **13,** 151-159.

Wang, R., Zhang, Y., Kieffer, M., Yu, H., Kepinski, S., and Estelle, M. (2016). HSP90 regulates temperature-dependent seedling growth in Arabidopsis by stabilizing the auxin co-receptor F-box protein TIR1. Nature Communications **7,** 10269.

Weigel, D., and Glazebrook, J. (2002). Arabidopsis: a Laboratory Manual. (CSHL Press).

White, P.J., and Broadley, M.R. (2000). Tansley Review No. 113 Mechanisms of caesium uptake by plants. New Phytologist **147,** 241-256.

Wiederkehr, A., Meier, K.D., and Riezman, H. (2001). Identification and characterization of Saccharomyces cerevisiae mutants defective in fluid-phase endocytosis. Yeast **18,** 759-773.

Wilkins, K.A., Matthus, E., Swarbreck, S.M., and Davies, J.M. (2016). Calcium-mediated abiotic stress signaling in roots. Frontiers in Plant Science **7,** 1296.

Xiong, L., Schumaker, K.S., and Zhu, J.-K. (2002). Cell signaling during cold, drought, and salt stress. The Plant Cell **14,** S165-S183.

Xu, J., and Scheres, B. (2005). Dissection of Arabidopsis ADP-RIBOSYLATION FACTOR 1 function in epidermal cell polarity. The Plant Cell **17,** 525-536.

Yadeta, K., Elmore, J.M., and Coaker, G. (2013). Advancements in the analysis of the Arabidopsis plasma membrane proteome. Frontiers in Plant Science **4,** 86.

Yamada, T., Kuroda, K., Jitsuyama, Y., Takezawa, D., Arakawa, K., and Fujikawa, S. (2002). Roles of the plasma membrane and the cell wall in the responses of plant cells to freezing. Planta **215,** 770-778.

Yamaki, T., Otani, M., Ono, K., Mimura, T., Oda, K., Minamii, T., Matsumoto, S., Matsuo, Y., Kawamukai, M., and Akihiro, T. (2017). Isolation and characterization of rice cesium transporter genes from a rice-transporter-enriched yeast expression library. Physiologia Plantarum **160,** 425-436.

Yang, X., Dong, G., Palaniappan, K., Mi, G., and Baskin, T.I. (2017). Temperature-compensated cell production rate and elongation zone length in the root of Arabidopsis thaliana. Plant, Cell & Environment **40,** 264-276.

Yin, C., Karim, S., Zhang, H., and Aronsson, H. (2017). Arabidopsis RabF1 (ARA6) Is Involved in Salt Stress and Dark-Induced Senescence (DIS). International Journal of Molecular Sciences **18,** 309.

Yokoyama, R., Hirakawa, T., Hayashi, S., Sakamoto, T., and Matsunaga, S. (2016). Dynamics of plant DNA replication based on PCNA visualization. Scientific Reports **6**.

Zelazny, E., and Vert, G. (2014). Plant nutrition: root transporters on the move. Plant Physiology **166,** 500-508.

Zhang, J., Hwang, J.U., Song, W.Y., Martinoia, E., and Lee, Y. (2017). Identification of amino acid residues important for the arsenic resistance function of Arabidopsis ABCC1. FEBS Letters **591,** 656-666.

Zhang, W., and Chen, W. (2010). Autophagy induction upon reactive oxygen species in Cd-stressed Arabidopsis thaliana. In Imaging, Manipulation, and Analysis of Biomolecules, Cells, and Tissues VIII. (eds: Daniel L. Farkas, Dan V. Nicolau, Robert C. Leif) pp. 75681Y. International Society for Optics and Photonics.

Zhao, F., Ma, J., Meharg, A., and McGrath, S. (2009). Arsenic uptake and metabolism in plants. New Phytologist **181,** 777-794.

Zheng, L., Peer, T., Seybold, V., and Lütz-Meindl, U. (2012). Pb-induced ultrastructural alterations and subcellular localization of Pb in two species of Lespedeza by TEM-coupled electron energy loss spectroscopy. Environmental and Experimental Botany **77,** 196-206.

Zhong, R., and Ye, Z.-H. (2004). Amphivasal vascular bundle 1, a gain-of-function mutation of the IFL1/REV gene, is associated with alterations in the polarity of leaves, stems and carpels. Plant and Cell Physiology **45,** 369-385.

Zhu, J., Zhang, K.-X., Wang, W.-S., Gong, W., Liu, W.-C., Chen, H.-G., Xu, H.-H., and Lu, Y.-T. (2015). Low temperature inhibits root growth by reducing auxin accumulation via ARR1/12. Plant and Cell Physiology **56,** 727-736.

Zhu, Y.G., and Smolders, E. (2000). Plant uptake of radiocaesium: a review of mechanisms, regulation and application. Journal of Experimental Botany **51,** 1635-1645.